

✓ TI-839

6/18/53

✓  
WADC TECHNICAL REPORT 52-130

DTI 186 624

AD A076043

**INVESTIGATION OF DISCREPANCIES BETWEEN FLIGHT-MEASURED  
AND CALCULATED F-80A DERIVATIVES AND RESPONSES  
INCLUDING A STUDY OF AEROELASTIC EFFECTS**

**LEONARD SEGEL  
CORNELL AERONAUTICAL LABORATORY, INC.**

*AUGUST 1952*

**WRIGHT AIR DEVELOPMENT CENTER**

**20011010001**

## NOTICES

When Government drawings, specifications, or other data are used for any purpose other than in connection with a definitely related Government procurement operation, the United States Government thereby incurs no responsibility nor any obligation whatsoever; and the fact that the Government may have formulated, furnished, or in any way supplied the said drawings, specifications, or other data, is not to be regarded by implication or otherwise as in any manner licensing the holder or any other person or corporation, or conveying any rights or permission to manufacture, use, or sell any patented invention that may in any way be related thereto.

The information furnished herewith is made available for study upon the understanding that the Government's proprietary interests in and relating thereto shall not be impaired. It is desired that the Judge Advocate (WCJ), Wright Air Development Center, Wright-Patterson Air Force Base, Ohio, be promptly notified of any apparent conflict between the Government's proprietary interests and those of others.



WADC TECHNICAL REPORT 52-130

**INVESTIGATION OF DISCREPANCIES BETWEEN FLIGHT-MEASURED  
AND CALCULATED F-80A DERIVATIVES AND RESPONSES  
INCLUDING A STUDY OF AEROELASTIC EFFECTS**

*Leonard Segel*  
*Cornell Aeronautical Laboratory, Inc.*

*August 1952*

*Aircraft Laboratory*  
*Contract No. W33(038)-ac-17003*  
*RDO No. 458-414*

Wright Air Development Center  
Air Research and Development Command  
United States Air Force  
Wright-Patterson Air Force Base, Ohio

## FOREWORD

This report was prepared for the U.S.A.F. by the Cornell Aeronautical Laboratory, Inc., Buffalo, New York, as Cornell Aeronautical Laboratory Report No. TB-495-F-14, under U.S.A.F. Contract No. W33-038-ac-17003, Supplemental Agreement No. 14. The contract was initiated under the research and development project, identified by RDO No. 458-414C, Flight Test on the Effects of Down-wash Lag and Aeroelasticity on Longitudinal Stability, and it was administered under the direction of the Aerodynamics Branch, Aircraft Laboratory, Engineering Division, Wright Air Development Center, with Major C. B. Westbrook, U.S.A.F., acting as project engineer.

### ABSTRACT

Studies have been made to determine if discrepancies existing between calculated and measured tail loads, responses, and derivatives, as obtained for the F-80A, can be eliminated or explained. These discrepancies were evidenced as (1) a tail load smaller than that predicted, (2) the measured aerodynamic stiffness being significantly greater than that indicated by wind tunnel tests, and (3) an unreasonably large value of stabilizer effectiveness being obtained in the analysis of the flight data. Certain of these results indicated that investigations should be made to establish the manner in which aeroelasticity and unsteady flow aerodynamics influence the tail loads and rigid body response of the F-80A airplane. It was found that (a) the failure of measured tail loads to agree with calculations is primarily due to an error in measurement due to limitations in strain gage location, (b) the effect of aeroelasticity is small and not of a dynamic nature, (c) the lack of agreement between predicted and measured responses at low Mach numbers is due to prediction being based on a wind tunnel evaluation of tail-off static stability which was different from that obtained in flight, and (d) the stabilizer effectiveness and downwash cannot be accurately evaluated unless the tail-off damping in pitch is determined. It is recommended that studies be made to develop additional techniques for determining the tail-off stability derivatives and that efforts be directed towards analyzing longitudinal response data assuming a complex downwash.

### PUBLICATION REVIEW

This report has been reviewed and is approved.

FOR THE COMMANDING GENERAL:



R. G. RUEGG  
Colonel, USAF  
Chief, Aircraft Laboratory  
Directorate of Laboratories

## TABLE OF CONTENTS

|   | <u>Page No.</u> |
|---|-----------------|
| Forword   | ii              |
| Abstract  | iii             |
| List of Illustrations   | v               |
| List of Symbols   | vi              |
| Introduction  | 1               |
| Background  | 2               |
| Examination of the Discrepancy Existing Between Predicted<br>and Measured Tail Load   | 5               |
| Aeroelastic Effects on the Response of the F-80A Airplane   | 8               |
| Consideration of Means of Improving the Agreement Between<br>Predicted and Measured Longitudinal Responses                                | 13              |
| Examination of and Means for Improving and/or Simplifying<br>the Extraction of Stability Derivatives from Longi-<br>tudinal Response Data | 17              |
| Comments on Future Aeroelastic Research   | 35              |
| Conclusions and Recommendations   | 36              |
| References  | 38              |

# LIST OF ILLUSTRATIONS

| <u>Fig.<br/>No.</u> | <u>Title</u>   | <u>Page<br/>No.</u> |
|---------------------|--|---------------------|
| 1                   | Frequency Response 10,000 Ft. 27% MAC .3 Mach No.  | 39                  |
| 2                   | Frequency Response 10,000 Ft. 27% MAC .5 Mach No.  | 40                  |
| 3                   | Frequency Response 10,000 Ft. 27% MAC .7 Mach No.  | 41                  |
| 4                   | Frequency Response 10,000 Ft. 27% MAC .75 Mach No.   | 42                  |
| 5                   | Frequency Response 20,000 Ft. 23% MAC .5 Mach No.  | 43                  |
| 6                   | Frequency Response 20,000 Ft. 23% MAC .7 Mach No.  | 44                  |
| 7                   | Frequency Response 20,000 Ft. 23% MAC .75 Mach No.   | 45                  |
| 8                   | Frequency Response 20,000 Ft. 27% MAC .3 Mach No.  | 46                  |
| 9                   | Frequency Response 20,000 Ft. 27% MAC .5 Mach No.  | 47                  |
| 10                  | Frequency Response 20,000 Ft. 27% MAC .7 Mach No.  | 48                  |
| 11                  | Frequency Response 20,000 Ft. 27% MAC .75 Mach No.   | 49                  |
| 12                  | Frequency Response 20,000 Ft. 31.5% MAC .5 Mach No.  | 50                  |
| 13                  | Frequency Response 20,000 Ft. 31.5% MAC .7 Mach No.  | 51                  |
| 14                  | Frequency Response 20,000 Ft. 31.5% MAC .75 Mach No.   | 52                  |
| 15                  | Frequency Response 30,000 Ft. 27% MAC .5 Mach No.  | 53                  |
| 16                  | Frequency Response 30,000 Ft. 27% MAC .7 Mach No.  | 54                  |
| 17                  | Frequency Response 30,000 Ft. 27% MAC .75 Mach No.   | 55                  |
| 18                  | Tail Load Response 20,000 Ft. 27% MAC .3 Mach No.  | 56                  |
| 19                  | Tail Load Response 20,000 Ft. 27% MAC .5 Mach No.  | 57                  |
| 20                  | Tail Load Response 20,000 Ft. 27% MAC .7 Mach No.  | 58                  |
| 21                  | Tail Load Response 20,000 Ft. 27% MAC .75 Mach No.   | 59                  |
| 22                  | Effect of Strain Gage Location on Tail Load Measurement  | 60                  |
| 23                  | Aeroelastic Calculations: $n_z/\delta$ and $\phi_{n_z}$ vs. Frequency                                      | 61                  |
| 24                  | Aeroelastic Calculations: $\xi_{\delta}/\delta$ and $\phi_{\xi_{\delta}}$ vs. Frequency                    | 62                  |
| 25                  | Aeroelastic Calculations: $C_{N_z}/\delta$ and $\phi_{C_{N_z}}$ vs. Frequency                              | 63                  |
| 26                  | Aeroelastic Calculations: $\xi/\delta$ and $\phi_{\xi}$ vs. Frequency                                      | 64                  |
| 27                  | Percentage Reduction in Response Amplitude Due to Aeroelasticity vs. Frequency                             | 65                  |
| 28                  | $dC_m/dC_L$ , $dC_m/dC_L$ , $m_{\dot{\alpha}}$ , $\mu m_{\dot{\alpha}}$ , $m_{\ddot{\alpha}}$ vs. Mach No. | 66                  |
| 29                  | $dE/d\delta$ , $C_{L_{\alpha}}$ , $-C_{m_{\dot{\alpha}}}$ , $-m_{\ddot{\alpha}}$ vs. Mach No.              | 67                  |
| 30                  | $b_0$ , $K_0$ vs. Mach No.   | 68                  |
| 31                  | $\Delta_c \phi$ and $\omega r \tan \Delta_c \phi$ vs. $\omega r$   | 69                  |
| 32                  | $m_w'$ and $m_w''$ vs. Reduced Frequency   | 70                  |

# LIST OF SYMBOLS

|                |   |
|----------------|---|
| $U_0$          | True airspeed - ft./sec.  |
| $w$            | Incremental velocity along $Z$ axis - ft./sec.                  |
| $\dot{w}$      | Incremental acceleration along $Z$ axis - ft./sec. <sup>2</sup> |
| $q$            | Pitching velocity - rad./sec.                                   |
| $q$            | Dynamic pressure - lb/sq.ft.                                    |
| $I_y$          | Moment of inertia about $y$ axis - slug ft. <sup>2</sup>        |
| $b$            | Wing span - ft.   |
| $c$            | Mean aerodynamic chord - ft.                                    |
| $g$            | Acceleration of gravity - ft./sec. <sup>2</sup>                 |
| $m$            | Mass of airplane - slugs  |
| $S$            | Wing area - ft. <sup>2</sup>                                    |
| $\alpha$       | Incremental angle of attack - rad. or deg.                      |
| $\delta$       | Elevator deflection - rad. or deg.                              |
| $\epsilon$     | Downwash angle  |
| $\theta$       | Altitude angle - rad. or deg.                                   |
| $\dot{\theta}$ | Pitching velocity - rad./sec.                                   |
| $\rho$         | Mass density of air - slugs/ft. <sup>3</sup>                    |
| $\mu$          | Airplane density factor -                                       |
| $\tau$         | Aerodynamic time unit - sec.,                                   |
| $\phi_{xy}$    | Phase of $x$ with respect to $y$                                |
| $\omega$       | Angular frequency - rad./sec.                                   |
| $D$            | Non-dimensional differential operator - $D = \tau \frac{d}{dt}$ |
| $i_t$          | Horizontal tail incidence - rad. or deg.                        |
| $n_z$          | Incremental normal acceleration                                 |
| $i_B$          | Moment of inertia coefficient - $4I_y/mc^2$                     |

|                   |   |
|-------------------|---|
| $l_t$             | Tail length - ft.   |
| $S_t$             | Horizontal tail area - ft. <sup>2</sup>   |
| $\bar{V}$         | Tail volume coefficient - $\bar{V} = \frac{S_t}{S} \frac{l_t}{c}$                                   |
| $\Delta \alpha_t$ | Incremental tail angle of attack  |
| $\lambda$         | Elevator effectiveness - $\lambda = \frac{\partial \alpha_t}{\partial \delta}$                      |
| $C_L$             | Airplane lift coefficient   |
| $C_m$             | Airplane pitching moment coefficient  |
| $z_w$             | $-1/2 dC_L/d\alpha$ , 1/rad. or 1/deg.  |
| $m_\delta$        | Elevator power - $m_\delta = \frac{\partial C_m}{\partial \delta}$ - 1/rad. or 1/deg.               |
| $z_\delta$        | $m_\delta / 2 \frac{l_t}{c}$ , 1/rad. or 1/deg.   |
| $dC_m/dC_L$       | Static longitudinal stability parameter   |
| $m_w$             | $-2 z_w dC_m/dC_L$ , 1/rad. or 1/deg.   |
| $C_{m_{i_t}}$     | $\partial C_m / \partial i_t$ , 1/rad. or 1/deg.  |
| $m_w$             | $2 l_t / c C_{m_{i_t}} d\epsilon/d\alpha$ , 1/rad. or 1/deg.  |
| $m_g$             | $\partial C_m / \partial \frac{g c}{2 U_0}$ , 1/rad. or 1/deg.                                      |
| $N_t$             | Horizontal tail load - lbs.   |
| $C_{N_t}$         | Horizontal tail load coefficient, $C_{N_t} = \frac{N_t}{1/2 S_t U_0^2}$                             |
| $T$               | Aircraft thrust - lbs.  |
| $b_0$             | Non-dimensional fixed control airplane damping coefficient,<br>$b_0 = -z_w - \frac{m_g + m_w}{c_0}$ |
| $K_0$             | Non-dimensional fixed control airplane spring coefficient,<br>$K_0 = 1/c_0 (m_g z_w - \mu m_w)$     |

## INTRODUCTION

This report presents the results of a study program which was oriented to explain the discrepancies encountered between calculated and measured (longitudinal) responses obtained from flight tests of the F-80A airplane. The study described herein is therefore a continuation of an extensive program which was designed to investigate the dynamic stability and aerodynamic tail loads of an F-80 at high subsonic Mach numbers. Execution of the program was the responsibility of the Flight Research Department of the Cornell Aeronautical Laboratory under the sponsorship of the Aerodynamic and Structure Branches of the Aircraft Laboratory, Wright Air Development Center.

The reasons underlying the development of this theoretical investigation are pertinent to the reporting of this study and are presented in a following section of the report entitled "Background". This section also includes a comprehensive statement of the problem together with a description of the approach that was followed in obtaining a solution.

The contractual objective of the program was to make brief, but all inclusive, studies directed towards determining if discrepancies existing between calculated and measured responses and derivatives can be eliminated. Accordingly, consideration has been given to means of improving the agreement between predicted and measured responses and to means of improving or simplifying the extraction of stability derivatives from longitudinal response data. Since certain investigators had predicted significant aeroelastic and unsteady flow effects on the response of the F-80A, an investigation was planned to determine to what extent these phenomena would account for the observed discrepancies. The resulting theoretical study examined the discrepancies existing between the predicted and measured tail loads and in addition, required that calculations be made to determine the effect of structural flexibility on the longitudinal responses of the F-80A airplane. The above mentioned work is fully described in this report, followed by recommendations for future aeroelastic research.

## BACKGROUND

Dynamic stability and control research by means of direct measurement of the aircraft response is a field in which the Flight Research Department of the Cornell Aeronautical Laboratory has been active for a number of years. The development of the response measurement technique in research programs carried out in large, relatively slow speed aircraft ultimately led to an experimental investigation which was designed to measure the responses and stability derivatives of a fighter airplane at high subsonic Mach numbers. The purpose of this program was twofold, namely --

(1) to demonstrate that the response of a fighter airplane to a sinusoidal forcing function can be measured with airborne instrumentation without compromising measurement accuracies and

(2) to investigate the effects of the pertinent variables such as lift coefficient, C.G. position, Mach number, etc. on the measured responses and stability derivatives for comparison with wind-tunnel results and the applicable theory.

By the time the F-80A flight program was about to get under way, other organizations and investigators had become actively interested in the problem of aircraft response prediction and measurement. One of the questions which had been raised was: were the original simplifying assumptions made in the earlier work at Cornell still justifiable in view of the higher dynamic pressures and Mach numbers which would be obtained with the F-80A. These assumptions, which previous flight measurements indicated to be valid, were as follows:

(1) The effects of frequency upon the stability derivatives are unimportant in the range of frequencies normally considered, i.e.  $0 < \omega \leq 8$  radians per second.

(2) The downwash lag can be approximated by the time required for the flow to travel from the wing to the tail.

(3) The airplane is non-elastic, thus making rigid body dynamics applicable to the solution of the response prediction problem.

In an effort to obtain theoretical verification for the first two assumptions, the study described in reference (1) was undertaken to determine whether the contribution of non-uniform flow effects is significant in the range of frequencies used in the flight test procedure. This study, which was made in a rigorous and thorough manner and applied numerically to an F-80A, indicated that frequency effects and higher order aerodynamic derivatives are not important in the range of frequencies that describe the flight path response of the rigid airplane. Use of the exact unsteady flow theory did result in a conception of downwash lag which is different from the time lag concept used in the simple theory. Responses obtained with the use of this phase lag approach

have a slightly reduced resonance peak and in effect look as if the damping is somewhat greater than is predicted by the simple theory. It should be emphasized that this difference is small and that experimental verification should be difficult to obtain. F-80A responses were also computed by Walkowicz (see reference 2) in which he attempted to include both aeroelastic and non-stationary flow effects. These calculations do not indicate the effects of each phenomenon separately but at zero frequency, where non-stationary flow is non-existent, the effect of aeroelasticity is seen to be quite large. In view of the agreement which had been previously obtained between flight measurements and the simple theory, considerable doubts were had as to the validity of these calculations. Nevertheless, they would either be substantiated or disproved by the results of the F-80A flight test program.

Upon completion of the F-80A longitudinal flight tests it was seen that the normal acceleration and pitching velocity responses were basically in agreement with what is predicted by rigid body and steady flow aerodynamic theory. Certainly there were discrepancies, but they were in no wise comparable to the results predicted in reference (2). On the other hand, a sizable discrepancy was noted between the predicted tail load and the measured horizontal tail load. Moreover, this difference appeared to be similar to the effect indicated in reference (1) i.e. a reduction of the peak response, which resulted from treating the downwash lag in an exact manner. The resolution of this problem - namely, to what extent does aeroelasticity and non-stationary flow influence the flight path and tail load response of the F-80A and to what extent are any or all of the observed discrepancies between measurement and prediction caused by these two phenomena - was of basic importance at this time. Unfortunately, the test program and data analysis had encountered a large number of delays; and time and money were not available to carefully examine the experimental results in light of the various theoretical predictions which had been made. Calculations were made to check the influence of unsteady flow effects on the horizontal tail load of the F-80A airplane, but the results of these calculations did not explain the apparent discrepancy between the measured tail loads and the theoretical predictions.

The study program, presented herein, was developed primarily in an attempt to resolve the overall situation described above. Since the analysis of the F-80A longitudinal data proved to be rather difficult and somewhat disappointing in certain respects, it was felt that a definite need existed for examining the state of the art. In this respect, it was believed that the study should be performed with a completely open mind as to the causes of any and all disagreements between measurement and theory. In a technical investigation, such as this, very often the obvious causes are overlooked in a search for more sophisticated answers. It was felt that this tendency should be avoided and that efforts should be made to establish that apparent discrepancies are real and valid.

In accordance with this philosophy, it is believed that any failure of theoretical predictions to agree with measurement is the result of one or more of the following three situations:

- (a) stability derivatives used in the theoretical calculations are not in sufficiently close agreement with actual derivatives;
- (b) experimental measurements are incorrect;
- (c) the assumption - that second order aerodynamic derivatives, unsteady flow effects, and structural flexibility are negligible for the F-80A - is not valid.

These items are listed in the order in which they should logically be eliminated as possible causes of the discrepancies in question. In practice, however, the process of elimination is not very orderly when the researcher finds himself groping in the dark. In the ensuing discussion, the results of this investigation are presented mainly in the order in which they were obtained, although there has been some regrouping for the purpose of presenting a more coherent argument.

The tail load discrepancy is examined first, followed by a calculation of the effects of aeroelasticity on the response of the F-80A airplane. This section is succeeded by a discussion of the factors which caused the observed disagreement between the estimated and measured response and conclusions are reached regarding the necessity of including unsteady flow and aeroelastic phenomena in the prediction of the F-80A longitudinal response. Finally, in the last and major part of the theoretical discussion, efforts are directed towards examining the discrepancies existing between predicted and measured derivatives and the reasons for same. Consideration is also given to means of improving and/or simplifying the extraction of stability derivatives from longitudinal response data.

EXAMINATION OF THE DISCREPANCY EXISTING  
BETWEEN PREDICTED AND MEASURED TAIL LOAD

As was indicated previously, the lack of agreement between the calculated and flight measured horizontal tail load was the particular discrepancy which was primarily responsible for questioning whether

- (a) there are significant aeroelastic effects on the F-80A airplane.
- (b) the lag in downwash at the tail is significantly different from the manner in which it is treated in writing the simplified equations of motion.

This discrepancy can be seen in figures 1 through 17, which have been taken from reference (3) for the purpose of supplementing this discussion. Note that at those values of frequency where peak response is predicted, the amplitude of the measured horizontal tail load lies well below the calculated curve whereas measured and predicted values of phase angle are generally in excellent agreement. Note also that the measured normal acceleration and pitching velocity responses are often in disagreement with the predicted response, especially at low frequencies. Since there is disagreement between the measured and predicted motion responses, there should be similar disagreement between the measured and predicted tail loads. This means that it is not relevant to compare observed tail loads with predicted loads, but rather they should be compared with the loads necessary to produce the observed responses of normal acceleration and pitching velocity.

The horizontal tail loads can, in fact, be written as a function of the normal acceleration and pitching velocity responses. The incremental change in tail angle of attack can be expressed as

$$\Delta\alpha_t = \frac{W}{U_0} \left(1 - \frac{d\epsilon}{d\alpha}\right) + \frac{d\epsilon}{d\alpha} \frac{\dot{w}}{U_0} \frac{l_t}{U_0} + \dot{\theta} \frac{l_t}{U_0} + \pi \delta \quad (1)$$

The normal acceleration is

$$n_z = \frac{2Z_w}{C_L} \left(\frac{w}{U_0}\right) + \frac{2Z\dot{\theta}}{C_L} \delta \quad (2)$$

On substituting (2) in (1),  $j\omega$  for  $\frac{d}{dt}$ , and dividing (1) by  $\delta$ , we obtain

$$\begin{aligned} \frac{\Delta \alpha_t}{\delta} = & \left(1 - \frac{dE}{d\alpha}\right) \frac{C_L}{2Z_w} \left(\frac{n_z}{\delta}\right)_{obs.} + \frac{2L_t}{C} \left(\frac{q_c}{U_0 \delta}\right)_{obs.} + \left(1 - \frac{dE}{d\alpha}\right) \frac{Z_\delta}{Z_w} + \pi \\ & + j \left\{ \omega \frac{L_t}{U_0} \frac{dE}{d\alpha} \frac{C_L}{2Z_w} \left(\frac{n_z}{\delta}\right)_{obs.} + \omega \frac{L_t}{U_0} \frac{dE}{d\alpha} \frac{Z_\delta}{Z_w} \right\} \end{aligned} \quad (3)$$

where the subscript "obs." designates the measured or observed value of the response. The tail load is then given by

$$C_{N_t}/\delta = \frac{dC_{N_t}}{d\alpha_t} \frac{\Delta \alpha_t}{\delta} \quad (4)$$

Examination of equations (3) and (4) indicates that the tail load can be calculated for each frequency test point using the appropriate experimental values for  $C_L$ ,  $n_z/\delta$ , and  $\frac{q_c}{U_0 \delta}$ . These computations do require, however, that numerical values be assumed for  $\frac{dE}{d\alpha}$ ,  $\pi$ ,  $dC_{N_t}/d\alpha_t$ ,  $Z_\delta$ , and  $Z_w$ . (A slightly different approach, using equation (1) directly, would require only the estimation of  $\frac{dE}{d\alpha}$ ,  $\pi$ , and  $dC_{N_t}/d\alpha_t$ .) For the computed results shown plotted in figures 18 through 21, wind tunnel values were used for all parameters except  $Z_w$ , which was assumed to be as obtained in the analyses performed in reference (3). This latter assumption was made in order to be conservative, in that a smaller  $Z_w$  produces a larger tail load. The real meaning of "conservative", as used here, will become evident later in the section devoted to means of extracting stability derivatives from flight data.

Figures 18 through 21 present the amplitude and phase of the horizontal tail as obtained experimentally and as computed by means of equations (3) and (4). It is seen that, while there is excellent agreement in phase angle, differences in computed and experimental amplitudes are significant and increase appreciably with increase in Mach number. It is also seen that the percentage difference between the computed and experimental amplitudes decreases with increasing frequency of oscillation, except at 0.3 Mach number where the

difference between experiment and calculation is relatively small.

This disagreement between the experimental tail load and that load which is indicated by the observed responses is in no way similar to the effect which was shown in reference (1) to be due to an exact treatment of the downwash lag. In fact this amplitude difference is so large at the high Mach numbers, that any attempt to seek a rigorous aerodynamical explanation appears to be somewhat ludicrous. In view of the excellent agreement in phase angle, one is inclined to conclude that incorrect measurement of the tail load is responsible for this unusual situation, wherein incorrect amplitude values are obtained with phase angles which are substantially correct. An error in static sensitivity would produce the reduced amplitude measurements, but this would not explain the observed variation in amplitude discrepancy with Mach number. On noting that the dimensional load, in pounds, increases with Mach number due to increased dynamic pressure, it appears that one possible explanation is a non-linear relationship between load and strain gage output. Another possible cause, though an uncertain factor, is the relieving of tail load caused by fuselage bending or other aeroelastic effects. This is amplified further in the following section where it is demonstrated that the responses of the F-80A are somewhat reduced by aeroelasticity. Since aeroelastic effects are a function of dynamic pressure, this phenomenon may possibly be a factor here. Admittedly this is a speculation, but in view of the fact that the phase angles agree at 0.75 Mach number while a 40 percent difference in amplitudes exists at low frequencies, it appears that a measurement error, in possible conjunction with aeroelastic effects, is the only means of explaining this result.

The variation in percent amplitude difference with frequency can be explained as a function of change in spanwise load distribution with frequency. For example, reference 3 points out that incremental loads inboard of station 10 on the horizontal stabilizer were not measured by the strain gage installation on the F-80A airplane. The area inboard of station 10 is 15.9 percent of the total horizontal tail area. If the assumption is made that the spanwise load distribution contributed by the elevator is measured in toto and that the measured loading, contributed by  $\theta$ ,  $\alpha$ , and  $\dot{\alpha}$ , is in error by sixteen percent, we obtain the result shown in figure 22. Note that little change in phase occurs but that a reduction in amplitude does result in a manner similar to that obtained in the F-80A flight tests. It then becomes feasible to explain the variation in amplitude discrepancy with frequency by a measurement error similar to that assumed above, since at the lower frequencies the greater portion of the tail load is contributed by  $\theta$ ,  $\alpha$ , and  $\dot{\alpha}$  while at the higher frequencies the tail load is due mainly to elevator deflection.

## AEROELASTIC EFFECTS

### ON THE RESPONSE OF THE F-80A AIRPLANE

While the F-80A flight test data fail to corroborate the large aeroelastic effects reported in reference (2), there is sufficient justification for a quantitative aeroelastic study to be made as a part of this overall investigation. Such a study would indicate the actual magnitude of the effects to be expected for a relatively stiff airplane. In addition, these data would serve to substantiate the observed responses in demonstrating that the F-80A airplane is not suitable as an aeroelastic research test vehicle.

In performing these aeroelastic calculations, the assumption was made (as was done in reference 2) that structural deflections of the wing would be negligible and that only fuselage bending, stabilizer, and elevator twist need be considered. Stabilizer and elevator twist were not properly included as additional degrees of freedom in the rigid body equations of motion, as was fuselage bending, because of the complexities involved. Rather the computed static reduction in elevator effectiveness (stabilizer twist was found to be negligible) was assumed to be valid over the entire frequency range since the dynamics of the elevator structure are far removed from the frequency range of interest. This assumption of constant effectiveness is substantially correct, if the major part of the loading that causes the elevator to twist is caused by elevator deflection, as is presumed to be the case. The method used in computing the reduced zero frequency value of elevator effectiveness is that described in reference (4). For the configuration selected for calculation purposes (Mach number: .6, Altitude: 10,000 feet), a seven percent static reduction in elevator effectiveness was found for the F-80A airplane.

In introducing the additional degree of freedom into the equations of motion for the purpose of representing a flexible fuselage, it was assumed that the fuselage bending was in phase with the aerodynamic and inertia forces. Stated differently, the dynamics of the fuselage structure were neglected since the fuselage bending modal frequency is presumably much higher than the rigid body frequency range under consideration. This simplifying assumption permits the direct formulation of the fuselage bending equation:

$$\ddot{\xi} = \frac{\partial \xi}{\partial N_t} \Delta N_t + \frac{\partial \xi}{\partial N_z} \Delta N_z + \frac{\partial \xi}{\partial \delta} \Delta \delta \quad (5)$$

where  $\xi$  is the fuselage bending angle measured as the change in angle of attack of the horizontal stabilizer.

$\frac{\partial \mathcal{E}}{\partial N_t}$  is the coefficient of fuselage bending due to horizontal tail load.

$\frac{\partial \mathcal{E}}{\partial n_z}$  is the coefficient of fuselage bending due to normal acceleration of the c.g.

$\frac{\partial \mathcal{E}}{\partial \ddot{\theta}}$  is the coefficient of fuselage bending due to pitching acceleration.

The coefficient of fuselage bending due to horizontal tail load was checked experimentally and found to agree exceedingly well with the value computed in reference (2). In view of this excellent agreement, a value for  $\frac{\partial \mathcal{E}}{\partial N_t}$

was also taken directly from this source. By working backwards from the bending moment curve due to fuselage dead weight, the fuselage weight distribution curve was found. It was then possible to compute the fuselage bending moment due to angular acceleration about the c.g. and subsequently determine the coefficient of fuselage bending due to pitching acceleration. The results obtained were as follows:

$$\frac{\partial \mathcal{E}}{\partial N_t} = 1.61 \times 10^{-6} \text{ rad./lb.}$$

$$\frac{\partial \mathcal{E}}{\partial n_z} = -1.21 \times 10^{-3} \text{ rad./g"}$$

$$\frac{\partial \mathcal{E}}{\partial \ddot{\theta}} = -4.25 \times 10^{-4} \text{ sec.}^2$$

Equation (5) can be written in terms of the variables  $\alpha$ ,  $D\theta$ ,  $\delta$ , and  $\mathcal{E}$  by noting that

$$N_t = g S_t \frac{dC_{N_t}}{d\alpha_t} \left\{ \left(1 - \frac{d\mathcal{E}}{d\alpha_t}\right) \alpha + \frac{h_t}{V_0} \dot{\theta} + \frac{d\mathcal{E}}{d\alpha_t} \frac{h_t}{V_0} \alpha + \frac{\partial \alpha_t}{\partial \delta} \delta + \mathcal{E} \right\} \quad (6)$$

and

$$n_z = \frac{2\gamma}{C_L} (\alpha - \dot{\theta}) \quad (7)$$

On substituting equations (6) and (7) into (5), we obtain

$$\xi = (aD + b)\alpha + (cD + e)D\theta + f\delta \quad (8)$$

where

$$a = \frac{\frac{\partial \xi}{\partial N_t} g S_t \frac{dC_{N_t}}{d\alpha_t}}{1 - \frac{\partial \xi}{\partial N_t} g S_t \frac{dC_{N_t}}{d\alpha_t}} \frac{\partial \xi}{\partial \alpha} \frac{h_t}{U_0} \frac{1}{\tau} + \frac{\frac{\partial \xi}{\partial N_t} \frac{p}{C_t}}{1 - \frac{\partial \xi}{\partial N_t} g S_t \frac{dC_{N_t}}{d\alpha_t}}$$

$$b = \frac{\frac{\partial \xi}{\partial N_t} g S_t \frac{dC_{N_t}}{d\alpha_t}}{1 - \frac{\partial \xi}{\partial N_t} g S_t \frac{dC_{N_t}}{d\alpha_t}} \left(1 - \frac{d\xi}{d\alpha}\right)$$

$$c = \frac{\frac{\partial \xi}{\partial \theta} \frac{1}{\tau^2}}{1 - \frac{\partial \xi}{\partial N_t} g S_t \frac{dC_{N_t}}{d\alpha_t}}$$

$$e = \frac{\frac{\partial \xi}{\partial N_t} g S_t \frac{dC_{N_t}}{d\alpha_t}}{1 - \frac{\partial \xi}{\partial N_t} g S_t \frac{dC_{N_t}}{d\alpha_t}} \frac{h_t}{U_0} \frac{1}{\tau} - \frac{\frac{\partial \xi}{\partial N_t} \frac{p}{C_t}}{1 - \frac{\partial \xi}{\partial N_t} g S_t \frac{dC_{N_t}}{d\alpha_t}}$$

$$f = \frac{\frac{\partial \xi}{\partial N_t} g S_t \frac{dC_{N_t}}{d\alpha_t}}{1 - \frac{\partial \xi}{\partial N_t} g S_t \frac{dC_{N_t}}{d\alpha_t}} \frac{\partial \alpha_t}{\partial \delta}$$

The longitudinal equations of motion, with the longitudinal (x) degree of freedom neglected then become:

$$\begin{bmatrix} (D - z_w) & -1 & -z_\xi \\ m(-Dm_{\dot{w}} - m_w) & (i_0 D - m_g) & -m m_\xi \\ -(aD + b) & -(cD + e) & 1 \end{bmatrix} \begin{bmatrix} \alpha \\ D\theta \\ \xi \end{bmatrix} = \begin{bmatrix} z_\delta \\ m m_\delta \\ f_\delta \end{bmatrix}$$

where

$$z_\xi = -\frac{1}{2} \frac{dC_L}{d\alpha}_t \frac{S_t}{S}$$

and

$$m_\xi = \frac{\partial C_m}{\partial i_t}$$

We find therefore, under the assumptions expressed in equation (5), that the order of this system of equations is still two. This is as was to be expected since the structural transfer function of the fuselage has been assumed to be unity, which assumption is believed to be in accordance with the facts. Use of the above equations of motion permit the comparison of responses obtained for both a rigid airplane and one possessing a flexible fuselage. Figures 23 through 25 present the amplitude and phase of the pitching velocity, normal acceleration and horizontal tail load responses of the F-80A for both an elastic and rigid body computation. Note that little or no difference in phase angle is obtained in the responses of the elastic and non-elastic airplane. The reduction in response amplitude appears to be similar to what would result from a straight reduction in elevator effectiveness. This is not actually the case, however, since the fuselage deflection response varies with frequency (see figure 26) and therefore the percentage reduction in response amplitudes does likewise. A plot of the percent change in amplitude caused by the combined effect of reduced elevator effectiveness and fuselage bending is presented in figure 27 for the three responses shown in figures 23 through 25. Since at steady state (zero frequency) a 7 percent reduction is caused by elevator twist, the remaining 9 percent reduction in the pitching velocity and normal acceleration responses is caused by fuselage flexibility.

Experience indicates that it would be extremely difficult to detect the above calculated aeroelastic effects in the results of an actual experimental flight program. The nature of the computed effect is such that for the F-80 airplane, aeroelasticity acts more like a scalar factor instead of a vector quantity. Moreover, the average value of this scalar factor falls into the region of prevailing prediction and measurement errors. A careful examination of the response plots presented in figures 1 through 17 fails to produce any positive verification of these computed aeroelastic effects.

CONSIDERATION OF MEANS OF IMPROVING THE AGREEMENT  
BETWEEN PREDICTED AND MEASURED LONGITUDINAL RESPONSES

An examination of the F-80A response plots presented in figures 1 through 17 indicates that the measured responses are representative of a second order dynamic system. On the basis of this visual comparison between calculation and experiment, it cannot be determined whether this system possesses constant derivatives or parameters which vary with the frequency of excitation. It is pointed out in reference (1) that the differences in response calculations obtained with the use of the simple and exact, complex equations of motion are so small, that the inaccuracies of using the time-lag concept of downwash are no greater than those of the original theoretical assumptions or the experimental data. Thus, comparison of response data is not a valid means for evaluating the effects of certain phenomena when these effects are as small or smaller than the errors which are introduced by faulty measurement or faulty prediction. This resulting inability to detect these effects in this manner does not say that they are not present, however. On the other hand, if one attempts to account for these phenomena in the analysis, which is performed to determine the stability derivatives, one finds that one must deal with a complicated system whose analysis is extremely difficult or perhaps impossible.

In the following section of this report consideration is given to the analysis part of the above-mentioned problem. As far as improved agreement between response prediction and measurement is concerned, it appears that major attention should be first directed towards increasing the accuracy with which the longitudinal short period natural frequency and damping are originally estimated. Certain of the F-80A response plots (particularly those for the 23 percent and 27 percent c.g. positions) indicate that the aerodynamic stiffness of the airplane is considerably different from what was originally predicted. If there are differences between the flight measured and predicted values of damping for the airplane, the response plots indicate that these differences are not as large or as significant as the discrepancies encountered between the measured and predicted values of stiffness or natural frequency.

The above observations point out the necessity for accurately determining the static stability or neutral point of the airplane when attempting to predict its longitudinal response. In the case of the F-80A, these predictions were based on wind tunnel data which were obtained from reference (5). The large variation in neutral point or  $dC_m/dC_L$  shown by the dashed line in figure 28 is the result of the non-linearity found to exist in the pitching moment data obtained from the wind tunnel tests. This non-linearity necessitated that the slope of the pitching moment curve be determined for the

particular lift coefficient and Mach number configuration at which it was intended to test the airplane in flight. It is seen that any deviation in airplane weight and resulting lift coefficient in flight from that selected for calculation purposes will automatically cause a small discrepancy in  $dC_m/dC_L$ . The non-linearity of these pitching moment curves, therefore, complicates the task of accurately predicting the flight neutral point. Examination of the wind tunnel data shows that this non-linearity is due entirely to the pitching moment characteristics of the model minus the horizontal tail. Since the contribution of the horizontal tail to the static stability, in conjunction with wind tunnel measured values of stabilizer effectiveness leads to wind tunnel values of downwash which are in excellent agreement with downwash theory, there is reason to believe that the tail-off static stability data is primarily responsible for the observed disagreement in predicted and measured stiffness.

This hypothesis is substantiated by the results obtained in static flight tests made with the F-80A. Reference (6) shows that the neutral point of the F-80A is significantly farther aft (at high lift coefficients) than what was indicated by the above-mentioned wind tunnel tests. This result intimates that the extreme non-linearity noted in the wind tunnel test data is in error and that the airplane is considerably more stable at high angles of attack than is shown by the dashed line in figure 28. Since it has been noted that knowledge of the static stability is critical for an accurate prediction of the longitudinal frequency response, it would seem advisable that static flight tests be made, whenever possible, to check wind tunnel results. These static tests would permit the accurate evaluation of the elevator power,  $M_s$ , in addition to the location of the neutral point. Admittedly, flight tests are not a convenient means of investigating the effects of Mach number, but in this particular instance, it is the variation of static stability with angle of attack that is questionable.

Note that static flight tests should be performed in the glide configuration, in order to prevent the direct thrust effects from contributing to the static stability. In constant speed flight, which is the case for the short period mode, the jet thrust does not contribute to the airplane's stability. It does, however, contribute to the static stability when the speed is allowed to vary. This is demonstrated quite readily by writing the moment coefficient due to the thrust acting at some vertical arm to the airplane's center of gravity.

$$C_m = \frac{T Z_t}{q S c} \quad (9)$$

where  $Z_t$  is the distance from the c.g. to the thrust line.

If the airplane is considered in unaccelerated flight (i.e.  $C_L$  varies with speed) the dynamic pressure,  $q$ , will be the following function of lift coefficient:

$$q = \frac{W/s}{C_L}$$

Equation (9) becomes

$$C_m = \frac{T z_t}{W c} C_L \quad (10)$$

For a constant throttle setting, the thrust,  $T$ , is nearly independent of airplane speed and can be considered a constant. The stability contribution can be obtained by differentiating (10) with respect to  $C_L$ .

$$\frac{dC_m}{dC_L}_{\text{thrust}} = \frac{T z_t}{W c}$$

Although the direct thrust effect is not a factor, a jet power plant does contribute to the dynamic longitudinal stability of an airplane. These contributions include (a) the direct normal force effects at the air duct inlet, (b) the effect of the induced flow at the tail due to the inflow to the jet blast, and (c) an increment in  $m_z$  as given by Braun in reference (7). The geometrical configuration of the F-80A airplane is such that the first two effects are found to be negligible. The damping effect of the jet stream is also quite small but it can be a significant portion of the damping due to the fuselage and the wing. Since the dimensional damping moment,  $\frac{\partial M}{\partial \delta}_{\text{jet}}$ ,

is approximately constant with airspeed, the non-dimensional derivative,  $m_z)_{\text{jet}}$ , is found to vary inversely with airspeed at a given altitude. For an altitude of 20,000 feet,  $M = 0.3$ , it was computed that

$$m_z)_{\text{jet}} = -.367$$

For the same conditions (based on wind tunnel data),

$$M_g)_{tail} = -7.0$$

These numerical results are presented for the purpose of indicating the relative magnitude of the damping caused by the jet stream. In order to predict the damping of the short period as accurately as possible, the derivative,  $M_g$ , should be carefully estimated by including all sources of damping such as the jet damping mentioned above.

In this discussion of means of improving the agreement between predicted and measured responses, it should be noted that the damping in pitch of the F-80A was assumed, for calculation purposes, to be caused only by the horizontal tail. In other words, the tail off damping in pitch was assumed to be zero. While this rough approach to the estimation of the derivatives may be considered oversimplified from the aerodynamicists' point of view, it can be justified engineering-wise since the response predictions were desired primarily for the purpose of instrumentation selection and to provide a check on flight measurements.

It is believed that the above discussion sufficiently emphasizes the point which was made earlier; namely - the errors introduced by the estimation of the first order aerodynamic terms are large enough to completely mask the effects of the second order terms, the unsteady flow effects, and the possible aeroelastic effects for the F-80A airplane. From the response prediction standpoint, consideration of these latter items for the F-80A airplane appears to be purely academic.

EXAMINATION OF AND MEANS FOR IMPROVING AND/OR SIMPLIFYING THE EXTRACTION  
OF STABILITY DERIVATIVES FROM LONGITUDINAL RESPONSE DATA

1. General Considerations.

Before proceeding to analyze response data obtained in flight it is necessary to assume equations of motion which adequately describe the dynamics of the system. Past experience has shown that linear, second order differential equations mathematically represent the short period longitudinal mode of a rigid airplane with excellent accuracy even when the limitation of infinitesimal displacements is violated. In this case, the assumption of linearity and the restriction to first order aerodynamic and inertia forces not only eases the prediction problem but simplifies greatly the problem of analysis, which has as its objective the extraction of stability derivatives from experimentally obtained flight data. Often there is some question whether these linear equations, containing a limited number of terms, are valid for certain aircraft configurations and flight conditions. This question is prompted by any analysis in which the experimental scatter is found to be large or the derivatives appear to vary with the frequency of oscillation. Disregarding for the moment the possibility of measurement error, it becomes incumbent upon the analyst to consider other phenomena which conceivably might influence the aircraft response. At this point, considerable engineering judgement must be exercised in selecting the additional complexities to be introduced into the equations of motion. If these additional complexities cause the problem to become non-linear, it may not be possible to perform an analysis at all. Finally, if the effects of these additional phenomena are small (as they certainly are for the F-80A) it will be very difficult to accurately extract the pertinent parameters describing these effects.

Since increasing the rigor with which the dynamical system is represented simultaneously increases the complexity of the analysis, it appears that it would be wise to use the simplest approach in the analysis unless there is substantial evidence that unsteady flow or aeroelastic effects, for example, are present to a significant degree. If this evidence or knowledge is present, we soon discover that sizable advancements must be made in the science of solving the reverse dynamics problem in order that these more complicated systems may be successfully analyzed. In this section of the report some consideration will be given to a possible means of performing an analysis of longitudinal response data when the equations of motion are written in terms of the complex downwash rather than the time lag concept. The method will be indicated, rather than applied, for reasons to be given later. Before examining the results obtained in the original F-80A analysis, consideration is given below to the peculiar problems encountered in the analysis of longitudinal response data.

## 2. Analysis Methods.

In this section, discussion will be confined to techniques of analyzing the short period longitudinal mode only, since the experimental flight data cover a frequency range of approximately 1 rad./sec. to 8 rad./sec. It will be assumed that the motion of the airplane is represented by linear differential equations.

### a. Operational Analysis Using Tail Load Data to Determine Basic Derivatives

Previous investigators have shown that extracting the constants, found in the operational (longitudinal) equations, from response data obtained in flight is a relatively straightforward task. These constants are the transfer function coefficients, such as  $b_o$  and  $K_o$  - the damping and stiffness parameters obtained from the characteristic or determinantal equations of the system. Stability analysts have also determined that, in the case of a heavily damped short period mode, the transfer function or operational constants cannot readily be obtained from transient response time histories of the system. They can, however, be extracted from frequency response data (obtained either from steady state oscillations or by harmonic analysis of transient responses) by means of various curve fitting techniques, either numerical or graphical. The graphical technique has evolved from the methods of the servomechanism engineer and proves to be practical when the system is only second order. Note that these transfer function parameters are combinations of the actual stability derivatives and as such do not indicate the basic aerodynamic characteristics of the airplane. In reference (3) an analysis procedure was developed whereby the tail load data could be used to break down the quantities,  $b_o$  and  $K_o$ , into their component derivatives.

On neglecting speed changes and non-stationary terms, it was assumed in the original F-80A analysis that the pertinent derivatives were as follows:

$$m_w, m_{\dot{w}}, m_q, m_s, z_w, z_s$$

Since

$$m_q = m_{q_1} + \frac{e h_t}{c} C_{m_{i_t}}$$

$$m_{\dot{w}} = e \frac{h_t}{c} C_{m_{i_t}} \frac{dE}{d\alpha}$$

$$m_w = m_{w_1} + C_{m_{i_t}} \left(1 - \frac{dE}{d\alpha}\right)$$

$$z_s = m_s / e \frac{h_t}{c}$$

where the subscript "1" denotes the tail-off derivative, it is evident that the basic quantities to be evaluated are  $m_s$ ,  $z_w$ ,  $m_{w_1}$ ,  $m_{z_1}$ ,  $C_{m_1}$ , and  $\frac{d\epsilon}{d\alpha}$ . The normal acceleration and pitching velocity responses were put into the following operational form for convenience of analysis.

$$\eta_{z/s} = -\frac{m_s}{C_L \frac{L_0}{c}} \left[ \frac{z_w \cos \phi}{b_0 \sin \Delta_1 \phi} \cos(\omega t + \phi + \Delta_1 \phi) + \sin \omega t \right] \quad (11)$$

where

$$\phi = \tan^{-1} \frac{K_0 - (\omega \tau)^2}{b_0 \omega \tau}$$

$$\Delta_1 \phi = \tan^{-1} \frac{\omega \tau L_0}{2 \mu L_0 / c}$$

and

$$\frac{g\epsilon}{2V_0/s} = \frac{m_s}{L_0 b_0 \cos \Delta_2 \phi} \sin(\omega t + \phi + \Delta_2 \phi) \quad (12)$$

where

$$\Delta_2 \phi = \tan^{-1} \left[ \frac{z_w}{\omega \tau} - \frac{m_{w_1}}{2 \omega \tau L_0 / c} \right]$$

Using the experimental values of  $L_0$ ,  $C_L$ ,  $\tau$ , and  $\mu$  and the measured amplitudes and phases of the acceleration and pitching responses, reference (3) presents an iterative procedure whereby the values of  $z_w$ ,  $b_0$ , and  $K_0$  are evaluated for each frequency test point. The elevator effectiveness,  $m_s$ , is determined from the slope of a straight line defined by points calculated at all test frequencies.

To evaluate the remaining unknowns, this procedure was repeated using similar expressions based on tail-off equations of motion. The derivation of these equations is given below and it is seen that the horizontal tail load must be measured in order to carry out this analysis. On writing the longitudinal equations of motion in terms of the aerodynamic forces contributed by the horizontal tail and the airplane minus the tail, we have

$$z_w \alpha + z_{\dot{\theta}}, D\theta = -z_{w_t} \alpha - z_{\dot{\theta}_t} D\theta - z_{\dot{w}} D\alpha - z_{\dot{\theta}} \delta + D\alpha - D\theta$$

$$\mu m_{w_1} \alpha + m_{\dot{\theta}_1} D\theta = -\mu m_{w_t} \alpha - m_{\dot{\theta}_t} D\theta - \mu m_{\dot{w}} D\alpha - \mu m_{\dot{\theta}} \delta + L_0 D^2 \theta$$

where the subscript "t" denotes the horizontal tail contribution.

Since

$$-z_{w_t} \alpha - z_{\dot{\theta}_t} D\theta - z_{\dot{\alpha}} D\alpha - z_{\delta} \delta = -\frac{\bar{V}}{2l_{tc}/c} C_{N_t}$$

and

$$-\mu m_{w_t} \alpha - m_{\dot{\theta}_t} D\theta - \mu m_{\dot{\alpha}} D\alpha - \mu m_{\delta} \delta = -\mu \bar{V} C_{N_t}$$

we obtain on neglecting  $z_{\delta}$ , the following two equations of motion in which the horizontal tail load is now the forcing function instead of the elevator.

$$z_{w_t} \alpha + D\theta - D\alpha = -\frac{\bar{V}}{2l_{tc}/c} C_{N_t} \quad (13)$$

$$\mu m_{w_t} \alpha + m_{\dot{\theta}_t} D\theta - l_B D^2\theta = -\mu \bar{V} C_{N_t} \quad (14)$$

The normal acceleration and pitching velocity responses to sinusoidal tail loads can be written, similarly to equations (11) and (12), as follows:

$$n_y/C_{N_t} = -\frac{\bar{V}}{C_L l_{tc}/c} \left[ \frac{z_{w_t} \cos \phi_1}{b_0 \sin \Delta_1 \phi} \cos(\omega t + \phi_1 + \Delta_1 \phi) + \sin \omega t \right]$$

where

$$\phi_1 = \tan^{-1} \frac{K_0 - (\omega \tau)^2}{b_0 \omega \tau} \quad (15)$$

$$\Delta_1 \phi = \tan^{-1} \frac{\omega \tau l_B}{2\mu l_{tc}/c}$$

$$\frac{q_c}{2U_0}/C_{N_t} = \frac{\bar{V}}{l_B b_0 \cos \Delta_2 \phi_1} \sin(\omega t + \phi_1 + \Delta_2 \phi_1) \quad (16)$$

where

$$\Delta_2 \phi_1 = \tan^{-1} \left[ \frac{Z_{w_1}}{\omega \tau} - \frac{m_{w_1}}{2 \omega \tau l/c} \right]$$

As indicated previously, use of the above equations, together with the measured responses and the quantities  $l_B$ ,  $l_c$ ,  $\tau$ , and  $\mu$ , permits the evaluation of  $Z_{w_1}$ ,  $b_0$ , and  $K_0$ , for each frequency test point. The tail-off derivatives,  $m_{q_1}$  and  $m_{w_1}$ , are then found from definitions of the tail-off damping and stiffness parameters. Finally, the last two unknown parameters,  $C_{m_{i+}}$  and  $\frac{d\epsilon}{d\alpha}$ , are obtained from a simultaneous solution of the following two equations:

$$b_0 = -Z_w - \frac{1}{l_B} \left( m_{q_1} + \frac{2l_c}{c} C_{m_{i+}} + \frac{2l_c}{c} C_{m_{i+}} \frac{d\epsilon}{d\alpha} \right) \quad (17)$$

$$K_0 = \frac{1}{l_B} \left\{ Z_w \left[ m_{q_1} + \frac{2l_c}{c} C_{m_{i+}} \right] - \mu \left[ m_{w_1} + C_{m_{i+}} \left( 1 - \frac{d\epsilon}{d\alpha} \right) \right] \right\} \quad (18)$$

Values of the derivatives as obtained by this method were plotted against the non-dimensional frequency,  $\omega \tau$ , and averaged arithmetically. It was believed that this point by point analysis adequately accounted for the variations in aircraft weight and velocity which occurred during the test runs.

#### b. Equation of Motion Analysis

In order to extract stability derivatives directly from response data obtained in flight, it becomes necessary to curve-fit the data on the basis of the original equations of motion. Unfortunately, the longitudinal equations are such that a linear dependency exists between the variables of motion which, in the reverse dynamics problem, are the coefficients of the unknown derivatives.

Mathematically this means that a unique set of values for the derivatives cannot be obtained since the determinant of the coefficients (in this case, the variables of motion) proves to be zero. This is readily demonstrated by writing the equations of motion in a form adaptable to their inverse solution for the unknown derivatives, viz:

$$\begin{bmatrix} \alpha & \delta & D\theta & D\alpha \end{bmatrix}_i \begin{bmatrix} z_w \\ z_\delta \\ z_\theta \\ z_{\dot{w}} \end{bmatrix} = \begin{bmatrix} \frac{z^T}{U_0} \eta_z \end{bmatrix}_i$$

$$\begin{bmatrix} \alpha & \delta & D\theta & D\alpha \end{bmatrix}_i \begin{bmatrix} \mu m_w \\ \mu m_\delta \\ m_\theta \\ \mu m_{\dot{w}} \end{bmatrix} = \begin{bmatrix} i_\theta D^2\theta \end{bmatrix}_i$$

The subscript "i" varies from 1 to  $n$  where  $n$  is equal to the total number of unknowns. (In this case, four.) It is seen that, in the inverse solution, the coefficients of the unknowns are the four variables of motion  $\alpha$ ,  $\delta$ ,  $D\theta$ , and  $D\alpha$ . Since

$$\frac{z^T}{U_0} \eta_z = D\alpha - D\theta$$

we find that

$$z_w \alpha + z_\delta \delta + (z_\theta + 1) D\theta + (z_{\dot{w}} - 1) D\alpha = 0$$

which expression illustrates the linear dependency existing between the four quantities ( $\alpha$ ,  $\delta$ ,  $D\alpha$ ,  $D\theta$ ). It can then be shown that

$$\begin{vmatrix} \alpha_1 & \delta_1 & D\theta_1 & D\alpha_1 \\ \vdots & \vdots & \vdots & \vdots \\ \alpha_n & \delta_n & D\theta_n & D\alpha_n \end{vmatrix} = 0$$

In reference (8), Schumacher suggests that the linear dependency be removed from the longitudinal equations of motion by making the following substitutions for  $m_{\dot{w}}$  and  $z_{\dot{w}}$ .

$$m_{\dot{w}} \cong \frac{dE}{d\alpha} m_g \frac{1}{u}$$

$$z_{\dot{w}} = \frac{dE}{d\alpha} z_g$$

Note that this is an approximation which assumes that the tail-off damping in pitch is zero, since accurately expressed within the limitations of the time lag concept of downwash

$$m_{\dot{w}} = \frac{dE}{d\alpha} m_{g_t} \frac{1}{u}$$

With the approximate expression for  $m_{\dot{w}}$ , the longitudinal equations of motion (in the form suitable for their inverse solution) are reduced to three unknowns and three linearly independent coefficients, viz;

$$\begin{bmatrix} \alpha & \delta & (D\theta + \frac{dE}{d\alpha} D\alpha) \end{bmatrix}_i \begin{bmatrix} z_w \\ z_\delta \\ z_g \end{bmatrix} = \left[ \frac{g}{V_0} m_g \right]_i \quad (19)$$

$$\begin{bmatrix} \alpha & \delta & (D\theta + \frac{dE}{d\alpha} D\alpha) \end{bmatrix}_i \begin{bmatrix} \mu m_w \\ \mu m_s \\ m_g \end{bmatrix} = \begin{bmatrix} i_B D^2 \theta \end{bmatrix}_i \quad (20)$$

If the tail-off damping in pitch is not assumed to be zero, the above equations can be written more accurately as

$$\begin{bmatrix} \alpha & \delta & D\theta & (D\theta + \frac{dE}{d\alpha} D\alpha) \end{bmatrix}_i \begin{bmatrix} z_w \\ z_\delta \\ z_{g_1} \\ z_{g_2} \end{bmatrix} = \begin{bmatrix} \frac{g_T}{U_0} m_g \end{bmatrix}_i \quad (21)$$

$$\begin{bmatrix} \alpha & \delta & D\theta & (D\theta + \frac{dE}{d\alpha} D\alpha) \end{bmatrix}_i \begin{bmatrix} \mu m_w \\ \mu m_s \\ m_{g_1} \\ m_{g_2} \end{bmatrix} = \begin{bmatrix} i_B D^2 \theta \end{bmatrix}_i \quad (22)$$

In this case there are four linearly independent coefficients, namely:

$$\alpha, \delta, D\theta, \text{ and } D\theta + \frac{dE}{d\alpha} D\alpha$$

Note that the subscript "i" indicates that one substitutes values for the coefficients obtained at different time intervals, if he is dealing with transient data, or values obtained at discrete intervals of frequency, if he is working with frequency response data. In the latter case, each coefficient is a vector or complex quantity and must be treated as such when normalizing the equations written for a large number of frequency points to yield the same number of equations as there are unknowns. In reference (8), Schumacher chooses the method of least squares to average the data. This normalization procedure is indicated in matrix notation, as follows:

$$\sum_{i=1}^{i=N} \begin{bmatrix} \alpha \\ \delta \\ D\theta \\ D\theta + \frac{d\epsilon}{d\alpha} D\alpha \end{bmatrix}_i \begin{bmatrix} \alpha & \delta & D\theta & (D\theta + \frac{d\epsilon}{d\alpha} D\alpha) \end{bmatrix}_i = \sum_{i=1}^{i=N} \begin{bmatrix} \alpha \\ \delta \\ D\theta \\ D\theta + \frac{d\epsilon}{d\alpha} D\alpha \end{bmatrix}_i \begin{bmatrix} \quad \quad \quad \quad \end{bmatrix}_i$$

$N$  = total number of test points

Solutions of equations (19) through (22) by the above-indicated procedure yields values of  $\theta$  derivatives which are associated with the artificially created motion variable,  $D\theta + \frac{d\epsilon}{d\alpha} D\alpha$ . These derivatives will be

slightly in error when the assumption is made that the tail-off contribution to the pitching velocity derivatives is zero. The accuracy of these derivatives is also a function of the assumed values of  $\frac{d\epsilon}{d\alpha}$ , but Schumacher feels that

the effect of inaccuracies in the assumed values of  $\frac{d\epsilon}{d\alpha}$  should be minor. Both

the analysis method presented in reference (8) and the modification suggested above have been applied to some of the F-80A flight data in an effort to explain some of the discrepancies which are found to exist between the estimated and measured derivatives. The significant results are presented in the following section.

### 3. Examination of Discrepancies Between Measured and Predicted Derivatives - F-80A Airplane.

Figures 28 and 29 present a comparison between the estimated derivatives (based on wind tunnel data) and the measured derivatives as determined from the flight test data by the analysis method which makes use of tail load measurements. Figure 30 shows estimated and flight test determined values of the damping and stiffness parameters,  $b_0$  and  $K_0$ . These curves represent only one altitude and C.G. configuration of the total flight configurations represented by figures 1 through 17. They are, however, more than sufficient to indicate that significant differences exist between prediction and flight test results.

Examination of figure 30 shows that the flight measured values of the stiffness and damping of the airplane are greater than that predicted, with the measured values of  $K_0$  being drastically larger, especially at 0.3 Mach number. This discrepancy in stiffness is likewise reflected in figure 28, where the static stability,  $dC_m/dC_L$  is shown plotted versus Mach number.

The fact that the airplane is more stable than what was indicated in the wind tunnel tests is not the major cause for concern. What is disturbing, however, is that figures 28 and 29 indicate that this increase in stability is caused primarily by an increase in stabilizer effectiveness. This increase is of the order of 25 to 35 percent greater than those values of  $C_{m_{it}}$  yielded by the

wind tunnel tests reported in reference (5). Investigation showed that the value of the tail lift curve slope, corresponding to these values of stabilizer effectiveness, would be aerodynamically impossible to achieve even if the tail efficiency were assumed to be one hundred percent.

Further examination of figure 29 indicates that the measured elevator effectiveness,  $M_{\delta}$ , is correspondingly higher than the value obtained in the wind tunnel. The lift curve slope obtained from flight data is approximately 7.5 percent less than the estimated value, while the slope of the downwash appears to be unreasonably high. Since  $M_{\delta}$  and  $M_{\dot{\alpha}}$  were computed from the flight measured values of  $C_{m_{it}}$  and  $\frac{dC_L}{d\alpha}$ , these derivatives are likewise larger than the original prediction.

In order to check these discrepancies, efforts were first directed towards an examination of the tail-on analysis, which as indicated above yields values of  $b_0$ ,  $K_0$ ,  $M_{\delta}$ , and  $Z_w$ . The possible effects of measurement errors as they would influence results of this analysis were considered in this phase of the investigation. These studies indicated that errors in static sensitivity (for a particular recording channel) would affect only the evaluation of the derivatives  $M_{\delta}$  and  $Z_w$ . Examination of equation (11) reveals that the transfer function constants,  $b_0$  and  $K_0$ , are a function only of the phase angle,  $\phi$ . Further studies indicated that, whereas reference (3) proposes

an iterative procedure for determining  $\phi$  after first assuming a value of  $m$ , the angle,  $\phi$ , can be expressed empirically with excellent accuracy as

$$\phi \cong \varphi_{n\gamma/\delta} + \Delta \phi + 90^\circ \quad (23)$$

This empirical relation shows that the stiffness and damping parameters,  $K_0$  and  $b_0$ , can be established with the measurement of only one variable, which proves to be the phase angle,  $\varphi_{n\gamma/\delta}$ . If aircraft weight and velocity is held reasonably constant, it becomes exceptionally convenient to find  $b_0$  and  $K_0$  from the following rearrangement of the equation defining the angle,  $\phi$ :

$$\omega r \tan \phi = \frac{-(\omega r)^2}{b_0} + \frac{K_0}{b_0} \quad (24)$$

It is believed that the normal acceleration response, both amplitude and phase, was determined with good accuracy, and therefore it is possible to check the previously obtained values of  $b_0$  and  $K_0$  in a reliable manner without resort to the pitching velocity measurements in any way.

In the actual analysis performed in reference (3), the parameters,  $b_0$  and  $K_0$ , were calculated for each frequency test point in order to allow for the variation in aircraft weight and velocity. Examination of the results showed that the scatter in the values of  $b_0$  and  $K_0$  was considerably larger than the variation in speed and weight encountered in flight. The experimental scatter is seen to be a function of the accuracy of phase angle measurement. This result serves to emphasize the point that phase angle measurements are as important or even more important than amplitude measurements. The resultant scatter in  $b_0$  and  $K_0$  was likewise reflected throughout the remainder of the analysis, since these two parameters are basic to the calculation of the rest of the derivatives. Subsequent computations based on equations (23) and (24) proved that, regardless of the scatter with frequency, the originally determined values of  $b_0$  and  $K_0$  are substantially correct.

During this study, it was found that a mechanical harmonic analyzer could be used to significantly improve the accuracy with which amplitude ratios and phase angles are measured on the oscillograph records. If low frequency harmonic distortion is present in the record, it was formerly necessary to

fair a sine wave through the trace. Fairing was similarly required when a certain amount of high frequency noise was encountered in the oscillation data. This fairing was done by eye and necessarily introduced certain errors into the data. By using a harmonic analyzer to select the fundamental frequency of the input and output trace, an accurate amplitude ratio and phase angle can be obtained and the necessity for arbitrary fairing procedures is thereby eliminated.

It should be pointed out that the pitch rate gyro used in the F-80A longitudinal flight test produced an output trace whose wave form was appreciably distorted with additional harmonics and at times with high frequency hash as well. These performance characteristics made it very difficult to obtain a consistent calibration of the pitch rate channel and accordingly the accuracy of the pitching velocity measurements must be considered somewhat questionable. Indication that there was a consistent error in the pitching velocity phase angle measurement is given by figure 31 where  $\Delta_2 \phi$  is shown plotted versus the non-dimensional frequency,  $\omega \tau$ . From equation (12), we note that

$$\Delta_2 \phi = \tan^{-1} \left[ \frac{Z_w}{\omega \tau} - \frac{m_w}{2 \omega \tau l/c} \right]$$

Hence,

$$Z_w = \omega \tau \tan \Delta_2 \phi + \frac{m_w}{2 l/c}$$

Since  $Z_w$  and  $m_w/2 l/c$  are constants, the term  $\omega \tau \tan \Delta_2 \phi$  should be constant with frequency. The points shown on figure 31 are representative of the results obtained at other Mach numbers and indicate a consistent trend which is probably caused by a small phase error in the dynamic calibration of the pitch rate channel. Numerical studies indicated that static sensitivity errors in the pitch rate measurement would produce opposite effects on the extraction of the derivatives,  $m_s$  and  $Z_w$ . For example, if the pitch rate were assumed to be 20 percent greater than the correct theoretical value, an approximate 16 percent decrease in  $Z_w$  and 24 percent increase in  $m_s$ , would be obtained in the reduction to derivative form. Note that the F-80A analysis did produce results for  $Z_w$  and  $m_s$  which possess this qualitative trend with respect to the wind tunnel evaluation of these parameters. In any event, this investigation was somewhat over-simplified since the response of the pitch rate channel was not perfectly flat over the frequency range covered in the flight tests.

A recapitulation is now in order. The flight measured value of static stability is in drastic disagreement with the wind tunnel results, with the flight value being approximately one hundred percent greater at 0.3 Mach number.

Since the original F-80A analysis showed the tail-off static stability to be in substantial agreement with prediction, the increase in stability was explained by a stabilizer effectiveness which was considerably larger than the effectiveness obtained in the wind tunnel. Aerodynamic theory, however, refuses to acknowledge the possible existence of these unusually large values of  $C_{m_{\dot{\alpha}}}$  and therefore the flight measured parameters shown on figures 28 and 29 should be regarded as extremely questionable. The only other possible explanation for the flight observed values of stiffness is that (contrary to the original analysis) the tail-off static stability is different from that measured in the wind tunnel. Further examination of the problem proved that this was the case.

The method of evaluating the tail-off derivatives using the responses to a tail load input, was outlined in the previous section. In the original analysis performed in reference (3), an attempt was made to correct for the apparent errors in the tail load measurements, but in view of the results that have been obtained in this investigation, it is believed that the derived correction procedure was inadequate for the proposed task. No attempt was made in this study to duplicate the original techniques developed for analyzing the responses to tail loads. Instead the equation of motion method has been used, since it gives a better physical insight into the problem.

Schumacher's curve-fitting technique (i.e. equations of motion method) was first applied to the F-80A response data to determine whether agreement would be obtained between the two analysis methods. Computations were made on the basis of three variables and also on the basis of four variables, in the hope that the tail-off damping in pitch could be determined. The necessary calculations showed that  $M_{\dot{\alpha}}$  could not be extracted from the response data because it was obtained as a small difference of two large quantities. Values were obtained for  $z_w$ ,  $m_{\dot{\alpha}}$  and  $M_w$ , in the three variable solution, which agree exceedingly well with the results obtained previously. These computed results are shown plotted on figures 28 and 29 for 0.3 and 0.7 Mach number. The damping in pitch,  $M_{\dot{\alpha}}$ , was found to be quite large in this three variable solution, but in view of the assumption that  $M_{\dot{\alpha}} = M_{\dot{\alpha}^*}$ , it is believed that some error is introduced into the determination of this quantity. The derivative,  $M_{\dot{\alpha}}$ , is also plotted on figure 28.

Note that this equation of motion analysis can also be applied to the tail-off equations of motion as given by equations (13) and (14). In this case, values of  $M_w$ ,  $m_{\dot{\alpha}}$ , and  $z_w$ , could be determined without the necessity of assuming a value for  $d\epsilon/d\alpha$ , since  $D\alpha$  is not a variable and no linear dependency is present. This analysis scheme was first tried with theoretical data in which the tail-off damping in pitch was assumed to be zero. Again it was found that  $M_{\dot{\alpha}}$  is a small difference term and even when using supposedly perfect data a value of  $M_{\dot{\alpha}} = -1.54$  was obtained. This result re-emphasizes the difficulty with which  $M_{\dot{\alpha}}$  is to be extracted from flight data. The tail-off static stability, however, is obtained very conveniently by this method and

of course will possess the same accuracy as that inherent in the tail measurements. On examination of equation (14) it is seen that for a given total static stability, an increase in tail load (meaning an increased stability contribution from the tail) will result in larger values of negative (unstable) static stability being obtained for the tail-off airplane. Since the analysis performed in reference (3) produced an extremely large value for the slope of the tail lift curve, measured tail loads should have been correspondingly higher than the theoretical prediction. Just the opposite was found, however. It therefore becomes necessary to show that, when using the measured tail load data or a calculated load based on the actual airplane responses, it is impossible to justify the large positive values of  $M_w$ , obtained at  $M = 0.3$  in the original analysis.

In performing the tail-off equation of motion analysis, the tail loads computed in examining discrepancies between predicted and measured tail load have been utilized. These tail loads were based on the measured values of  $C_L$ , normal acceleration and pitching velocity. It was necessary, however, to assume values for  $dC_{L_t}/d\alpha$ ,  $dE/d\alpha$ , and  $z_w$ . It will be recalled that

wind tunnel values were used for the first two parameters and a flight measured value for  $z_w$ . On this basis the horizontal tail load was calculated for all Mach numbers at the 20,000 feet, 27 percent C.G. flight configuration. Using the tail load computed for 0.3 Mach number (as presented in figure 18)  $M_w$  was found to equal 0.411 or  $\frac{dC_m}{dC_{L_t}} = 0.0853$ . This value of tail-off static

stability is shown plotted on figure 28. Note that the difference between this point and the estimated tail-off stability is approximately equal to the total increase in stability exhibited by the airplane in flight over that indicated by the wind tunnel. At a Mach number of 0.7, using the computed tail load shown in figure 20, a value of  $M_w = 0.5061$  or  $\frac{dC_m}{dC_{L_t}} = 0.084$  was obtained.

This numerical value is in agreement with that previously determined, but again we note that an increase in stability is accompanied by a similar decrease in the instability of the tail-off configuration. In summary, it is seen that the static stability contribution of the tail now varies with Mach number in a reasonable manner. Furthermore, the magnitude of  $\frac{dC_m}{dC_{L_t}}$  is in substantial agreement with wind tunnel results.

The breakdown of  $\frac{dC_m}{dC_{L_t}}$  into values of  $C_{m_{it}}$  and  $\frac{dE}{d\alpha}$  is the final step required in the analysis. Since

$$\frac{dC_m}{d\alpha} = \left(1 - \frac{dE}{d\alpha}\right) C_{m_{it}}$$

we see that the large value of  $C_{mit}$  obtained in the original analysis, at 0.7 Mach number for example, is counteracted by a large value of  $\frac{d\epsilon}{d\alpha}$ . It is apparent that the results shown in figure 29 for  $C_{mit}$  and  $\frac{d\epsilon}{d\alpha}$  are in error. Given values of the transfer function constants,  $b_o$  and  $K_o$ , it can be demonstrated that  $M_{w_1}$  and  $M_{g_1}$  must be known before  $C_{mit}$  and  $\frac{d\epsilon}{d\alpha}$  can be correctly evaluated. On solving the two equations (17) and (18), it is found that

$$C_{mit} = \frac{i_o K_o + \mu M_{w_1} - \gamma_w M_{g_1} + \frac{\mu(i_o b_o + \gamma_w i_o + M_{g_1})}{2 h/c}}{2(\frac{h}{c} \gamma_w - \mu)}$$

The above expression can be simplified without any significant loss in accuracy to the following:

$$C_{mit} \approx \frac{i_o K_o}{2\mu} - \frac{i_o(b_o + \gamma_w)}{4 h/c} - \frac{M_{w_1}}{2} - \frac{M_{g_1}}{4 h/c}$$

On inserting typical numerical values, we find that the two terms on the extreme right are very important. In the original analysis,  $M_{w_1}$  was generally too large (positive) and  $M_{g_1}$  was assumed to be zero. Both factors caused the solution of this equation to yield values for  $C_{mit}$  which were too large. In the equation for  $\frac{d\epsilon}{d\alpha}$ , viz.

$$\frac{d\epsilon}{d\alpha} = - \left[ 1 + \frac{i_o b_o + \gamma_w i_o + M_{g_1}}{2 h/c C_{mit}} \right]$$

it can likewise be shown that  $M_{g_1}$  is far from being a negligible quantity. Values for  $C_{mit}$  and  $\frac{d\epsilon}{d\alpha}$  can also be obtained from a solution of the

below two expressions for  $M_{g_1}$  and  $M_{w_1}$ :

$$M_{q_t} = 2 \frac{h_t}{c} C_{m_t}$$

$$M_{w_t} = (1 - \frac{dE}{d\alpha}) C_{m_t}$$

where

$$M_{q_t} = M_q - M_{q_1}$$

and

$$M_{w_t} = M_w - M_{w_1}$$

Again it is seen that the tail-off derivatives must be known in order to accurately compute the magnitude of  $C_{m_t}$  and  $\frac{dE}{d\alpha}$ . Unfortunately, the

extraction of  $M_q$  from flight data does not appear to be feasible with presently available techniques. No serious attempts have been made to completely re-analyze the flight data presented in reference (3), since the required accurate tail load data are not available. For the purpose of this study, it was deemed sufficient to establish the causes of the subject discrepancies and to indicate methods for their removal rather than present a revised numerical analysis of the F-80 flight data.

#### 4. An Equation of Motion Analysis Incorporating a Complex Downwash.

Statler demonstrated, in reference (1), that a computed response will be essentially the same if either all the derivatives are treated as frequency dependent or just the downwash is assumed to be frequency dependent. The net result is such that the complex downwash appears to cause more damping than what would be predicted by steady flow theory. Computations made in Appendix C of reference (3) indicates that the frequency dependent damping constant,  $b_m$ , is generally higher than the steady flow value of  $b_0$ . This is particularly true at higher Mach numbers. Therefore, if there is any evidence to show that the complex downwash does affect the response in accordance with the theory present in reference (1), it should be noted as increased damping over and above that which would be predicted by the simple theory. Values of  $b_0$ ,

based on a linear analysis of the F-80A flight data, strongly indicate that this evidence exists. Examination of figure 30 shows that the measured damping is significantly higher than prediction, even when allowance is made for the tail-off damping which was neglected in the original calculations.

On the basis of this evidence, let us assume that the aircraft's dynamics are more accurately represented by equations of motion containing the complex form of downwash rather than the time lag concept. What are the implications of analyzing such a system as if it were non-complex? Presumably, values would be obtained for  $b_o$  and  $K_o$  which would be an average of the actual variation with frequency. The damping parameter,  $b_o$ , would then be larger than is normally defined by "steady flow" derivatives. Accordingly, we should expect that the experimentally determined lift curve slope of the tail will be greater than that indicated by the wind tunnel for steady flow conditions. This result, of course, will affect the experimental determination of all the basic aerodynamic parameters. Based on the data which have been examined in this study, it is believed that the above situation actually exists and has influenced to an uncertain degree the analysis of the F-80A flight measured responses.

If we use a theory which consists of all derivatives constant with frequency except  $m_w$  (a complex  $d\epsilon/d\alpha$ ) and which is devoid of the so-called "time lag" term,  $m_w''$ , it appears that an approximate analysis technique may be developed which will handle the introduced complex term. In accordance with these assumptions, the longitudinal moment equation becomes

$$\mu [m_w' + i m_w''] \alpha + (m_z - i c_D) D \theta = -\mu m_{\delta} \delta \quad (25)$$

where  $m_w'$  is the real part of  $m_w$

and  $m_w''$  is the imaginary part of  $m_w$

Figure 32 presents a plot of  $m_w'$  and  $m_w''$  as a function of the reduced frequency,  $\frac{\omega c}{2U_o}$ . These data were obtained from reference (1). If the

variation in  $m_w'$  is assumed to be linear with frequency and the curve of  $m_w''$  is assumed to be of parabolic form, we may write

$$m_w' = A + B \frac{\omega c}{2U_o}$$

and

$$m_w'' = C \frac{\omega c}{2U_o} + E \left( \frac{\omega c}{2U_o} \right)^2$$

Substituting the above into equation (25) we obtain:

$$(\mu A + B\omega\tau)\alpha + (C + E\frac{\omega\epsilon}{2U_0})D\alpha + (m_g - i\epsilon D)D\theta = -\mu M_g\delta$$

Since the frequency,  $\omega$ , appears in the coefficients of the variables, it should be possible to obtain a unique solution for the unknowns  $A$ ,  $B$ ,  $C$ ,  $E$ ,  $M_g$ , and  $M_w$ , using Schumacher's equation of motion approach. Theoretically this method permits an approximate determination of a complex  $M_w$  by means of the constants  $A$ ,  $B$ ,  $C$ , and  $E$ . Practically, it may be found that the constants  $B$  and  $E$  may be subject to the "small difference difficulty". It is seen that if we must assume  $B$  and  $E$  equal to zero, we again have the equivalent of the simple system with a time lag downwash term, where

$$A = M_w$$

and

$$C = \mu M_w$$

No efforts have been expended to apply this proposed analysis scheme, since it was felt that the available time should be spent on the pitfalls and weaknesses of the analysis of a non-complex linear system. The above analysis method is presented, primarily, to indicate the nature of the simplifications required to transform the complex  $M_w$  derivative into derivatives which are independent of frequency.

## COMMENTS ON FUTURE AEROELASTIC RESEARCH

The subject of aeroelasticity can logically be divided into three separate topics. The first of these might properly be called "static" aeroelastic effects and would include such items as loss and reversal of aileron control, wing and wing-aileron divergence, loss and reversal of elevator control, and stabilizer-elevator divergence, and the less spectacular but sometimes important effects of deflection on various derivatives. These phenomena may be observed on stiff as well as elastic aircraft and are primarily functions of the dynamic pressure or the aerodynamic loading. The second topic is the well known phenomenon called "flutter" which results from the dynamic coupling existing between the unsteady aerodynamic forces and the combined structural bending and torsion modes of an aerodynamic surface or control. This phenomenon is a function of true airspeed and the natural frequency of the structural flutter mode and generally occurs at frequencies far above the natural frequency of the aircraft's rigid body motions. The third topic consists of the relatively newer phenomenon in which the structural dynamics have been observed to significantly affect the rigid body response of the airplane. This aeroelastic effect is a function of the natural frequencies of the aircraft structure and increases in magnitude as these frequencies approach those of the aircraft rigid body response.

Although the influence of aeroelasticity on the dynamics of the F-80A was quantitatively investigated, it should be realized that this configuration does not provide an example of the third named aeroelastic effect in which structural motions are found to couple dynamically with the motion of the airplane's center of gravity. Since the F-80A is a structurally stiff airplane, it is seen that aeroelastic effects are essentially scalar rather than dynamic. Note, also, that the structural motion (fuselage bending) is very small as is indicated by figure 26. These considerations lend weight to the argument that the F-80 airplane is not a suitable aeroelastic research test vehicle.

As aircraft continue to become larger and more flexible, coupling between the structural and rigid body modes will naturally become more pronounced. This trend has already been dramatically demonstrated by difficulties encountered in present day aircraft in which structural modes have coupled with various types of automatic control systems. The problem then arises of being able to theoretically predict the response of the flexible airplane which has a large number of structural degrees of freedom. This situation is further complicated by the introduction of the swept wing since wing bending then produces changes in the span-wise load distribution. These facts would indicate that the demonstration of the feasibility of accurately predicting the response of an "aeroelastic" airplane is certainly in order. Such a demonstration should certainly involve the full scale flight tests of a truly aeroelastic aircraft.

## CONCLUSIONS AND RECOMMENDATIONS

On completion of the study described herein, it has been concluded that:

1. Whereas the determination of the short period longitudinal stiffness and damping parameters from dynamic flight data is a straightforward task, all of the basic aerodynamic quantities cannot be determined (including  $dc/d\alpha$  and  $C_{m_{\dot{\alpha}}}$ ) unless means are available for determining the tail-off static stability and damping in pitch.
2. The tail load discrepancy observed in reference (3) is, to a large degree, due to an error in measurement due to limitations in possible strain gage locations.
3. The effects of fuselage bending and elevator twist on the response of the F-80A are predominantly scalar and therefore difficult to perceive in the experimental measurements.
4. The lack of agreement, shown in reference (3), between predicted and measured responses at low Mach numbers is due to prediction being based on a wind tunnel evaluation of tail-off static stability which is different from that obtained in flight.
5. From the response prediction standpoint, the errors introduced by the estimation of the first order aerodynamic derivatives are large enough to completely mask the effects of the second order terms, the unsteady flow effects, and the possible aeroelastic effects for the F-80A airplane.
6. The numerical results obtained in the original F-80A analysis for stabilizer effectiveness and slope of the downwash are in error due to incorrect values of tail-off static stability and tail-off damping in pitch being used in the analysis.
7. There is evidence that the measured damping of the F-80A airplane is significantly higher than what would be predicted by linear theory, giving indication that the complex downwash does effect the response in accordance with the calculations made in reference (1).
8. The most significant dynamic aeroelastic problem at this time is the increasing coupling between structural, automatic control system, and rigid body modes resulting from present day aircraft design trends toward more flexible aircraft.
9. The F-80A airplane is not a suitable airplane for examining dynamic aeroelastic effects.

Additional or secondary conclusions may be stated as follows:

10. Since careful estimation of the static stability is necessary for accurate prediction of the longitudinal response, it would seem advisable that static flight tests be made to verify wind tunnel results.

11. In the analysis of tail-on longitudinal response data, the damping and spring constants,  $b_o$  and  $K_o$ , are defined by the measured phase angle,  $\phi_{12/18}$ . A static sensitivity error in the elevator, pitching velocity, and normal acceleration traces, therefore, affects only the extraction of the derivatives,  $\dot{z}_w$  and  $\dot{m}_\delta$ .

12. A mechanical harmonic analyzer can be used to significantly improve the accuracy with which amplitude ratios and phase angles can be measured from sinusoidal oscillation data in which a disturbing amount of harmonic distortion is present.

13. It does not appear possible to extract the tail-off damping in pitch,  $\dot{m}_\delta$ , from longitudinal response data with any of the analysis techniques tried to date.

The investigation reported on herein, together with the above-stated conclusions, has led to the following recommendations.

1. Further studies should be made to develop methods which would simplify and expedite the measurement of horizontal tail loads. These studies should be accompanied by the development of additional analytical techniques for determining the tail-off stability derivatives.

2. Efforts should also be directed toward analyzing longitudinal response data on the basis of equations of motion consisting of all derivatives constant with frequency except  $\dot{m}_w$  (a complex  $dE/da$ ) and which are devoid of the so-called "time lag" term,  $\dot{m}_w$ .

3. The feasibility of accurately predicting the response of an aeroelastic airplane should be demonstrated by means of full scale flight tests with a truly aeroelastic aircraft.

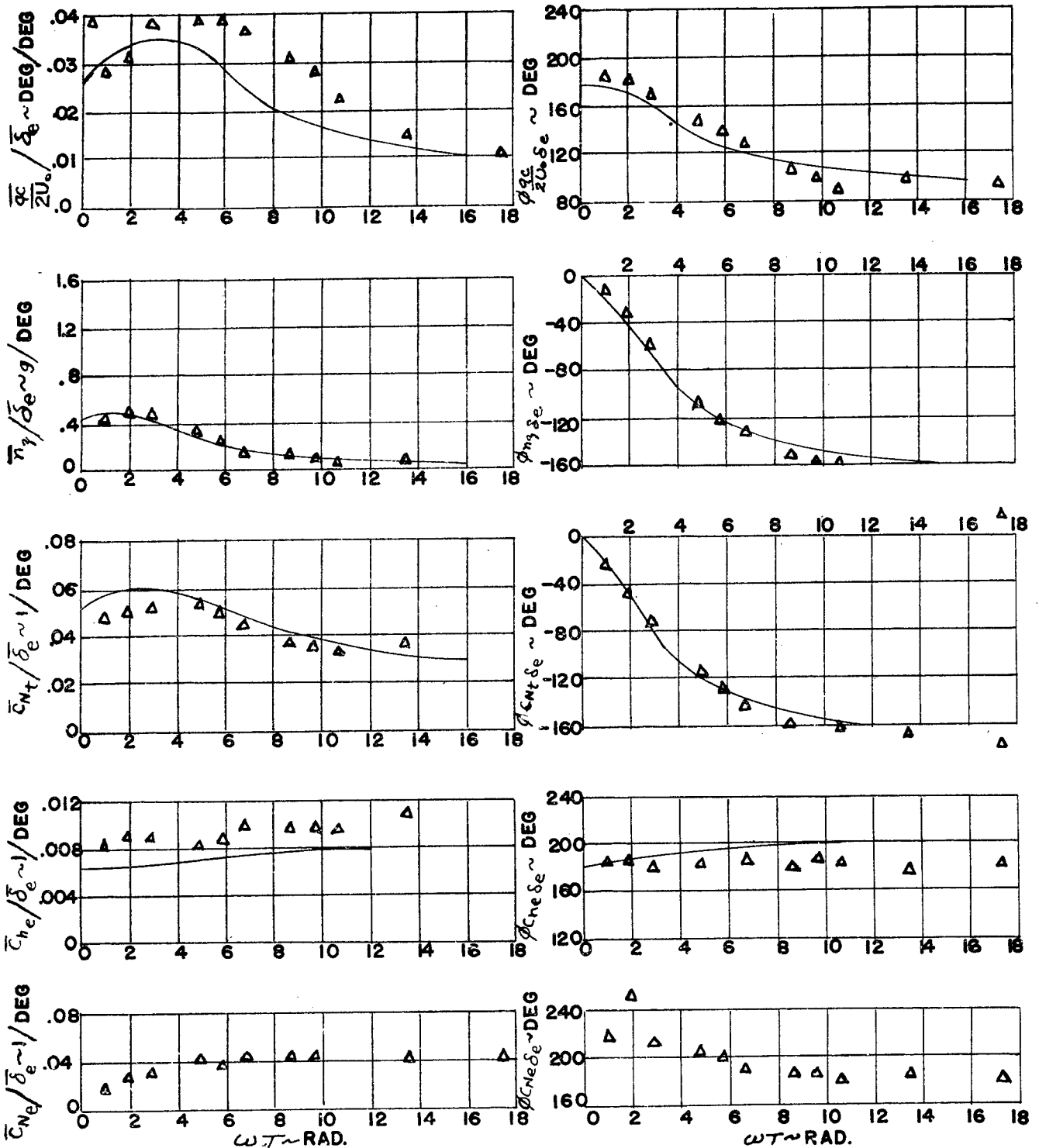
## REFERENCES

- (1) I. C. Statler. Derivation of Dynamic Longitudinal Stability Derivatives for Subsonic Compressible Flow from Non-Stationary Flow Theory and Application to an F-80A Airplane. Cornell Aeronautical Laboratory Report No. TB-495-F-9.
- (2) T. F. Walkowicz. Dynamic Longitudinal Response of an Airplane at High Subsonic Mach Numbers. D.Sc. Thesis, Massachusetts Institute of Technology.
- (3) R. C. Kidder. Dynamic Longitudinal Stability Flight Tests of an F-80A Airplane by the Forced Oscillation and Step Function Response Methods Including Measured Horizontal Tail Loads. Cornell Aeronautical Laboratory Report No. TB-495-F-11.
- (4) S. M. Harmon. Determination of the Effect of Horizontal-Tail Flexibility on Longitudinal Control Characteristics. NACA ACR L5B01.
- (5) J. W. Cleary, L. J. Gray. High-Speed Wind Tunnel Tests of a Model of the Lockheed YP-80A Airplane Including Correlation with Flight Tests and Tests of Dive Recovery Flaps. NACA RM A7A29.
- (6) E. A. Kidd. Stability and Control of the P-80A Airplane. Lockheed Aircraft Corporation Report No. 8151.
- (7) G. W. Braun. Damping Influence of an Aero-Jet Duct. ATSC-(T-2)IRE-22.
- (8) L. E. Schumacher. A Method for Evaluating Aircraft Stability Parameters from Flight Test Data. WADC-TR-52-71.

# F-80A DYNAMIC RESPONSE CURVES

ALTITUDE 10,000 FT; CG POSITION 27% MAC.

MACH NO.30; GROSS WEIGHT 10,000 LBS.



## LEGEND

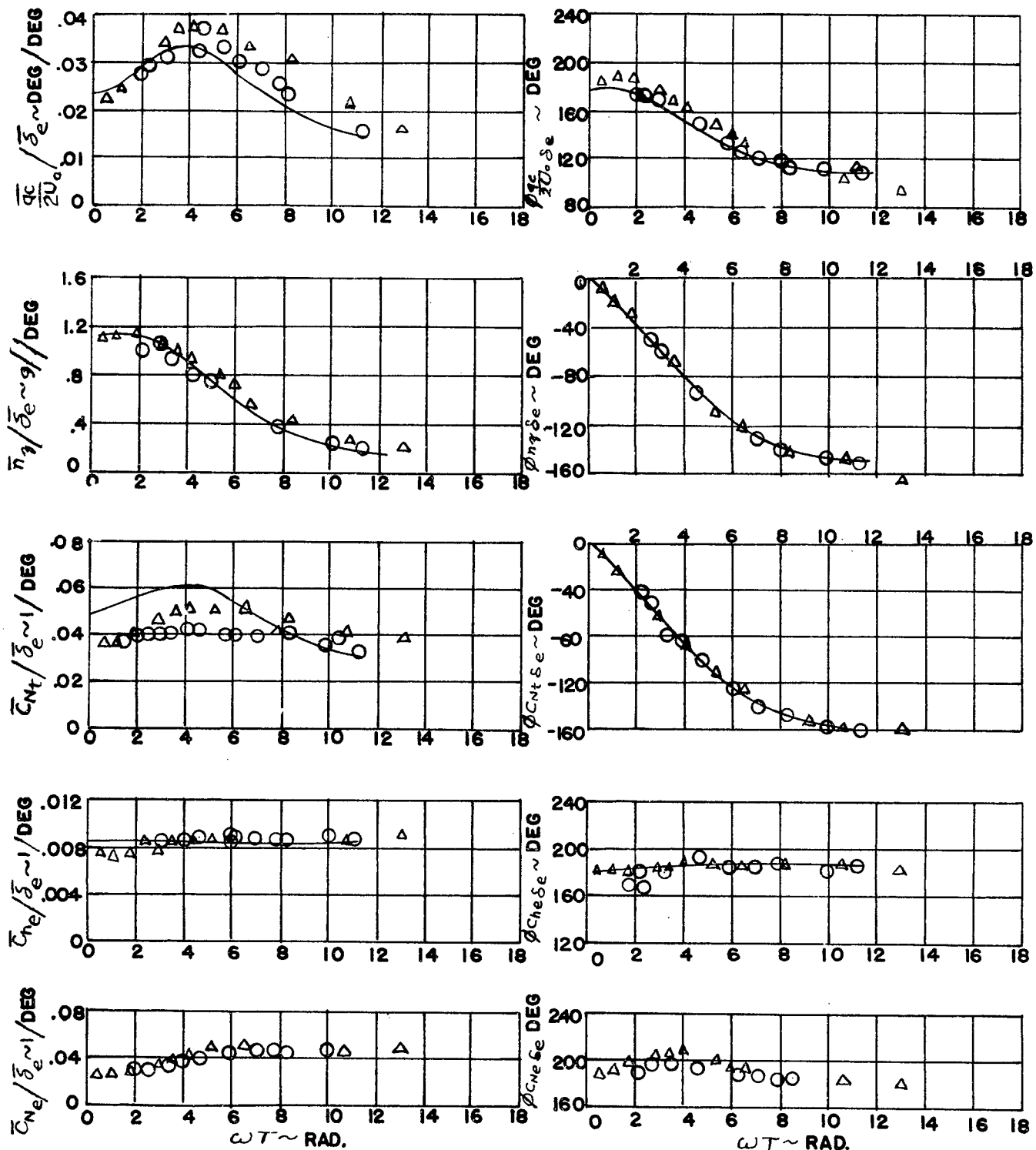
Δ STEP FUNCTION DATA  
— CALCULATED RESPONSE

Figure 1

# F-80A DYNAMIC RESPONSE CURVES

ALTITUDE 10,000 FT; CG POSITION 27% MAC.

MACH NO. 50; GROSS WEIGHT 10,000 LBS.



## LEGEND

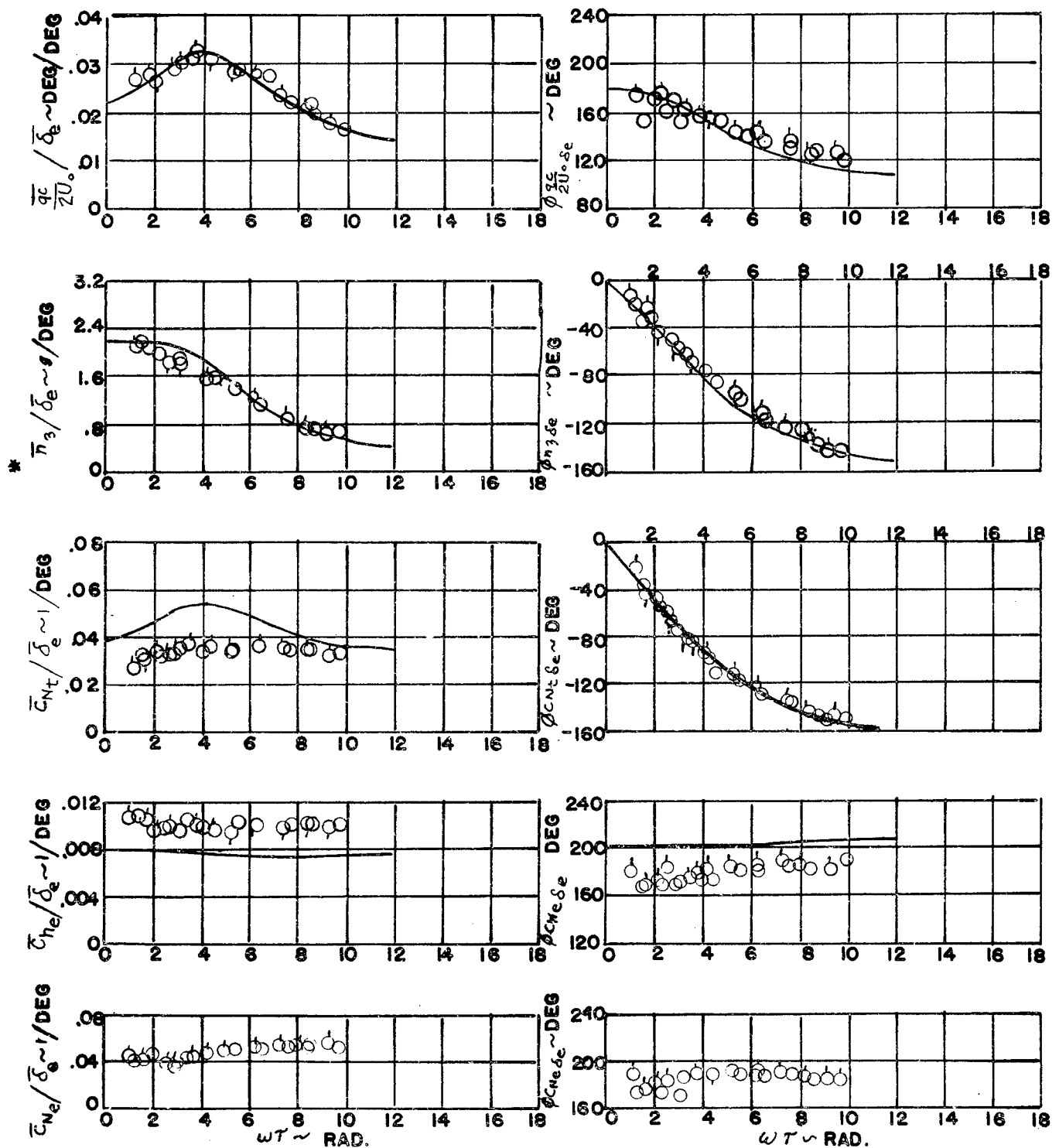
- OSCILLATION DATA
- △ STEP FUNCTION DATA
- CALCULATED RESPONSE

Figure 2

# F-80A DYNAMIC RESPONSE CURVES

ALTITUDE 10,000 FT; CG POSITION 27% MAC.

MACH NO. 70; GROSS WEIGHT 10,000 LBS.



## LEGEND

- OSCILLATION DATA
- ◊ OSCILLATION DATA ADDITIONAL FLIGHT
- CALCULATED RESPONSE

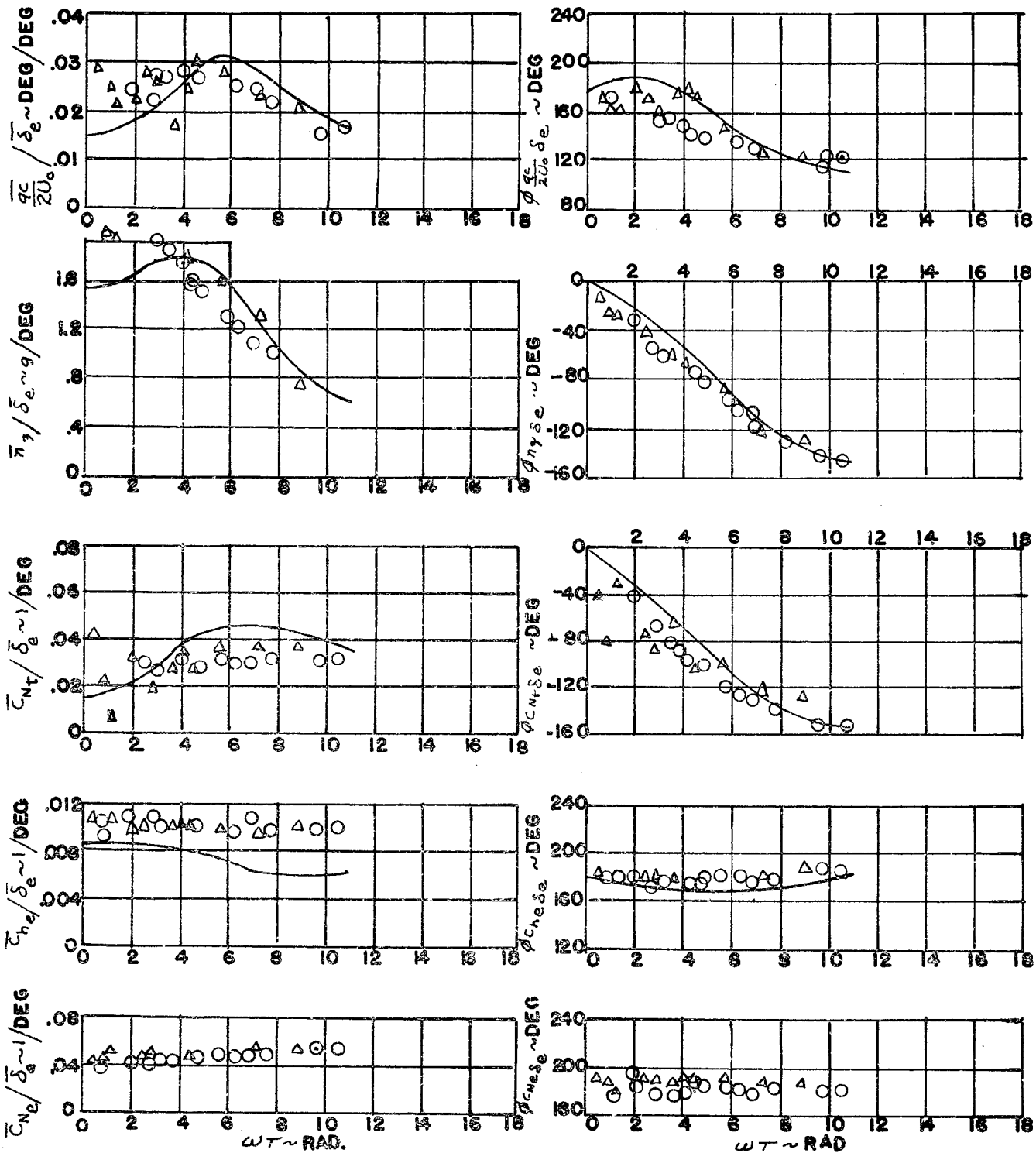
\* NOTE SCALE CHANGE

Figure 3

# F-80A DYNAMIC RESPONSE CURVES

ALTITUDE 10,000 FT; CG POSITION 27% M.A.C.

MACH NO. 75 GROSS WEIGHT 10,000 LBS.



## LEGEND

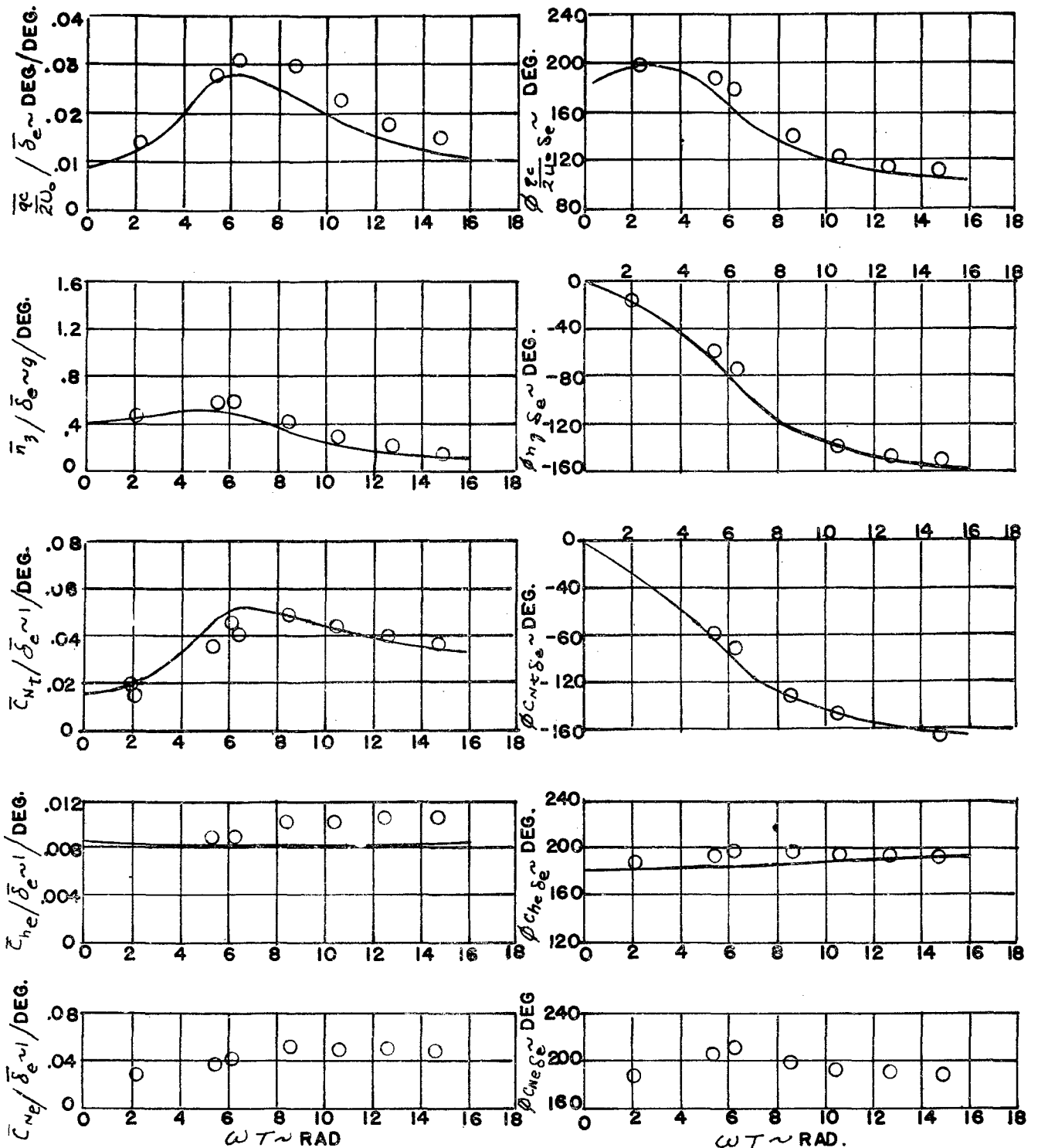
- OSCILLATION DATA
- △ STEP FUNCTION DATA
- CALCULATED RESPONSE

Figure 4

# F-80A DYNAMIC RESPONSE CURVES

ALTITUDE 20,000 FT; CG. POSITION 23% M.A.C.

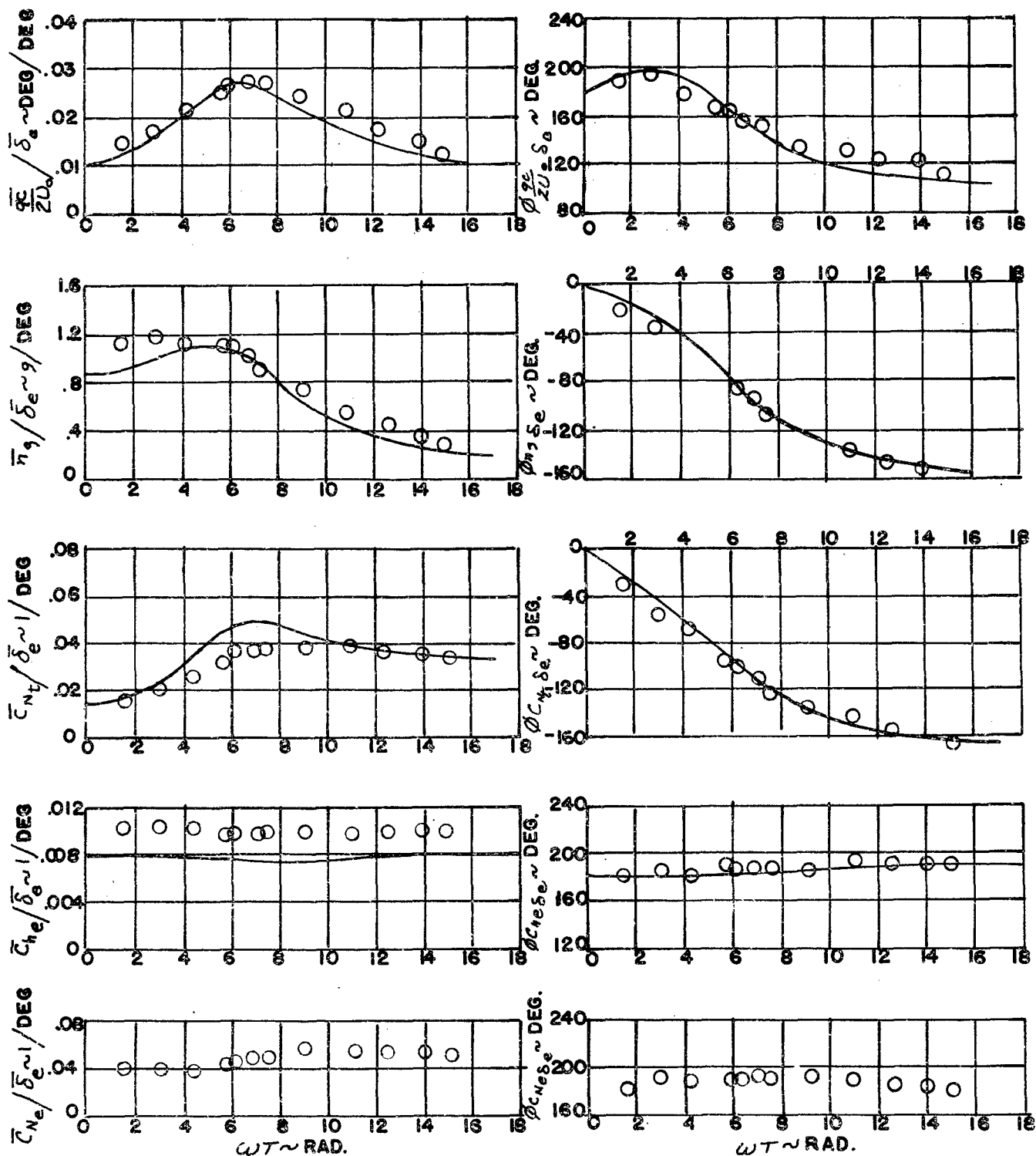
MACH NO. 50; GROSS WEIGHT 10,000 LBS.



LEGEND  
 ○ OSCILLATION DATA  
 — CALCULATED RESPONSE

Figure 5

**F-80A DYNAMIC RESPONSE CURVES**  
 ALTITUDE 20,000 FT.; CG POSITION 23% M.A.C.  
 MACH NO. .70; GROSS WEIGHT 10,000 LBS.



**LEGEND**  
 ○ OSCILLATION DATA

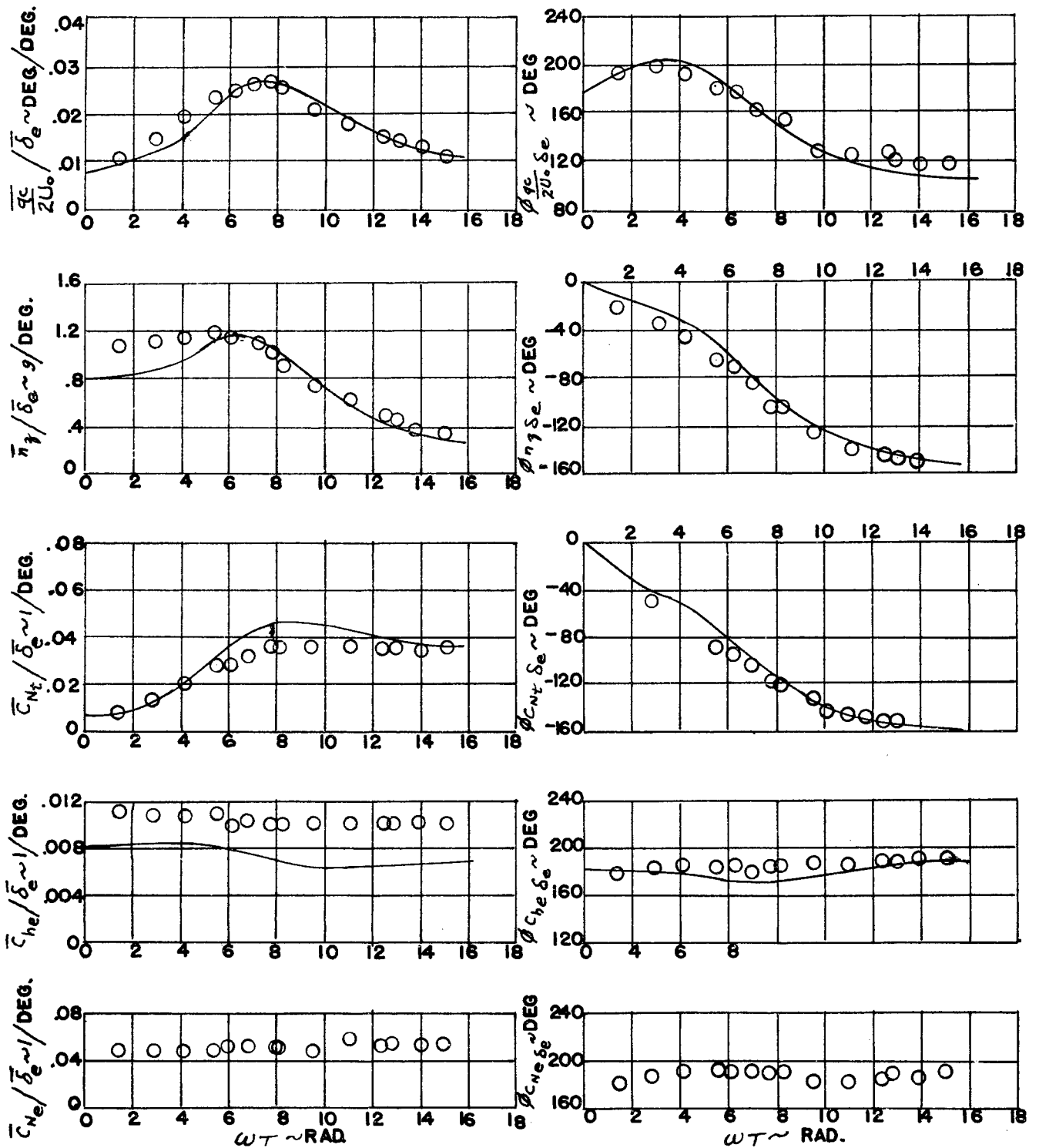
— CALCULATED RESPONSE

Figure 6

# F-80A DYNAMIC RESPONSE CURVES

ALTITUDE 20,000 FT; CG POSITION 23% MAC.

MACH NO. 75; GROSS WEIGHT 10,000 LBS.



LEGEND  
O OSCILLATION DATA

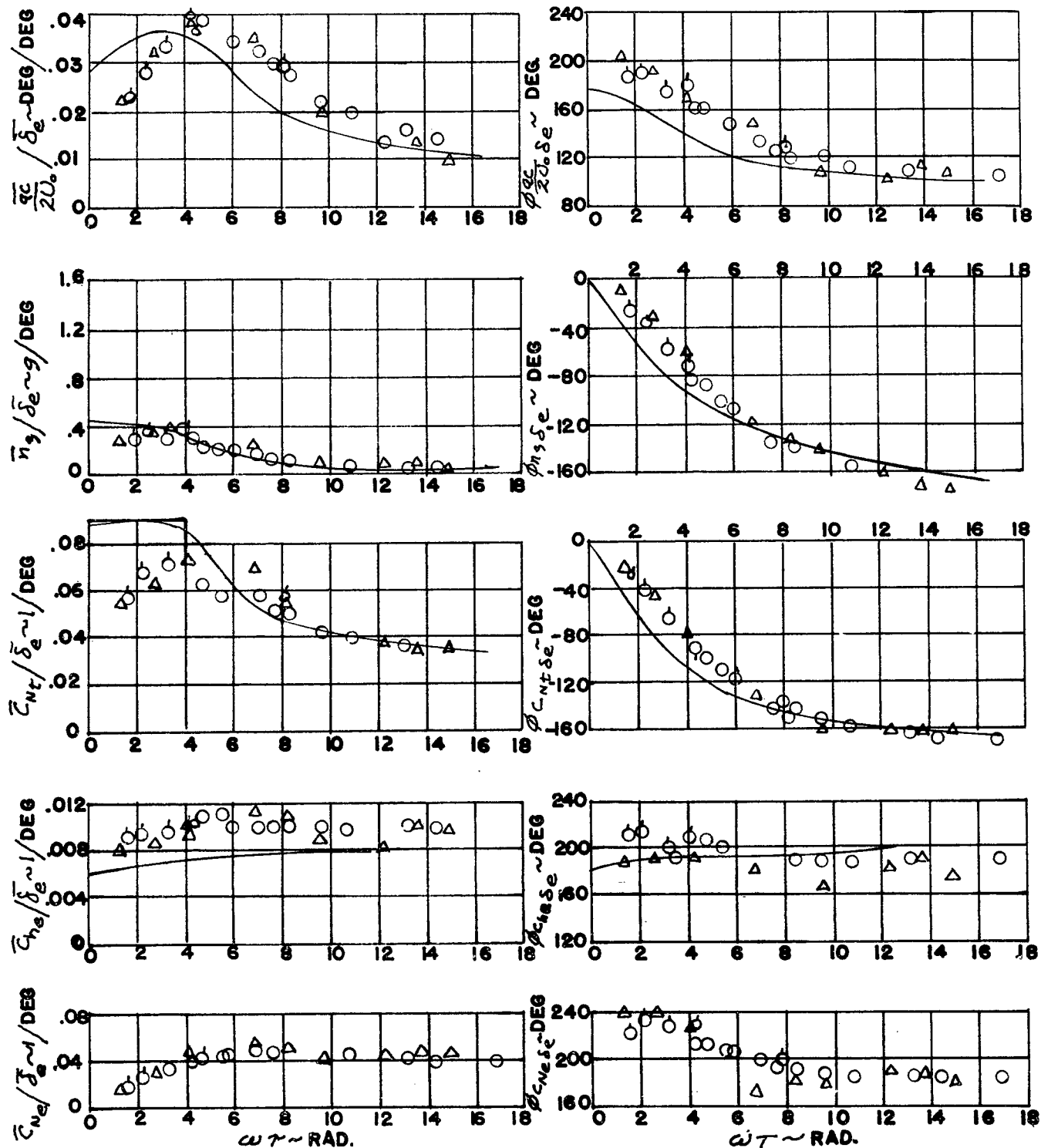
— CALCULATED RESPONSE

Figure 7

# F- 80A DYNAMIC RESPONSE CURVES

ALTITUDE 20,000 FT, CG POSITION 27% M.A.C.

MACH NO. .30; GROSS WEIGHT 10,000 LBS.



## LEGEND

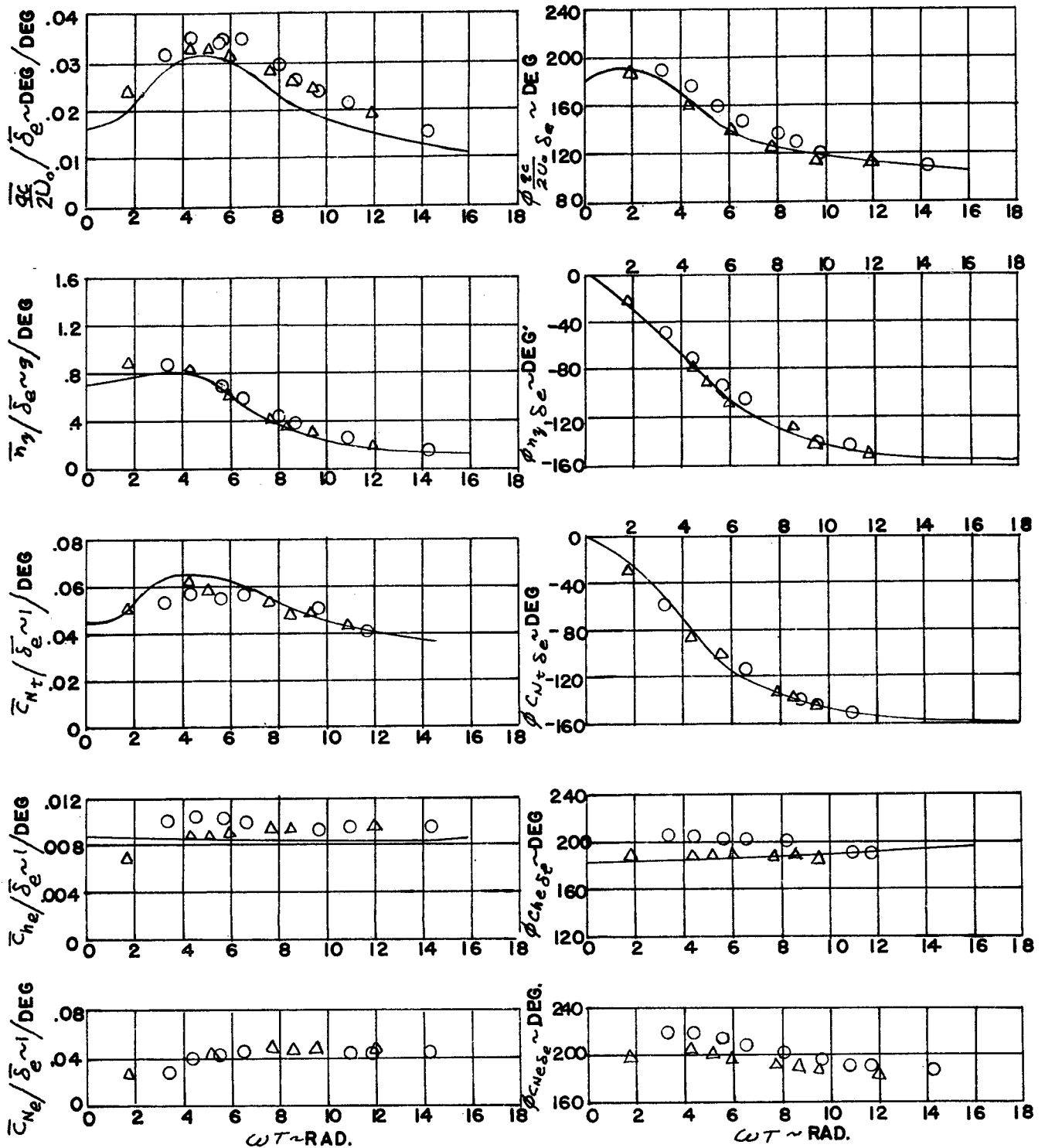
- OSCILLATION DATA
- △ STEP FUNCTION DATA
- CALCULATED RESPONSE
- ADDITIONAL FLIGHT

Figure 8

# F-80A DYNAMIC RESPONSE CURVES

ALTITUDE 20,000 FT; CG. POSITION 27% M.A.C.

MACH NO. .50; GROSS WEIGHT 10,000 LBS.



## LEGEND

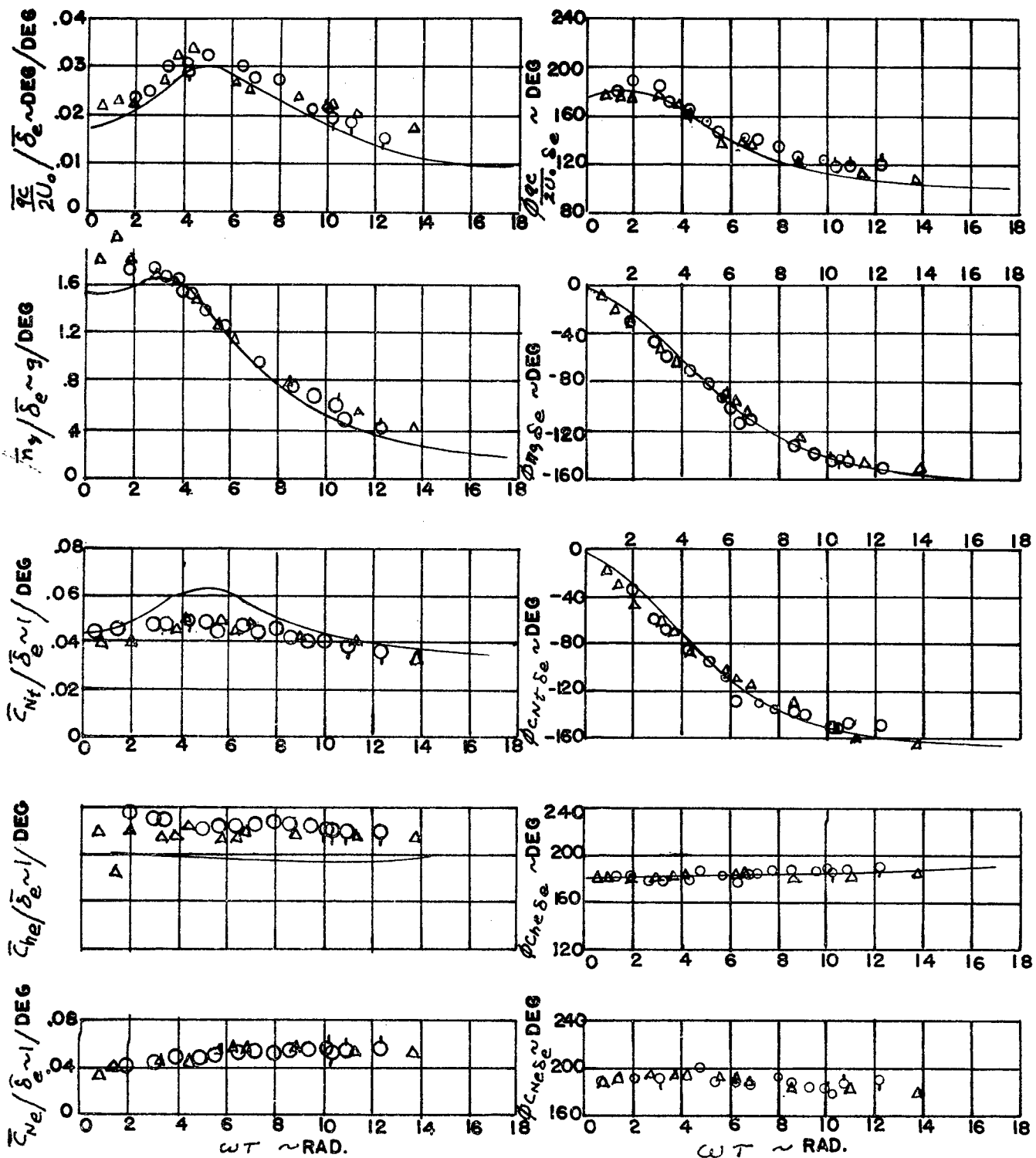
- OSCILLATION DATA
- △ STEP FUNCTION DATA
- CALCULATED RESPONSE

Figure 9

# F- 80A DYNAMIC RESPONSE CURVES

ALTITUDE 20,000 FT, CG POSITION 27 % MAC.

MACH NO. .70, GROSS WEIGHT 10,000 LBS.



## LEGEND

- OSCILLATION DATA
- △ STEP FUNCTION DATA
- CALCULATED RESPONSE
- ◇ ADDITIONAL FLIGHT

Figure 10

# F- 80A DYNAMIC RESPONSE CURVES

ALTITUDE 20,000 FT; CG POSITION 27% M.A.C

MACH NO .75; GROSS WEIGHT 10,000 LBS.

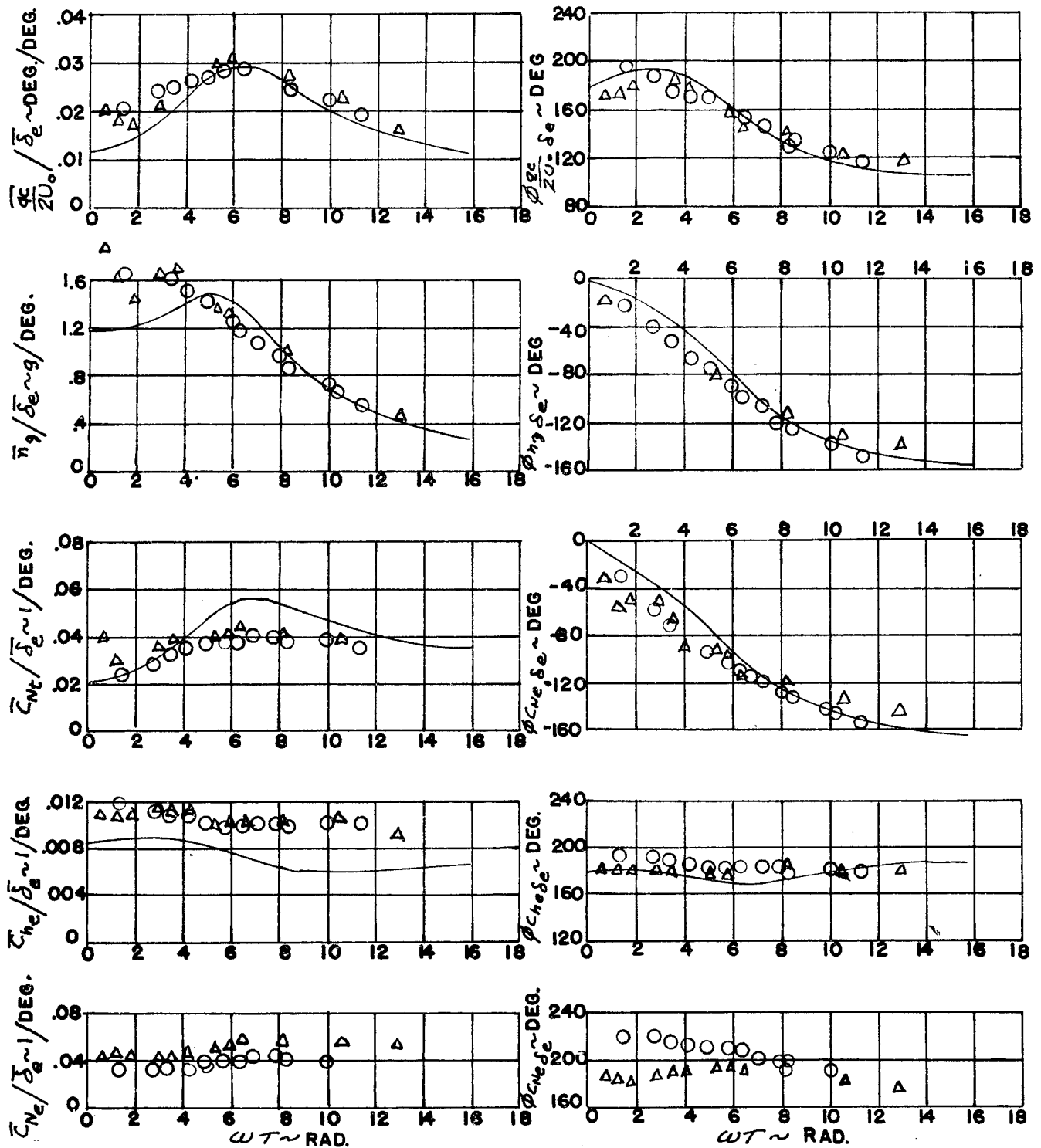
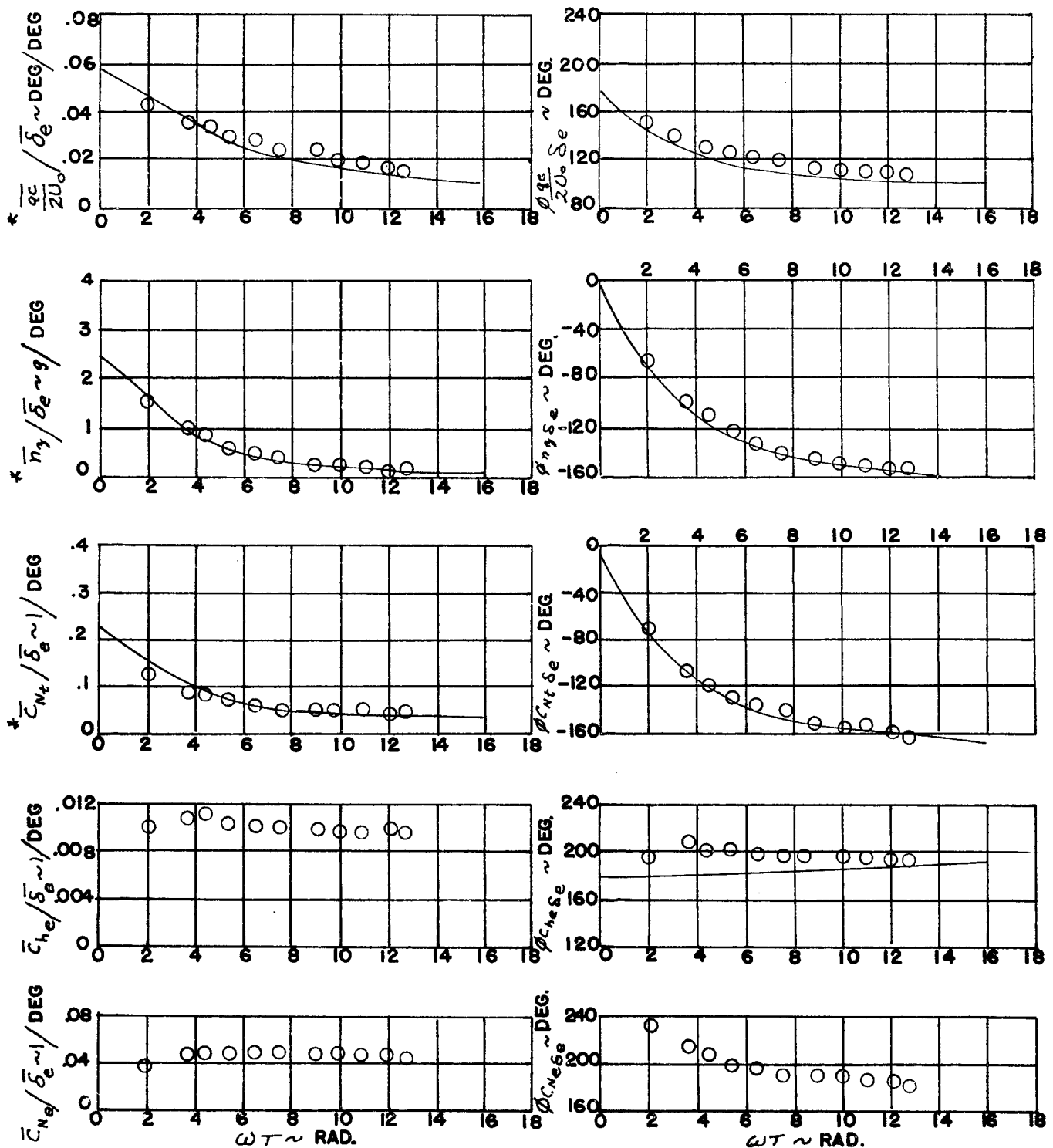


Figure 11

# F-80A DYNAMIC RESPONSE CURVES

ALTITUDE 20,000 FT; CG POSITION 31.5% MAC.

MACH NO..50; GROSS WEIGHT 10,000 LBS.



LEGEND  
○ OSCILLATION DATA

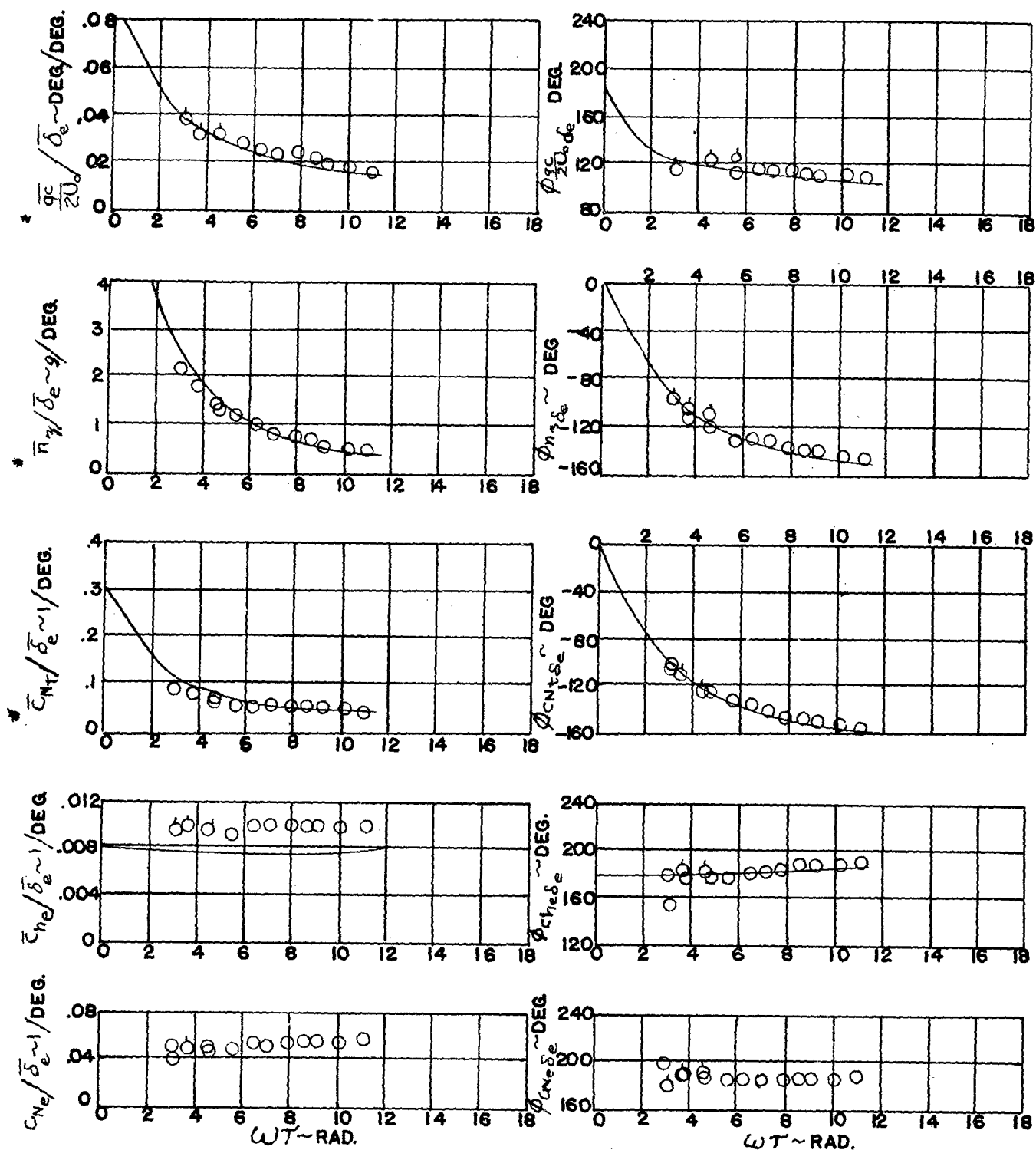
— CALCULATED RESPONSE

NOTE SCALE CHANGE

Figure 12

# F-80A DYNAMIC RESPONSE CURVES

ALTITUDE 20,000 FT; CG POSITION 31.5 MAC.  
MACH NO. .70; GROSS WEIGHT 10,000 LBS.



## LEGEND

- OSCILLATION DATA
- ◊ ADDITIONAL FLIGHT
- CALCULATE RESPONSE

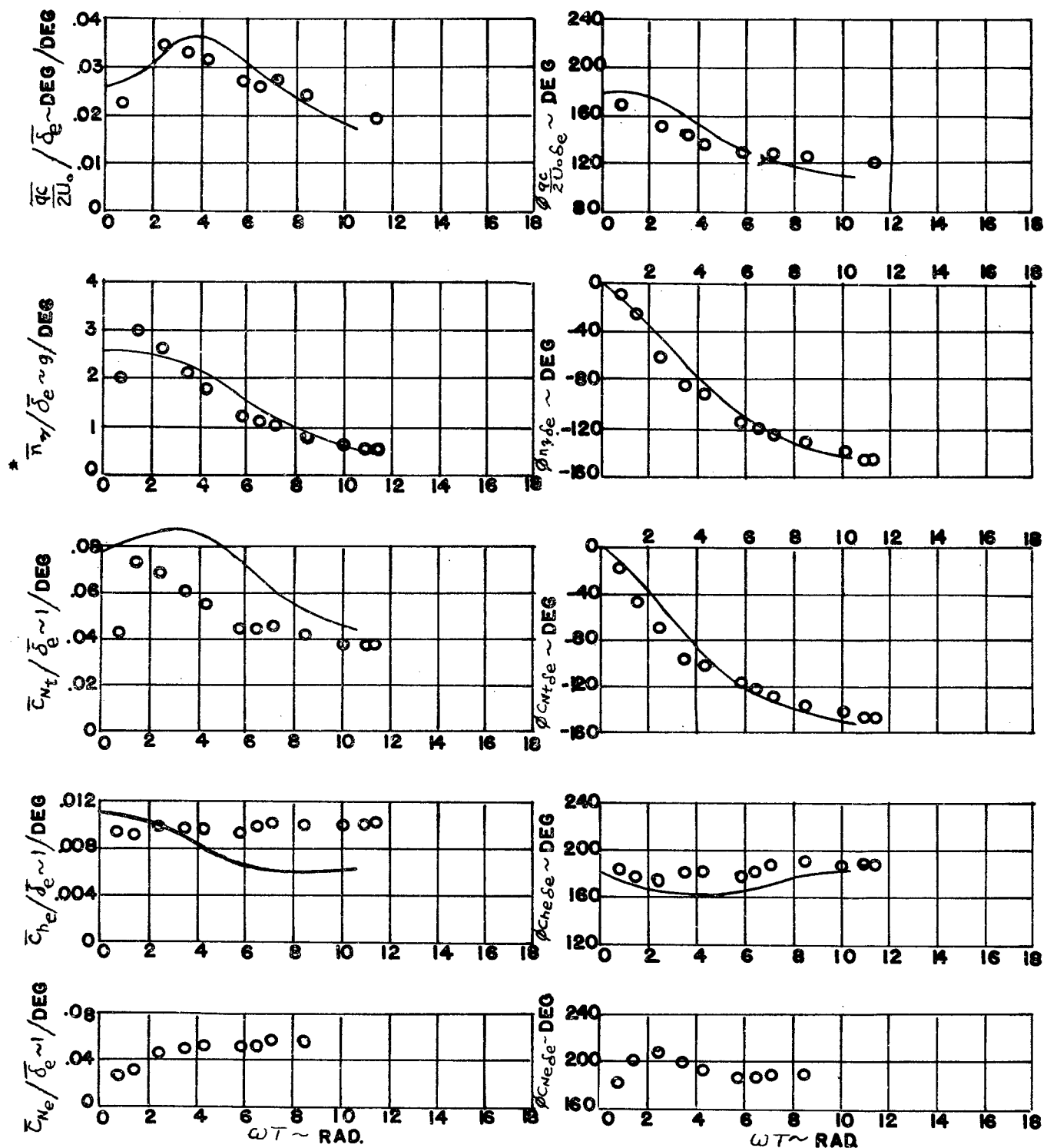
\* NOTE SCALE CHANGE

Figure 13

# F-80A DYNAMIC RESPONSE CURVES

ALTITUDE 20,000 FT. CG POSITION 31.5% MAC.

MACH NO .75; GROSS WEIGHT 10,000 LBS.



## LEGEND

○ OSCILLATION DATA

— CALCULATED RESPONSE

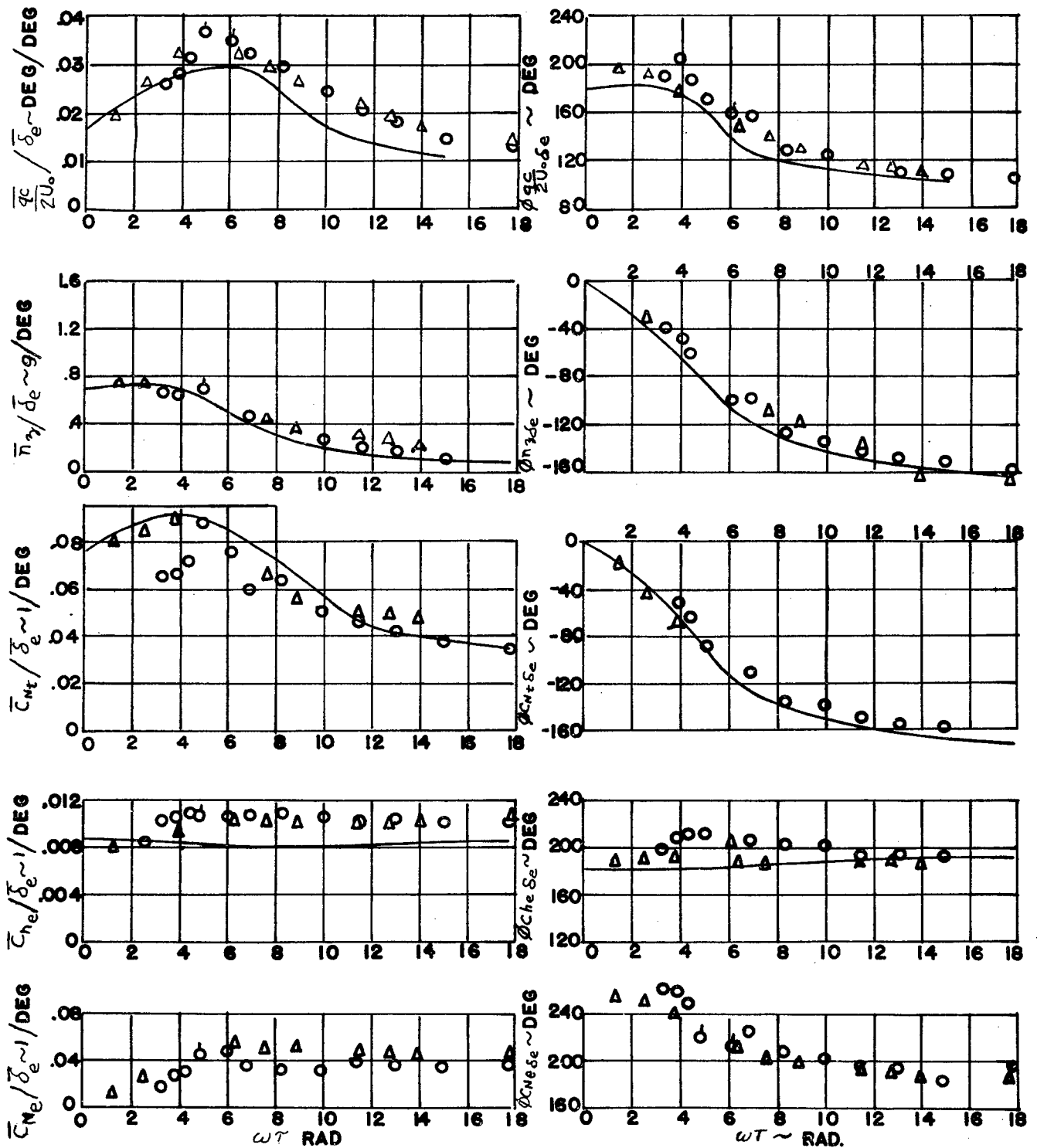
\* NOTE SCALE CHANGE

Figure 14

# F- 80A DYNAMIC RESPONSE CURVES

ALTITUDE 30,000 FT. CG. POSITION 27% M.A.C.

MACH NO.50; GROSS WEIGHT 10,000 LBS.



## LEGEND

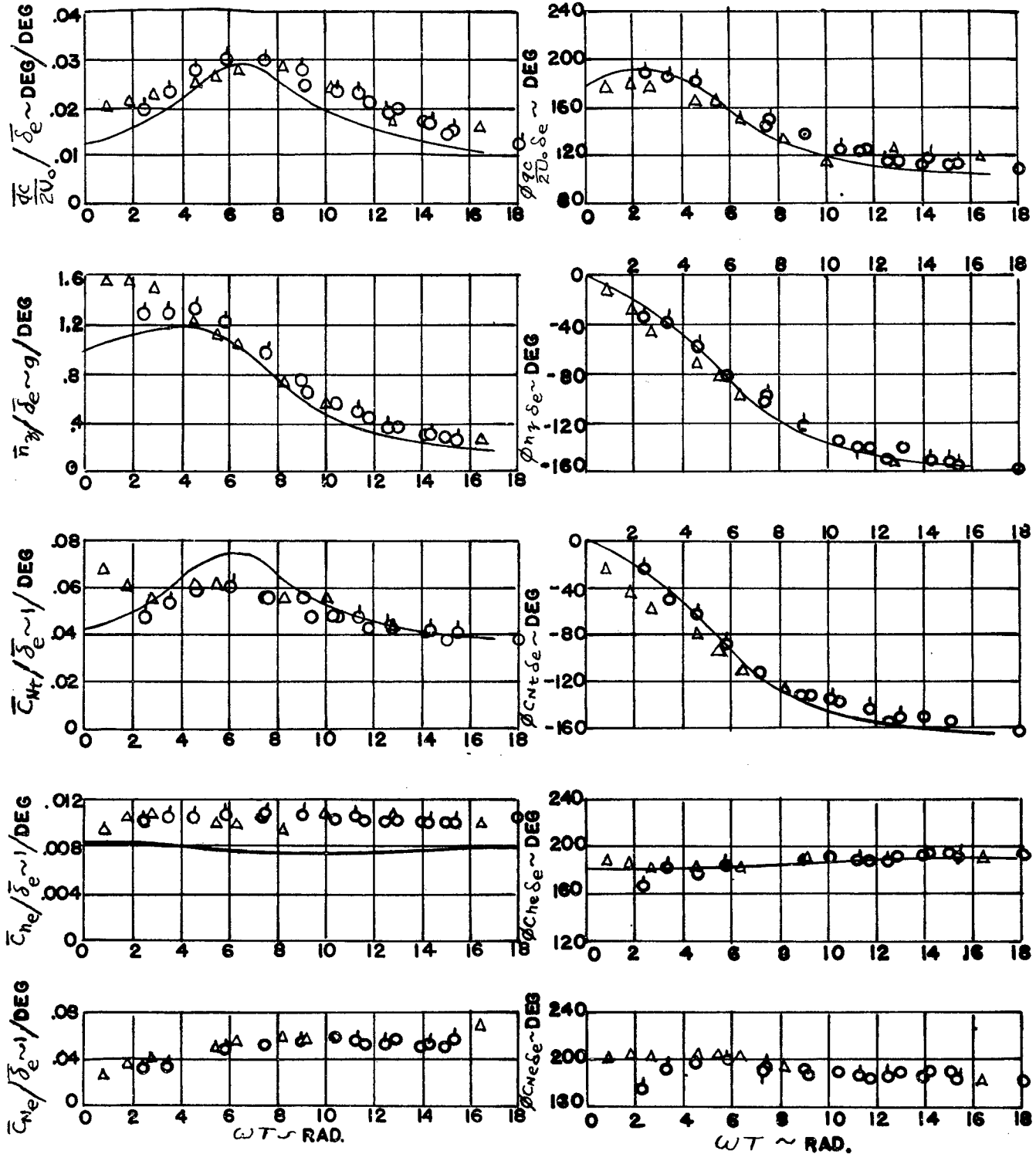
- OSCILLATION DATA
- △ STEP FUNCTION DATA
- CALCULATED RESPONSE
- ◊ ADDITIONAL FLIGHT

Figure 15

# F-80A DYNAMIC RESPONSE CURVES

ALTITUDE 30,000 FT. CG POSITION 27% M.A.C.

MACH NO.70; GROSS WEIGHT 10,000 LBS.



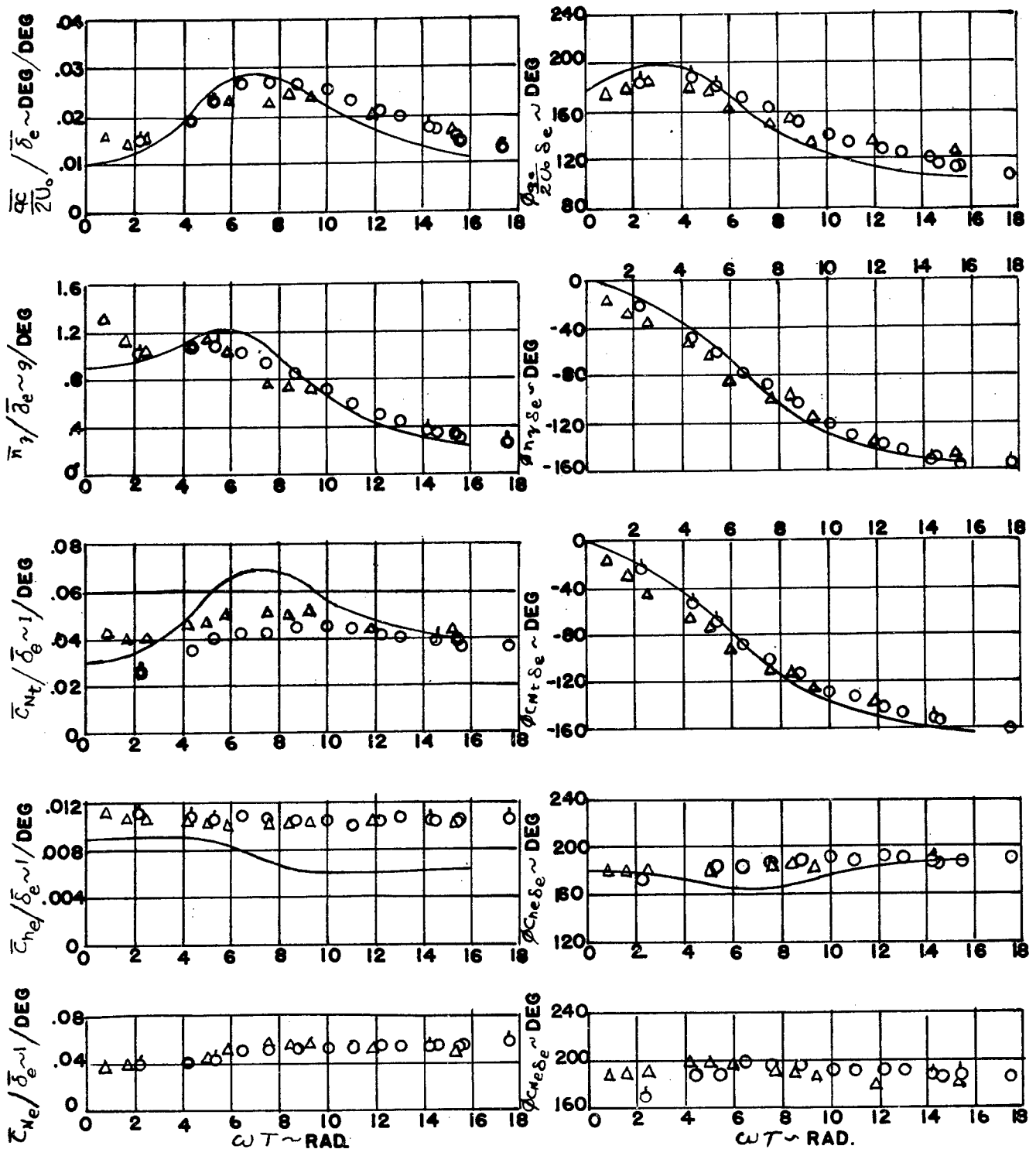
## LEGEND

- OSCILLATION DATA
- △ STEP FUNCTION DATA
- CALCULATED RESPONSE
- ◊ ADDITIONAL FLIGHT

Figure 16

# F-80A DYNAMIC RESPONSE CURVES

ALTITUDE 30,000 FT CG POSITION 27% MAC  
MACH NO .75. GROSS WEIGHT 10,000 LBS.



## LEGEND

- OSCILLATION DATA
- △ STEP FUNCTION DATA
- CALCULATED RESPONSE
- ◊ ADDITIONAL FLIGHT

Figure 17

# F-80A DYNAMIC RESPONSE CURVES

HORIZONTAL TAIL LOAD AMPLITUDE AND PHASE VS. FREQUENCY

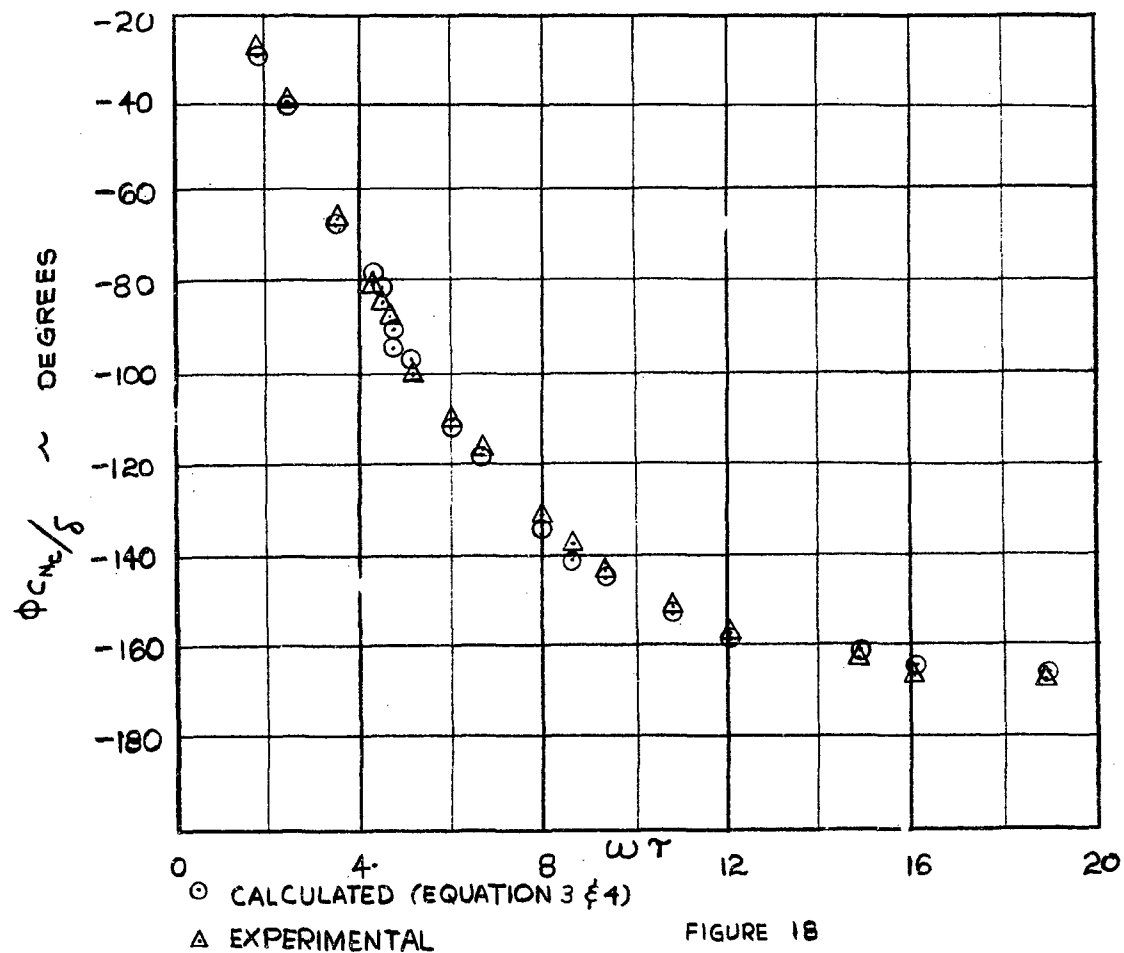
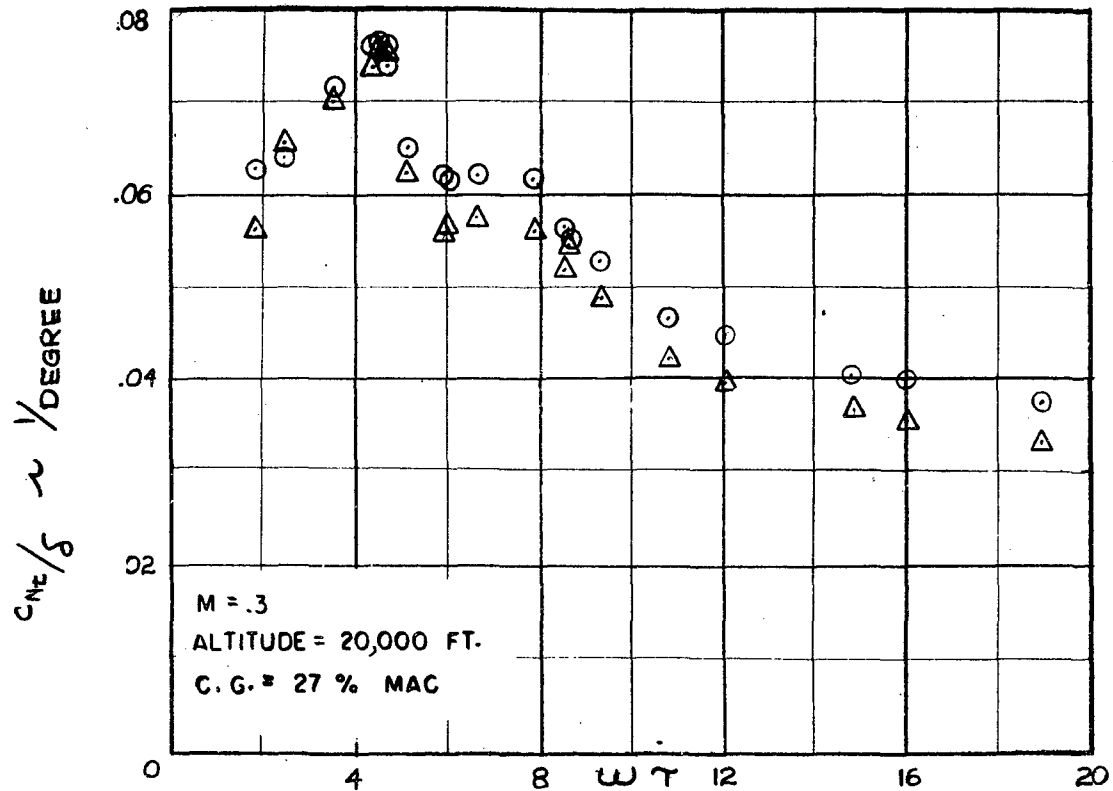
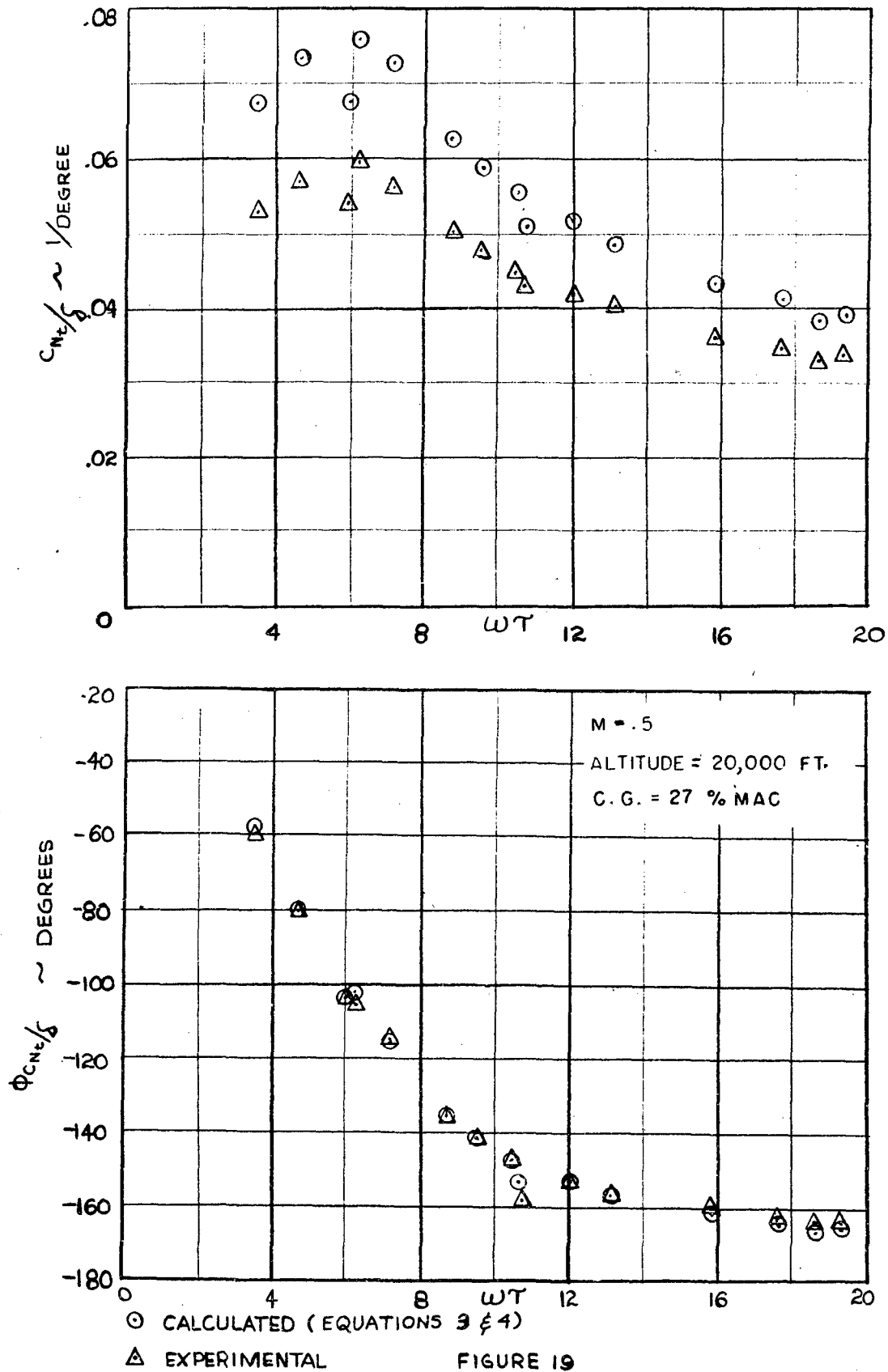


FIGURE 18

F-80A DYNAMIC RESPONSE CURVES  
HORIZONTAL TAIL LOAD AMPLITUDE AND PHASE VS. FREQUENCY



# F-80A DYNAMIC RESPONSE CURVES

## HORIZONTAL TAIL LOAD AMPLITUDE AND PHASE VS. FREQUENCY

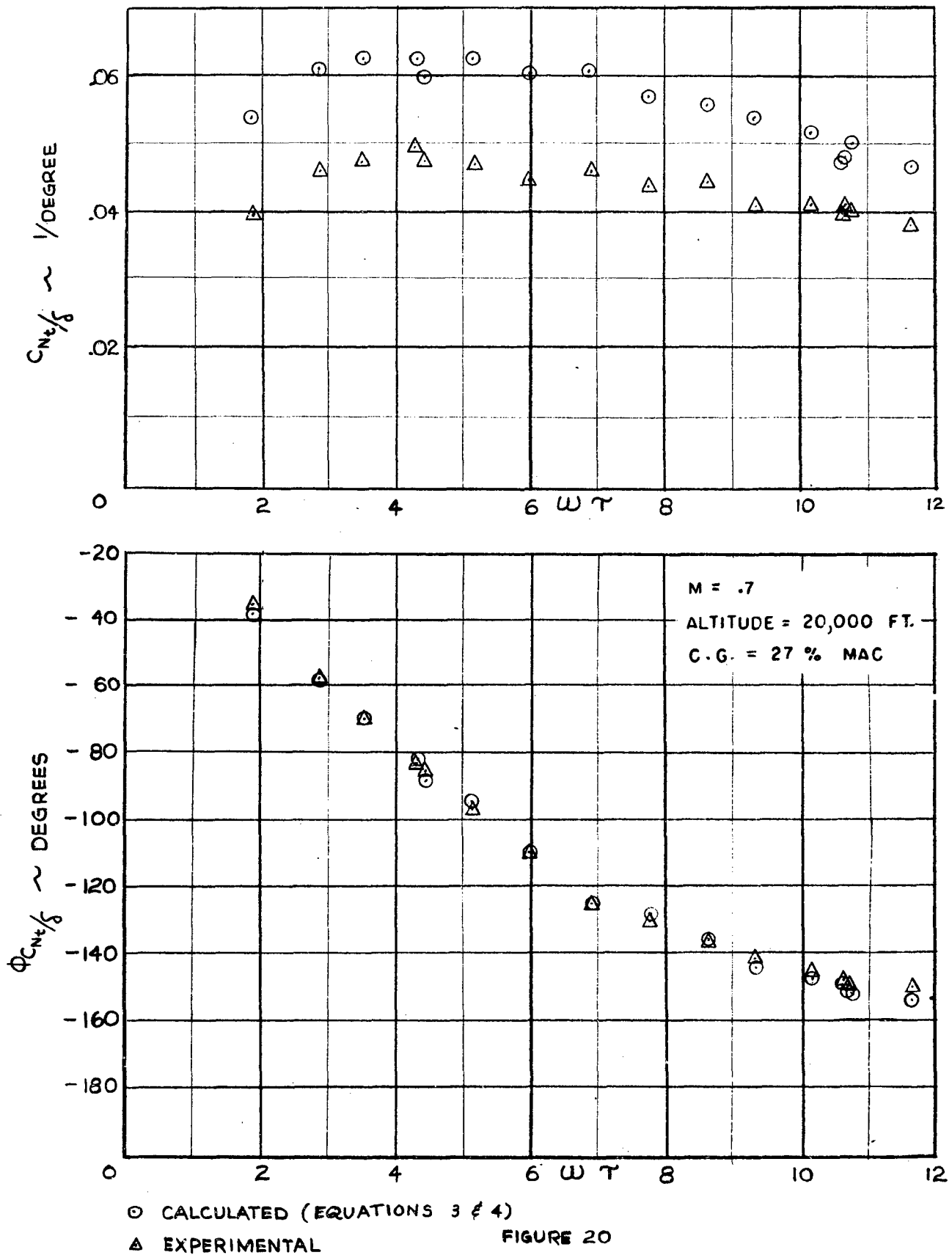
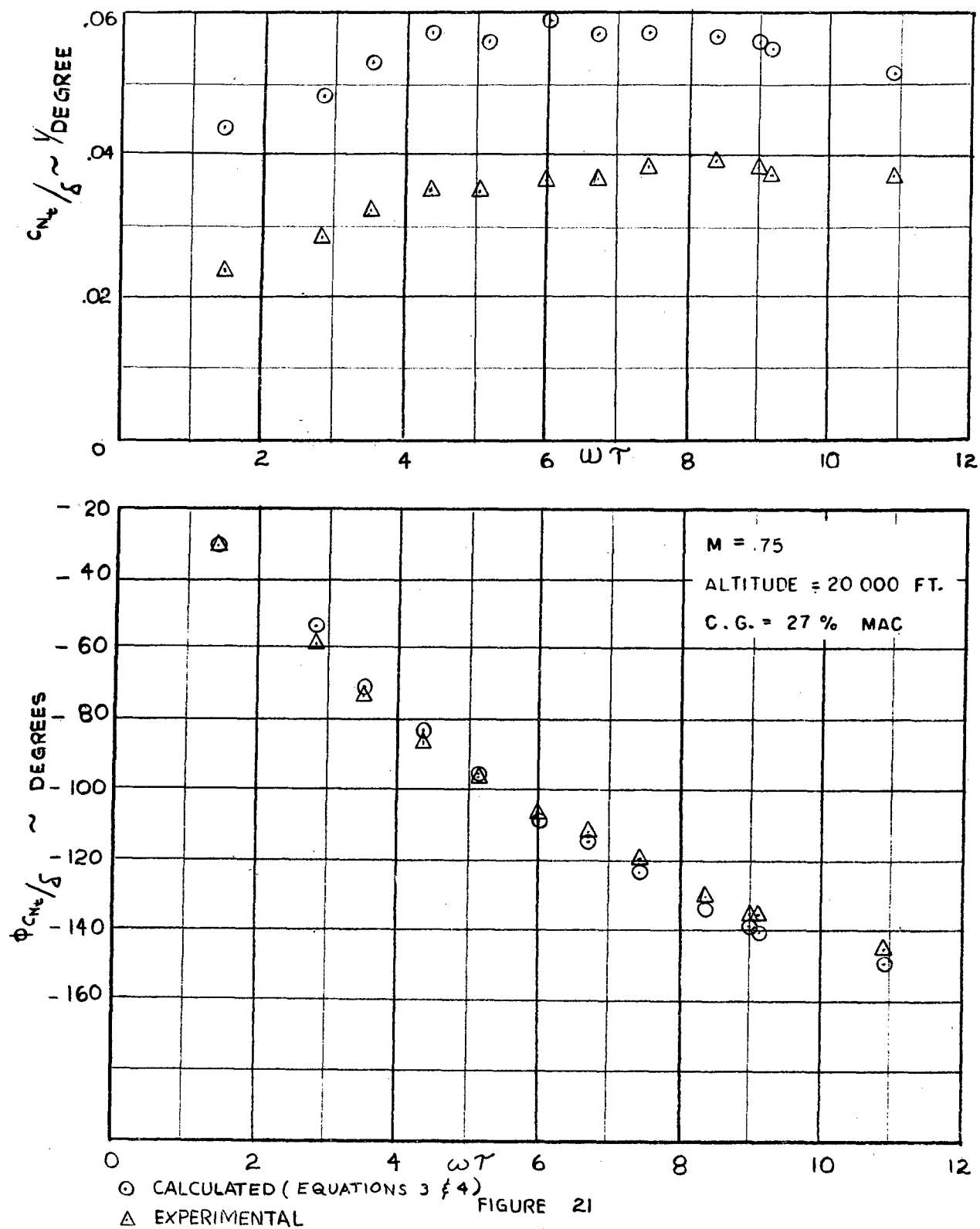
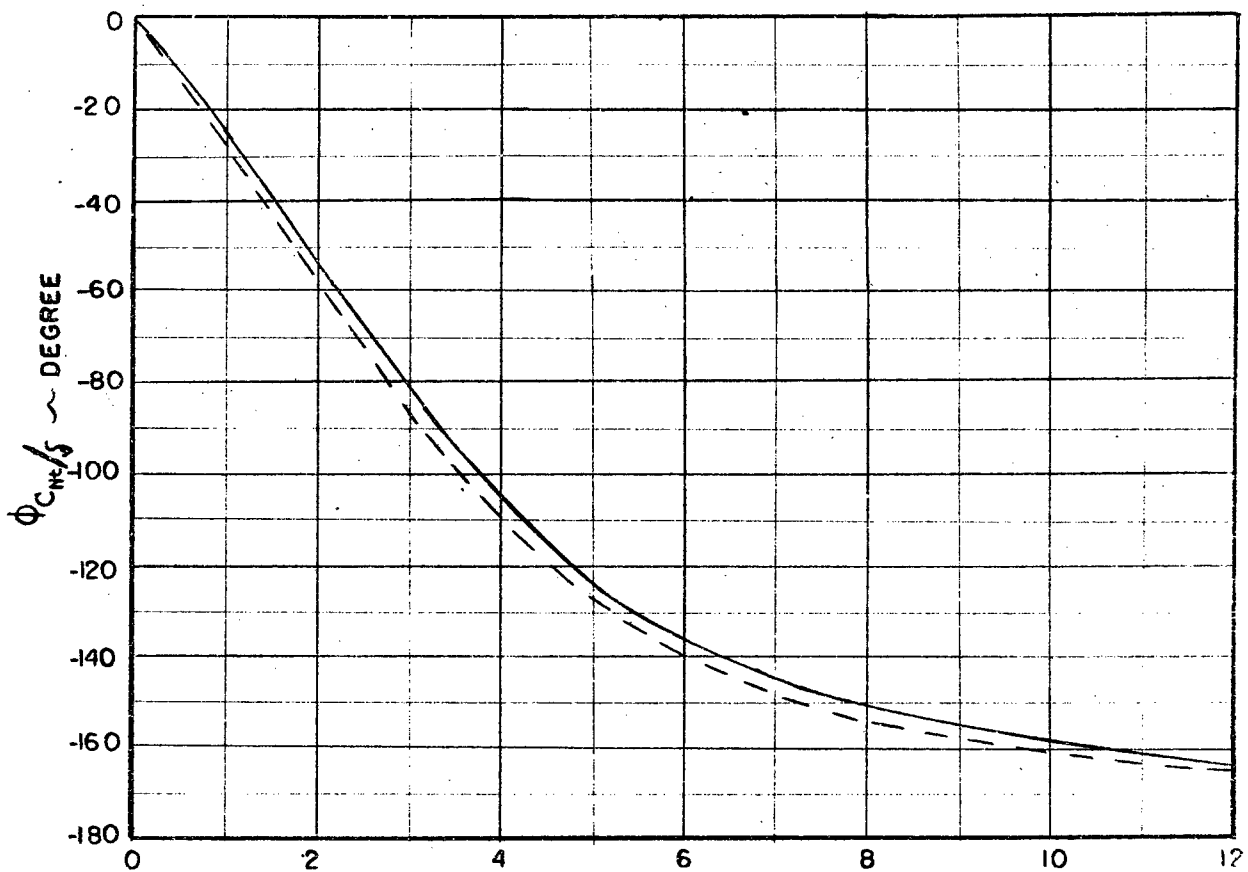
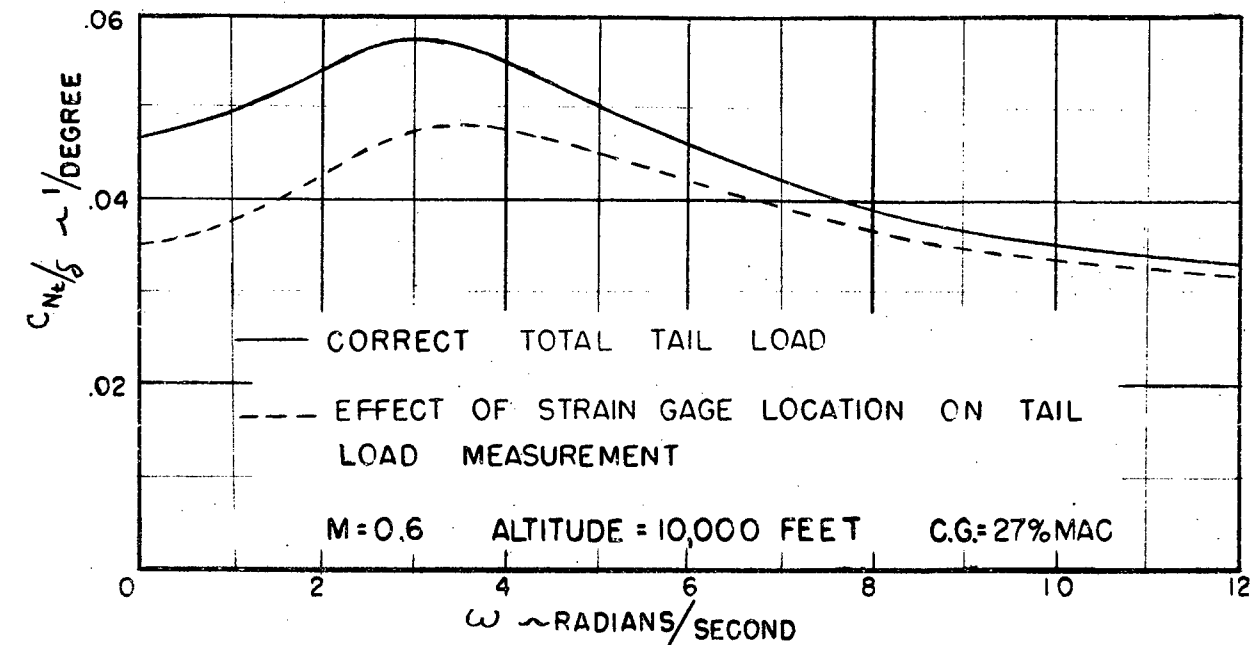


FIGURE 20

# F-80A DYNAMIC RESPONSE CURVES

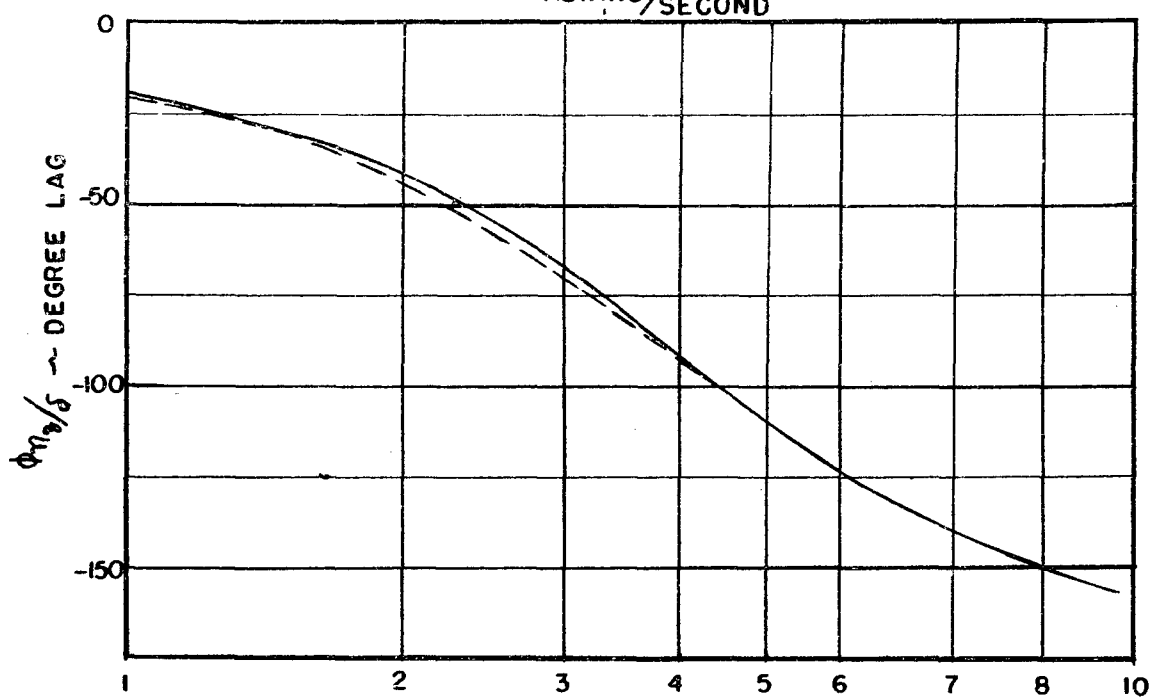
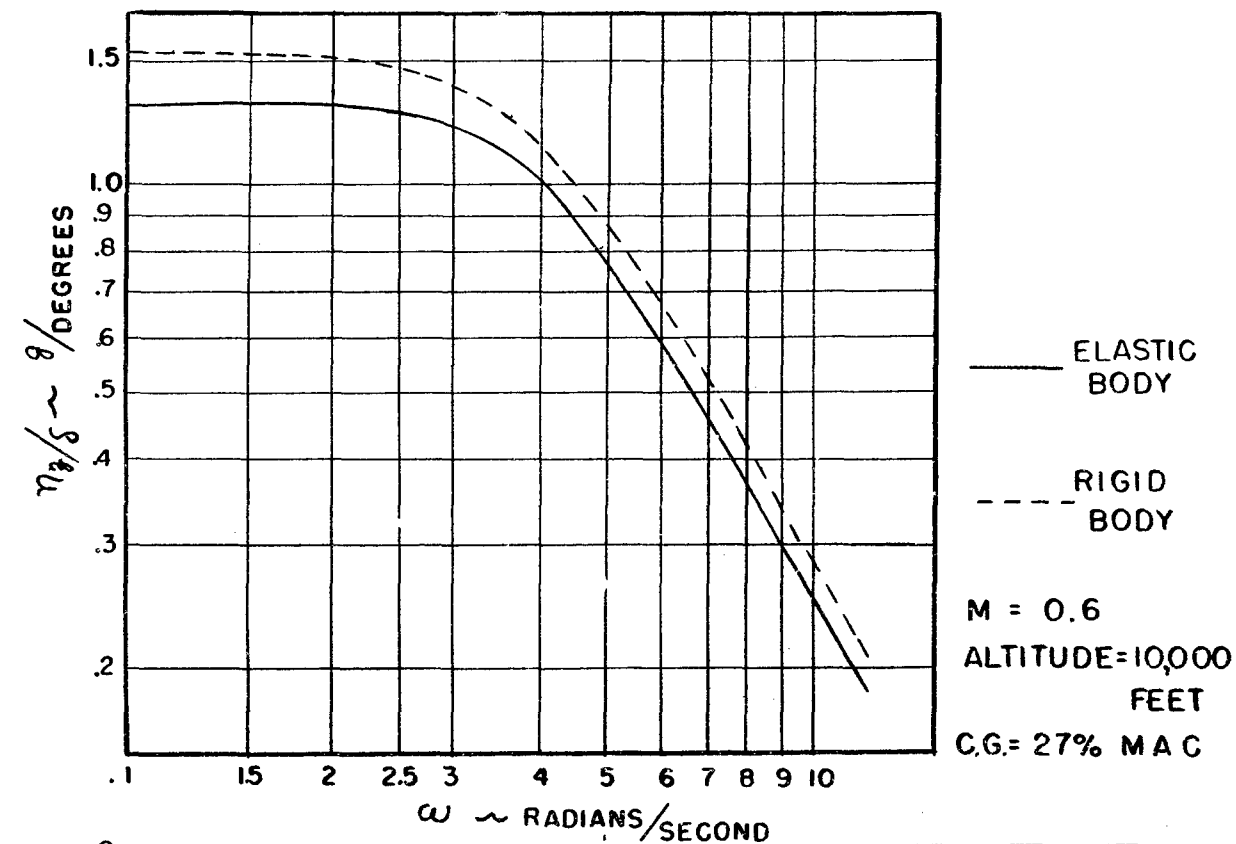
HORIZONTAL TAIL LOAD AMPLITUDE AND PHASE VS. FREQUENCY





F-80A DYNAMIC RESPONSE CURVES  
HORIZONTAL TAIL LOAD AMPLITUDE AND PHASE VS. FREQUENCY  
EFFECT OF STRAIN GAGE LOCATION ON ACTUAL MEASUREMENT  
OF HORIZONTAL TAIL LOAD

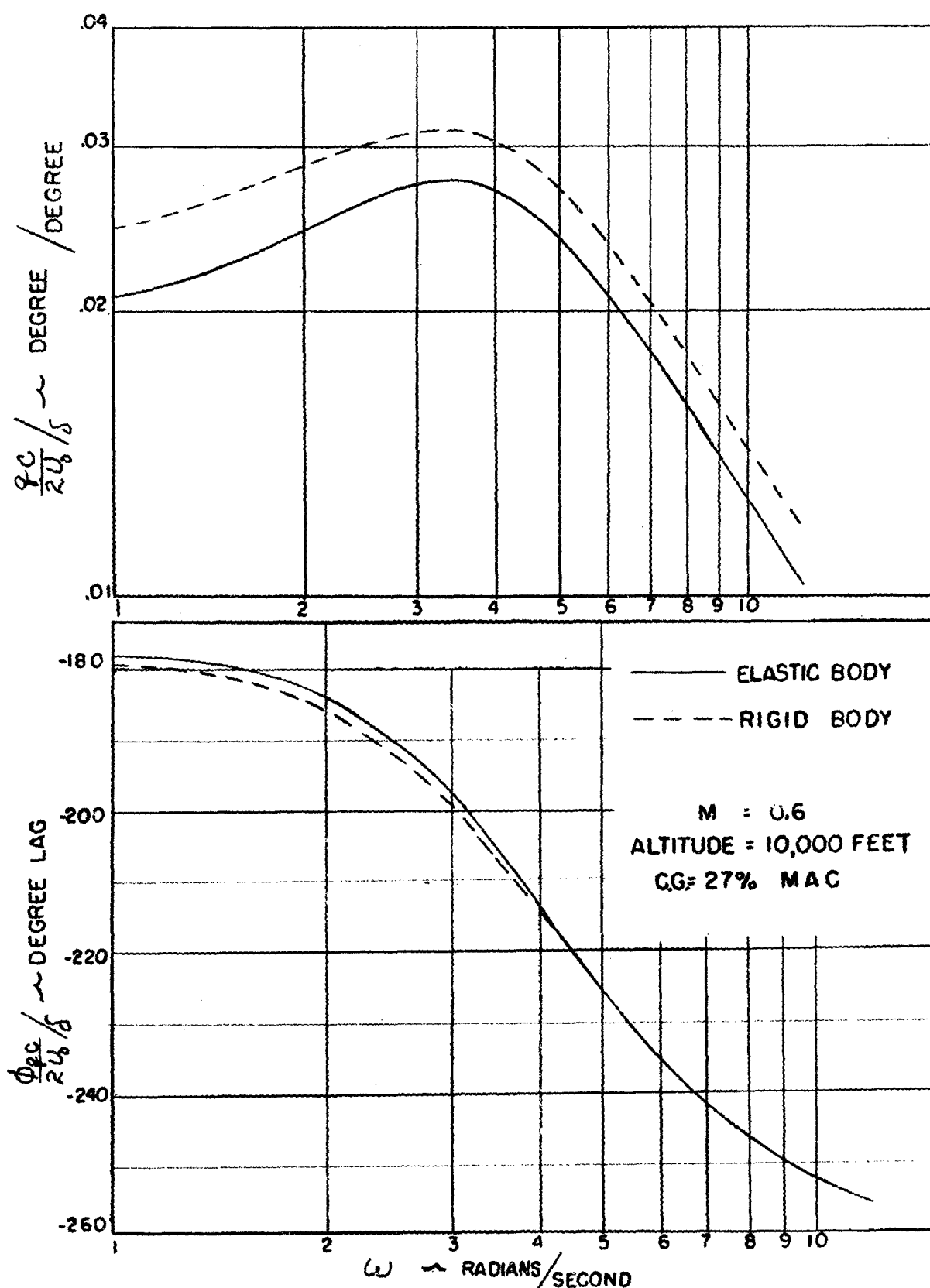
FIGURE 22



### F-80A DYNAMIC RESPONSE CURVES

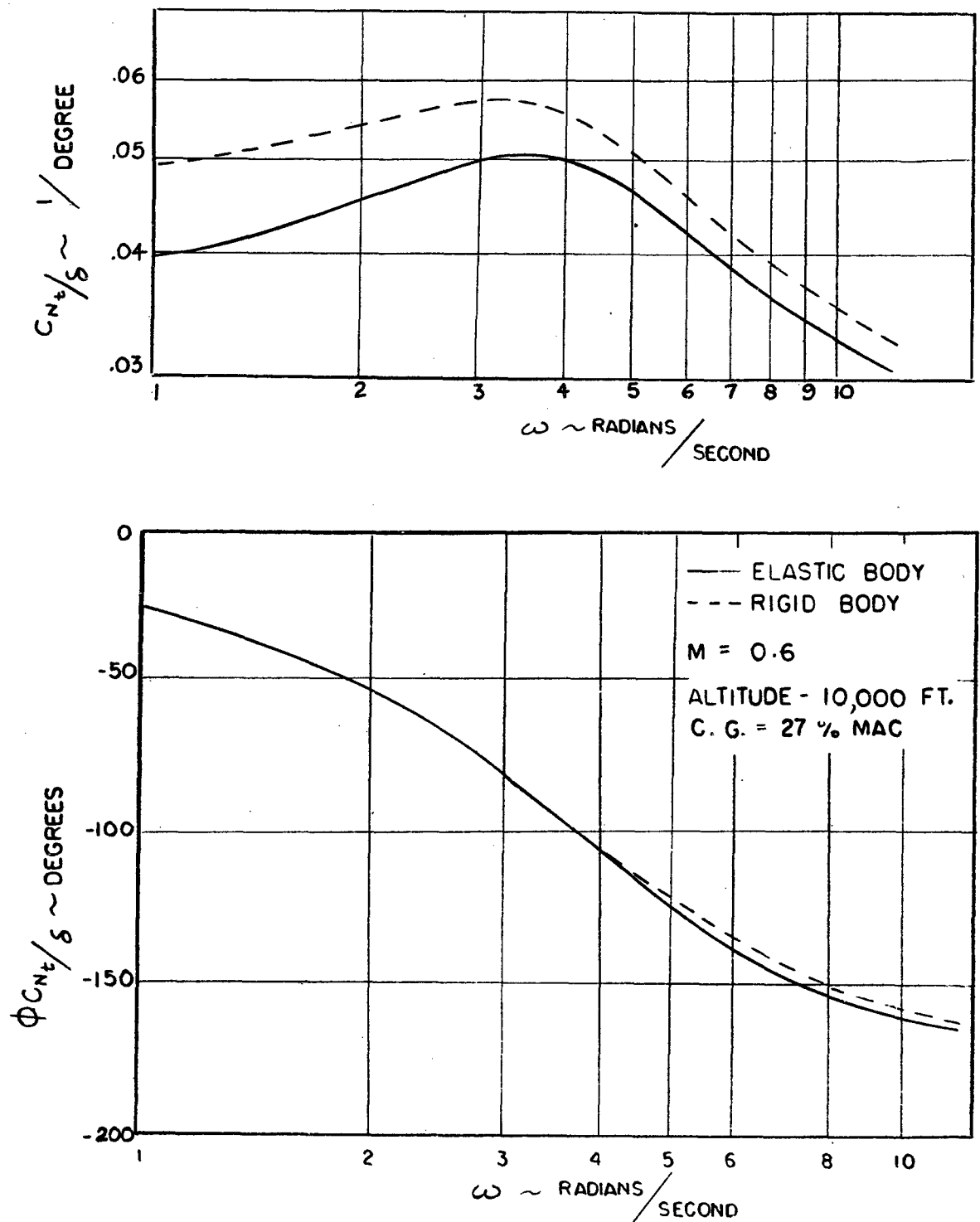
NORMAL ACCELERATION AMPLITUDE AND PHASE VS. FREQUENCY

FIGURE 23



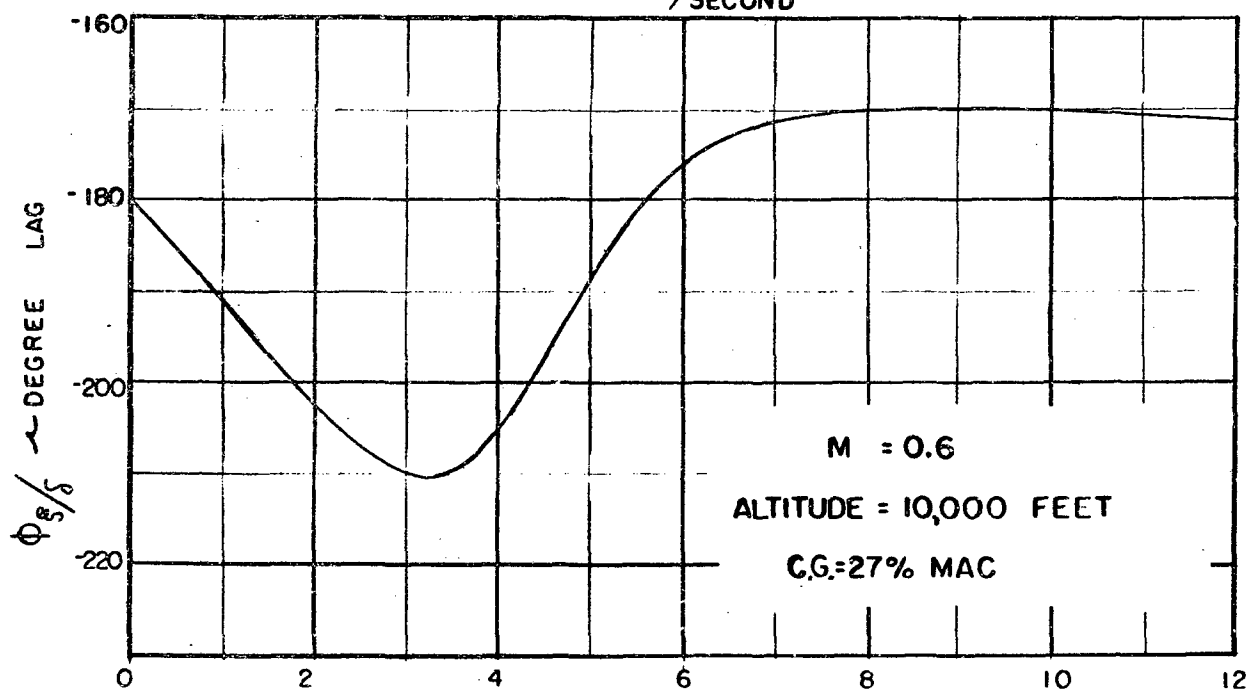
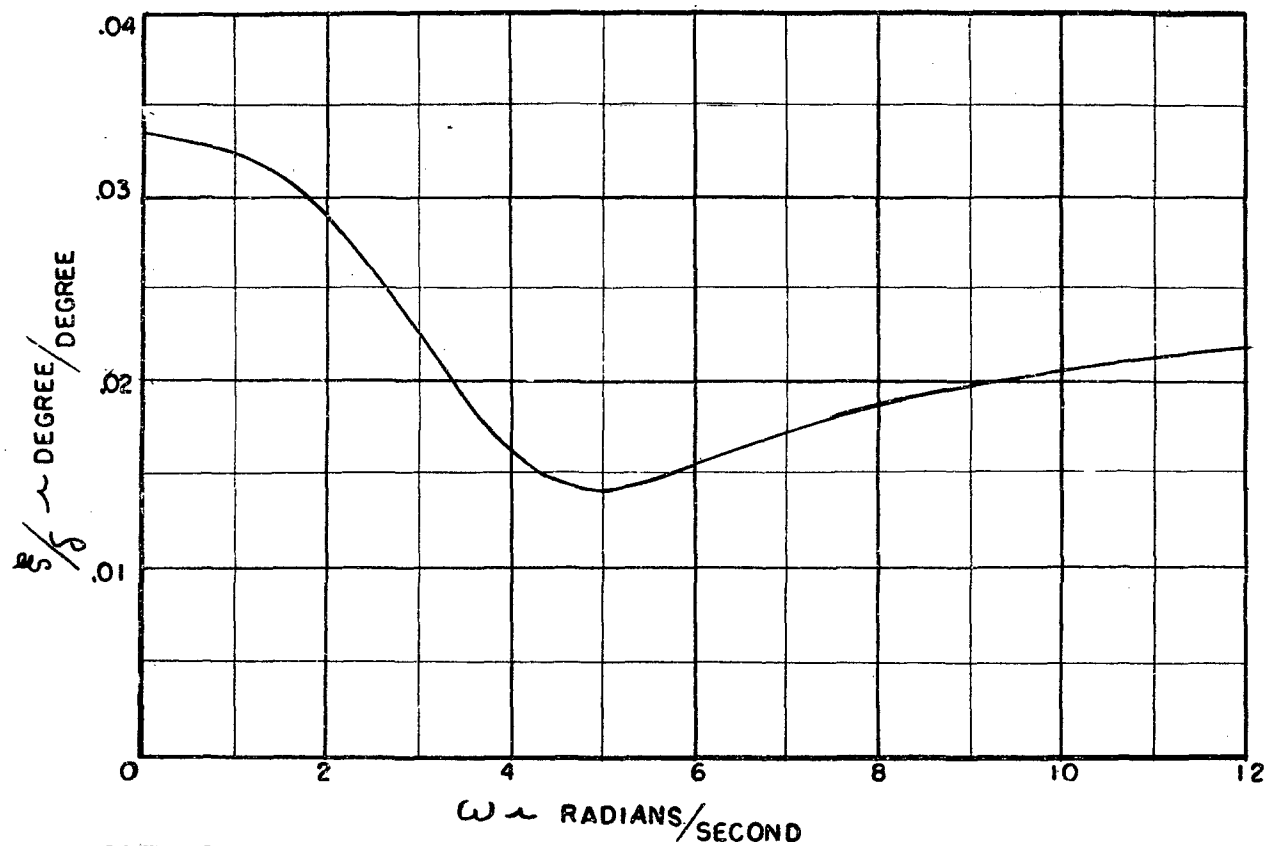
F-80A DYNAMIC RESPONSE CURVES  
 PITCHING VELOCITY AMPLITUDE AND PHASE VS. FREQUENCY

FIGURE 24  
 - 62 -



F-80A DYNAMIC RESPONSE CURVES  
HORIZONTAL TAIL LOAD AMPLITUDE AND PHASE VS.  
FREQUENCY

FIGURE 25



### F-80A DYNAMIC RESPONSE CURVES

FUSELAGE BENDING AMPLITUDE AND PHASE V S. FREQUENCY

FIGURE 26

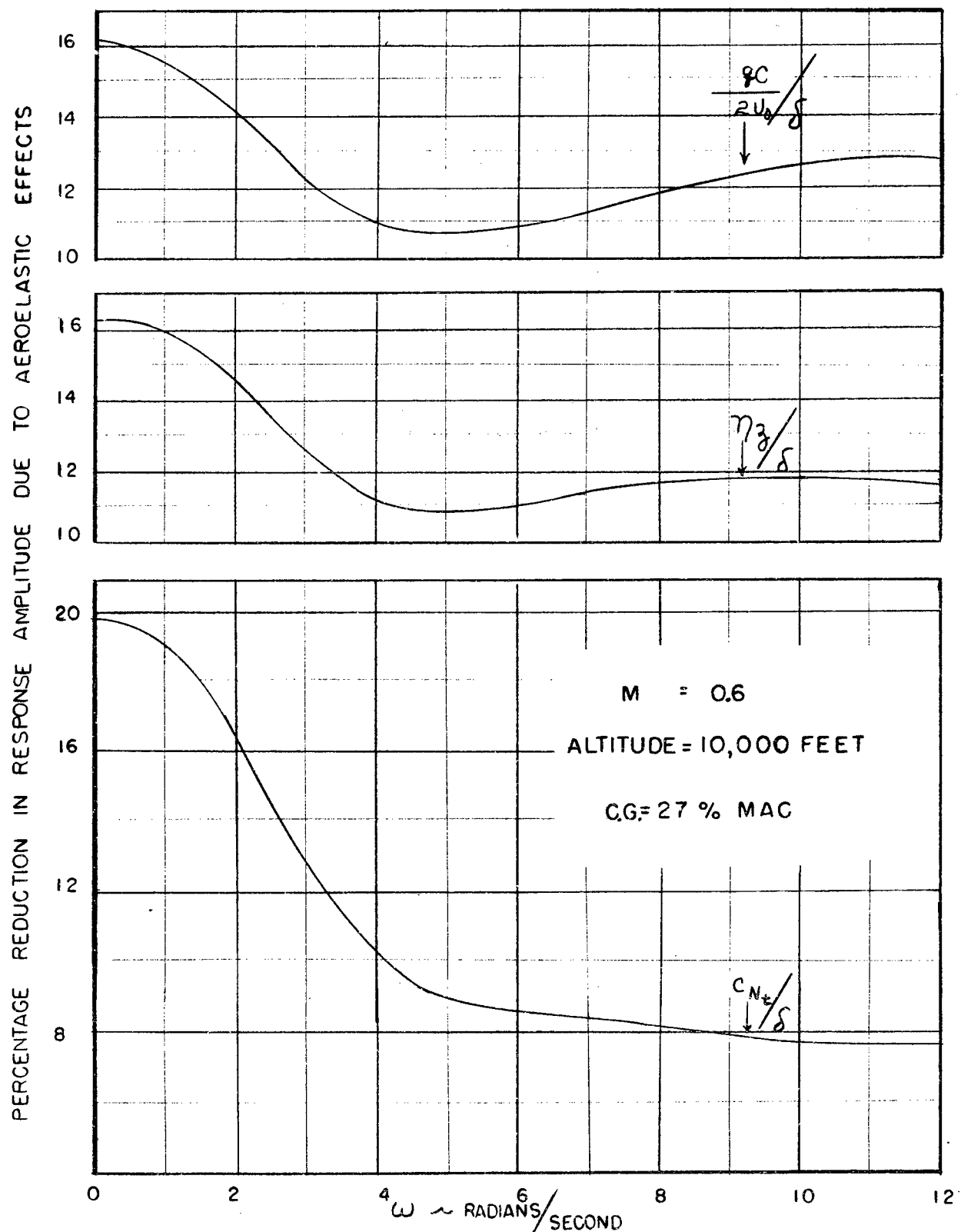
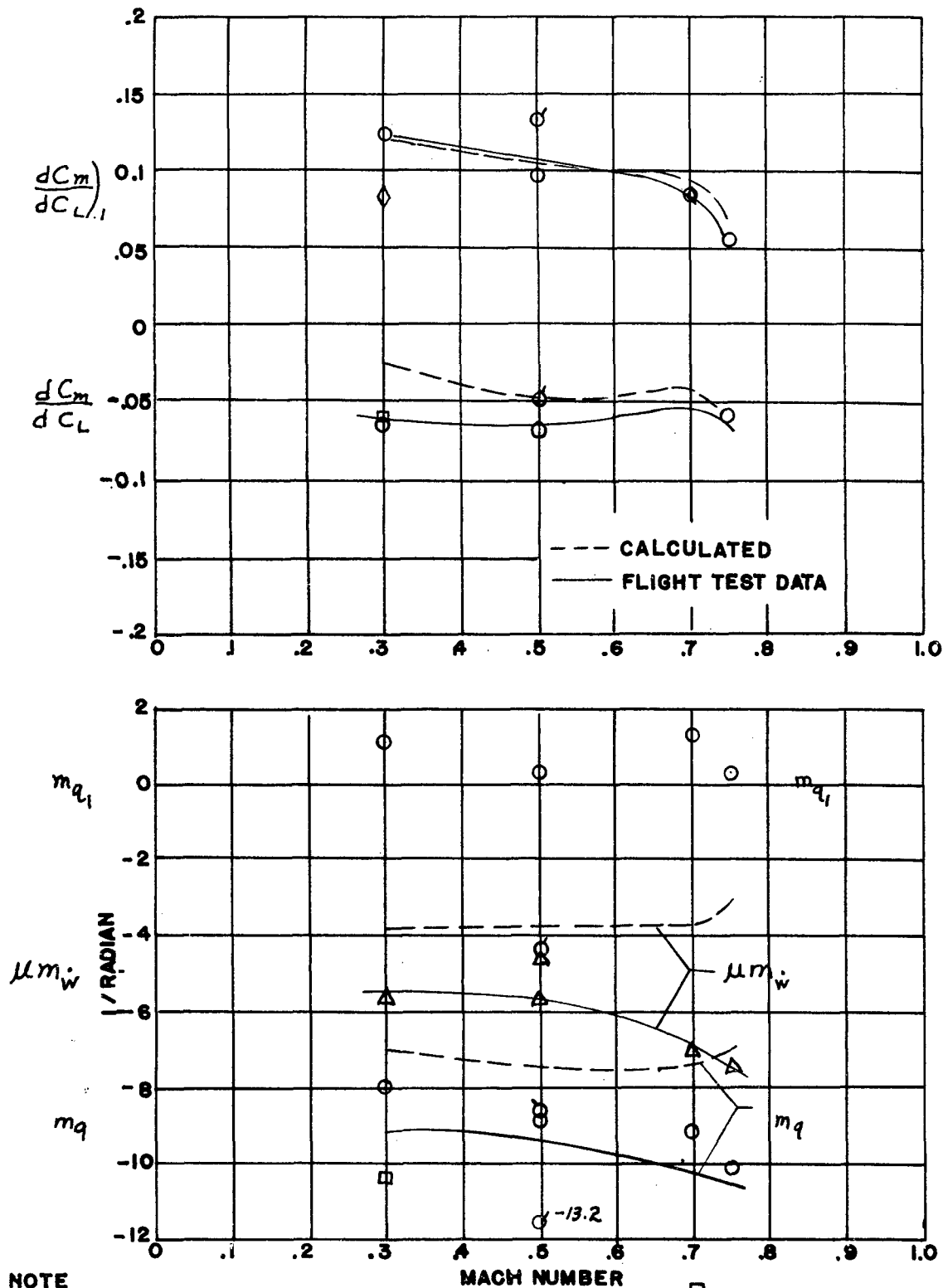


FIGURE 27

# F-80A STABILITY DERIVATIVES

ALTITUDE 20,000 FT; C.G. POSITION 27% M.A.C.



NOTE  
 □ DATA POINT YIELDED BY EQUATION OF MOTION ANALYSIS  
 ◇ DATA POINT YIELDED BY EQUATION OF MOTION ANALYSIS USING A COMPUTED TAIL LOAD (I.E. A TAIL OFF ANALYSIS)

Figure 28

# F-80A STABILITY DERIVATIVES

ALTITUDE 20,000 FT., C.G. POSITION 27% M.A.C.

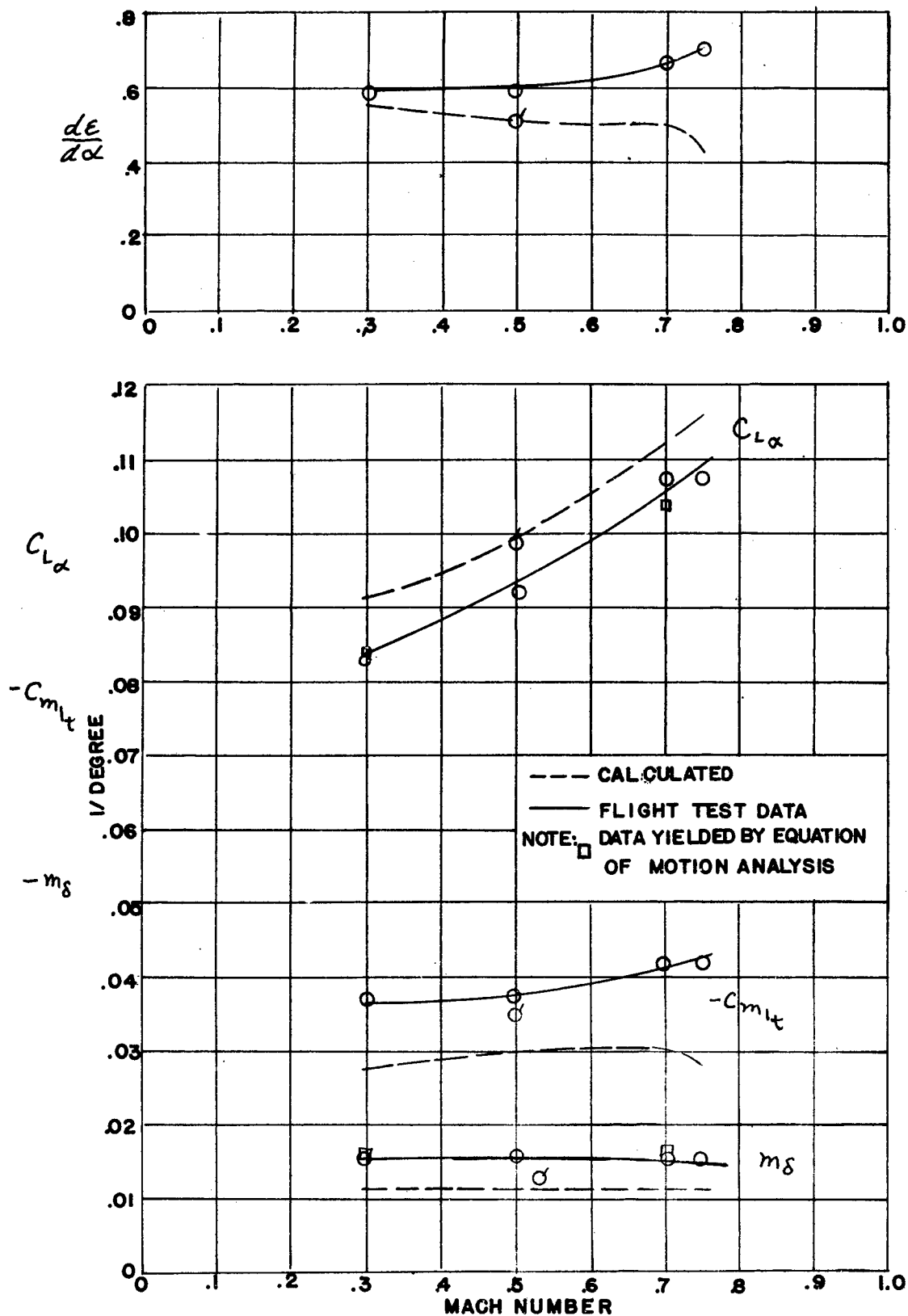


Figure 29

# **F-80A STABILITY DERIVATIVES** **ALTITUDE 20,000 FT; C.G. POSITION 27% M.A.C.**

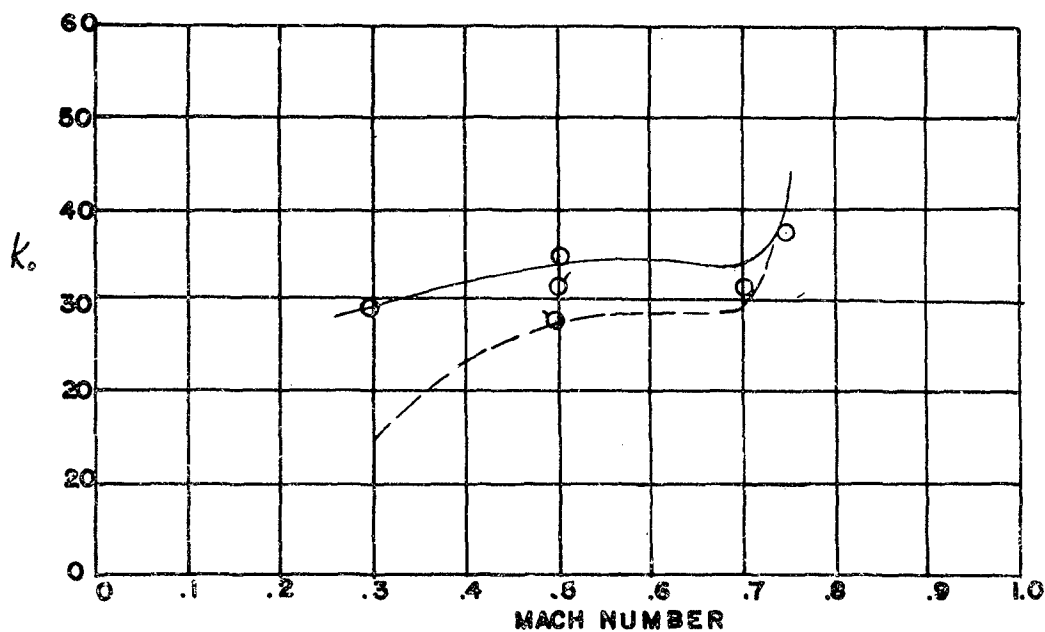
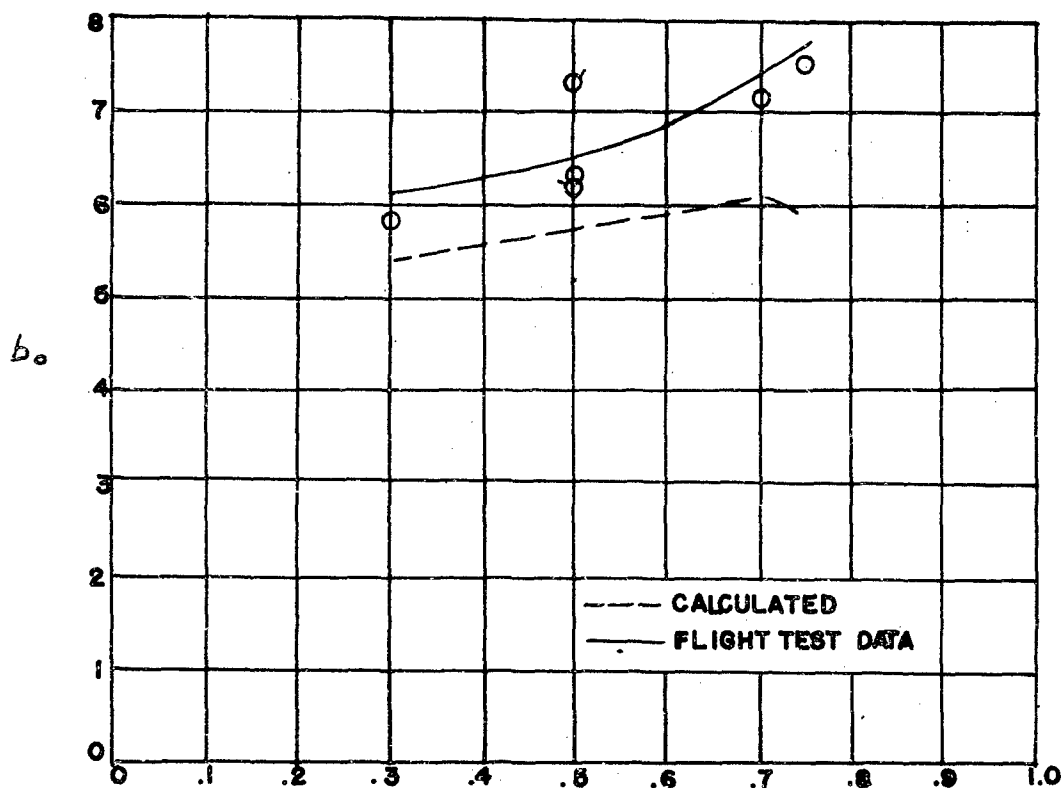
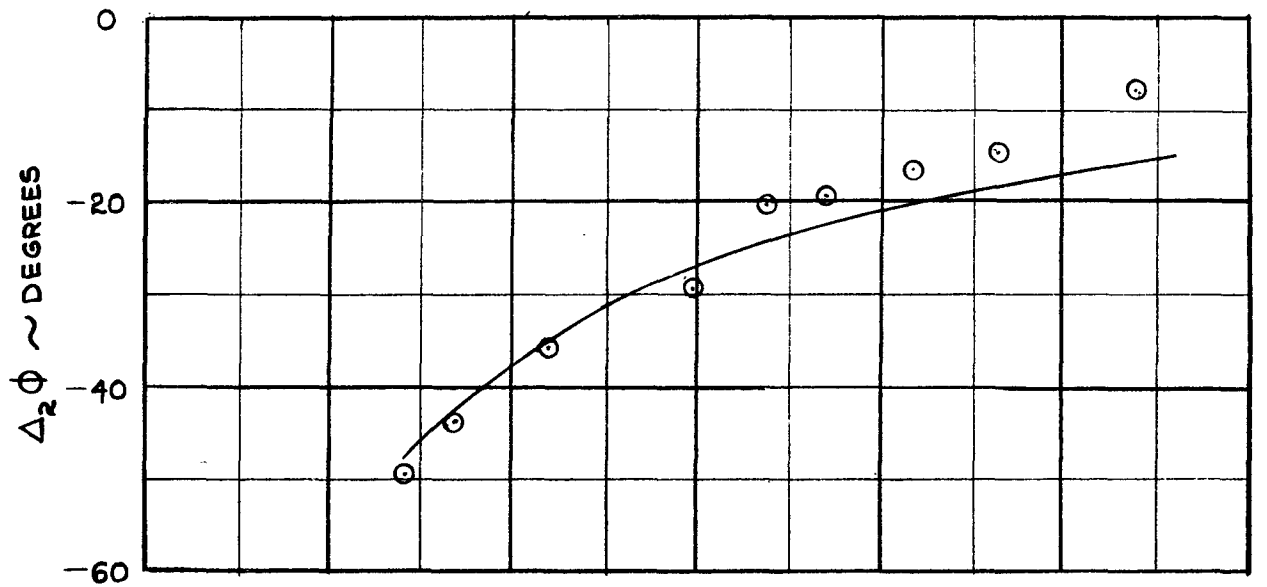


Figure 30

$\Delta_2\phi$  AND  $(\omega\tau)\tan\Delta_2\phi$  VS.  $\omega\tau$



— COMPUTED FROM EXPERIMENTAL  
VALUES OF  $\beta_w$  AND  $m_w$

$M = 0.75$

ALTITUDE = 20,000 FEET

C.G. = 27% MAC

○ FLIGHT MEASUREMENT

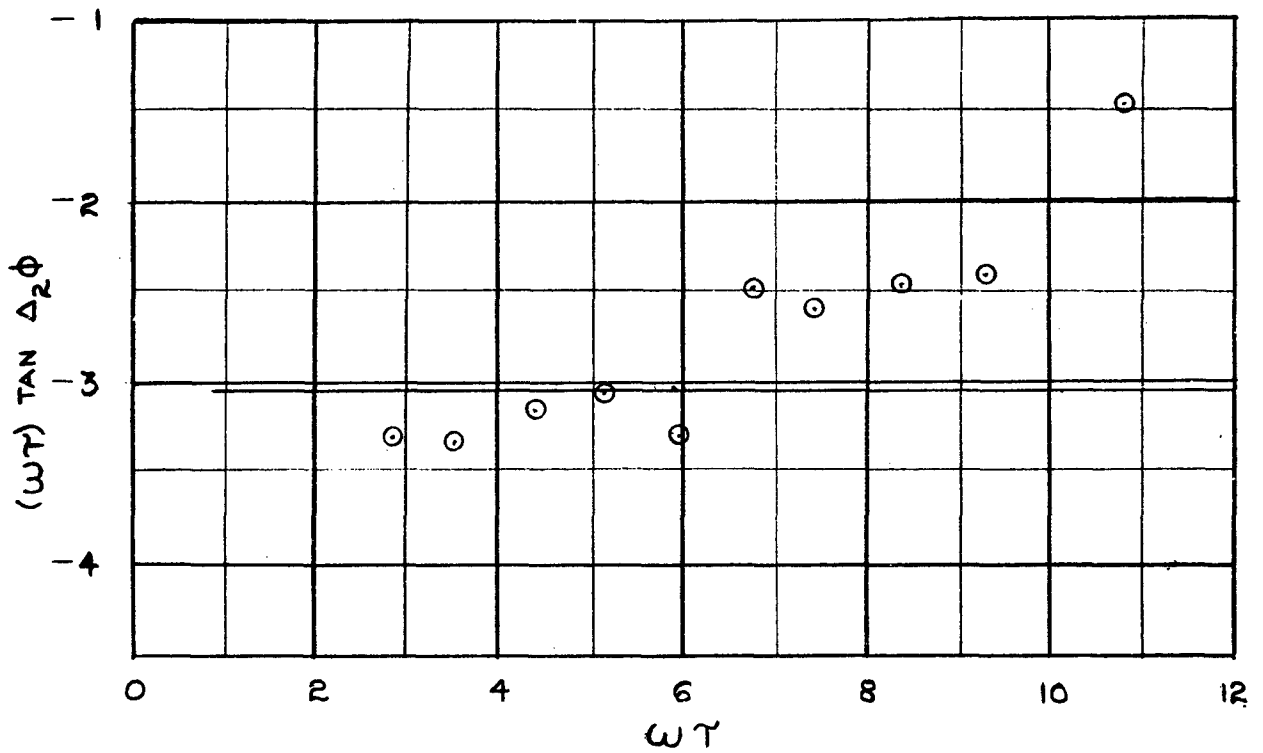


FIGURE 31

# $m_w'$ AND $m_w''$ VS. REDUCED FREQUENCY

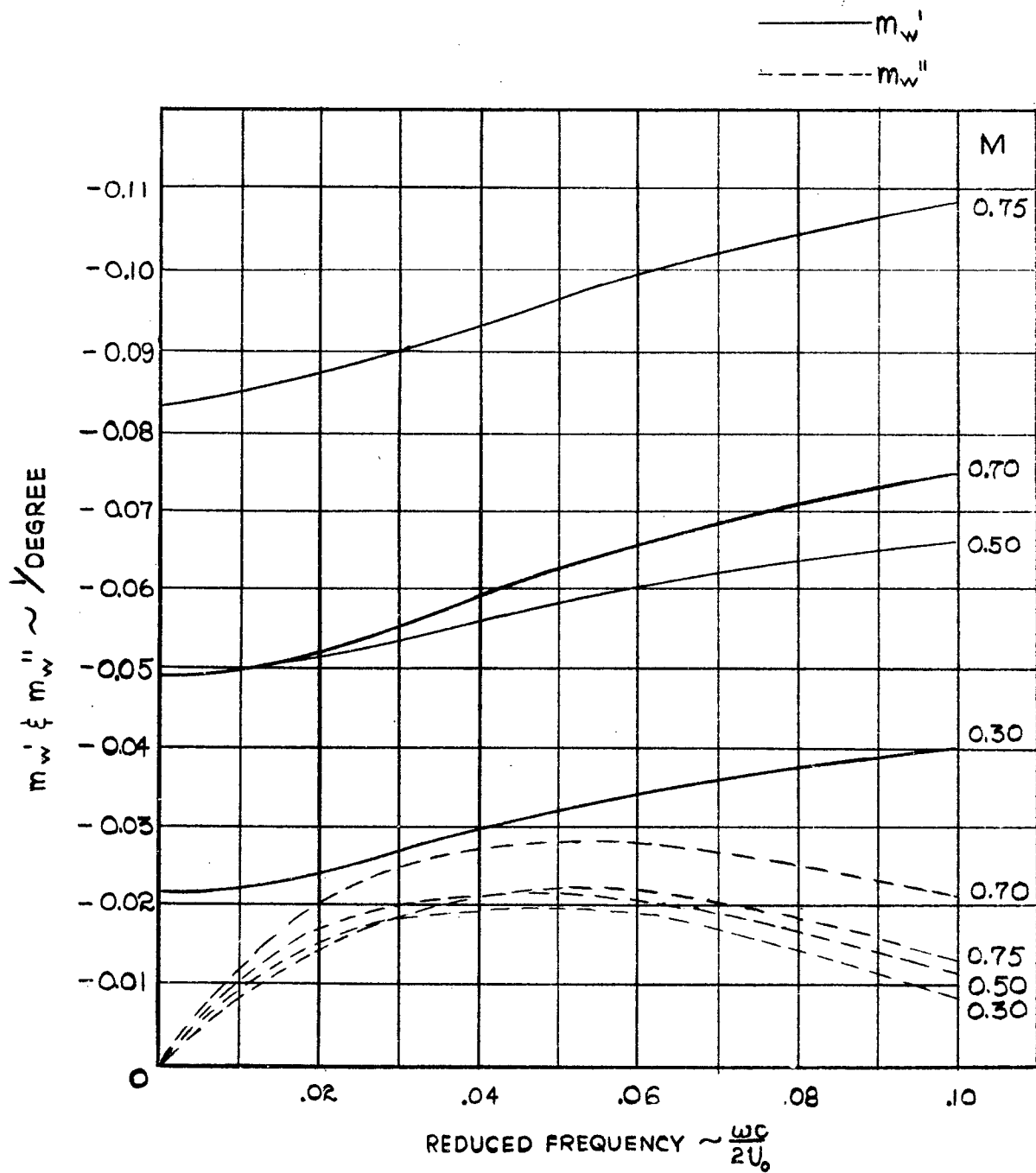


FIGURE 32